THE TECTONIC GEOMORPHOLOGY AND QUATERNARY

GEOLOGY OF THE KATALLA RIVER

VALLEY, ALASKA

by

Kelly Ann Good

A thesis submitted to the faculty of
The University of Utah
in partial fulfillment of the requirements for the degree of

Master of Science

in

Geology

Department of Geology and Geophysics

The University of Utah

December 2013

The University of Utah Graduate School

STATEMENT OF THESIS APPROVAL

The thesis of   **Kelly Ann Good**

has been approved by the following supervisory committee members:

Ronald L. Bruhn	, Chair	**7/13/13**
		Date Approved
Marjorie Chan	, Member	**7/2/13**
		Date Approved
John Bartley	, Member	**7/2/13**
		Date Approved

and by   **John Bartley**   , Chair/Dean of

the Department/College/School of   **Geology and Geophysics**

and by David B. Kieda, Dean of The Graduate School.

ABSTRACT

The paleoseismology record of southeastern Alaska documents several

megathrust earthquakes during the late Holocene, including the Mw 9.2 earthquake of

1964, when the Katalla River Valley was uplifted as much as 2 m (Plafker, 1965;

Richards, 2000). The Katalla River Valley is exceptional because uplifted terraces and

beach berms suggest net tectonic uplift relative to sea level during the late Holocene,

when the greater coastal region experiences net subsidence. This study addresses the

question: is the valley truly undergoing net tectonic uplift, and if so, what is the cause?

Research methods included geomorphic analysis using LIDAR and other digital

elevation data, sampling of Quaternary deposits by coring and hand trenching,

radiocarbon dating of deposits, construction of paleogeography, and analysis of structural

geology.

There are four major results of this study. 1) Katalla behaves similarly to

southeastern coastal Alaska during megathrust cycles: coseismic uplift is followed by

interseismic subsidence. 2) In the last 7000 years, Katalla experienced net uplift with

respect to sea level, and radiocarbon dates and stratigraphic profiles indicate tectonic

uplift. 3) An uplift event documented in the stratigraphy of Katalla dated at 500 BP does

not correlate with any known uplift events in southeastern Alaska. 4) The Ragged

Mountain fault, which has been interpreted as both a thrust and normal fault, underwent extension in at least the last 10,000 years.

There are three possible hypotheses for uplift in Katalla, each of which partially explains long-term extension along the Ragged Mountain fault: 1) uplift driven by buried imbricate thrusting, 2) uplift driven by slow aseismic anticlinal folding that is accommodating shortening, and 3) uplift driven by exhumation as the upper plate of the Ragged Mountain fault moves west.

TABLE OF CONTENTS

ACKNOWLEDGMENTS

CHAPTER 1

INTRODUCTION

The Aleutian megathrust, located in the Gulf of Alaska, is the active thrust

boundary between the Pacific plate and the North American plate (Figure 1) (Kanamori,

1977; Bruns, 1983; Plafker *et al.*, 1994). Subduction zones, like the Aleutian megathrust,

are responsible for the largest earthquakes recorded on Earth (Kanamori, 1977). Between

ruptures, the underlying plate and overriding plate become locked (Figure 2). This causes

the areas closest to the plate boundary, or trench, to subside as the underlying plate

continues to subduct. The areas further inland of the thrust boundary "bulge up" with

respect to sea level interseismically. When the fault ruptures, the areas closest to the

trench coseismically uplift and the inland areas correspondingly subside due to the

elasticity of the crust (Plafker, 1972). Abrupt uplift along the trench and coast often

results in an abrupt environmental change, for example, a change from a marine

environment to a freshwater environment. Coseismic subsidence results in the reverse

change: freshwater environments flooded by seawater. This abrupt environmental change

is evident in the coastal stratigraphy. In the case of coseismic uplift, marine sand might

be sharply overlain by freshwater peat. A gradual change back to marine sand indicates

interseismic subsidence (Atwater, 1987).

The Pacific plate is subducting beneath the North American plate at a rate of ~50 mm/yr (Elliot *et al.*, 2010). In 1964, the Aleutian megathrust ruptured along its eastern margin, causing the second largest recorded earthquake in history. The Mw 9.2 event took 128 lives, most of which were taken by a tsunami generated by the underwater coseismic uplift. Also known as the Good Friday Earthquake, this megathrust event caused uplift of the coastal regions with respect to mean sea level and subsidence of the interior relative to the same datum. Uplift was as great as 10 m (Plafker, 1965). The potential for another large earthquake along this plate boundary is a serious threat. The damage caused by the 2011 Tohoku, Japan earthquake was largely tsunami related. Rupture along the Aleutian megathrust could have similarly devastating effects.

Along the coast of Alaska, there is increasing evidence of active, smaller faults causing local uplift (Chapman, 2011). Though small in area, these uplift events are likely to generate large tsunamis because the amount of uplift is greater than that caused by megathrust events. For example, a fault under Montague Island in the Prince William Sound (Figure 1) coseismically ruptured with the Aleutian megathrust in 1964, and was responsible for the 10 m of uplift recorded after that earthquake (Plafker, 1965). The Kayak Island zone, located in the Gulf of Alaska, and its onshore equivalent, the Suckling Hills fault may also act similarly in megathrust events (Chapman, 2011).

The Quaternary coastal stratigraphy along plate margins can indicate the type, magnitude, and recurrence interval of megathrust earthquakes. Atwater (1987) first showed how a change in coastal vegetation following a large earthquake is preserved in the stratigraphic record. Studying the coast of Washington, he found evidence of submerged peat deposits as well as tsunami sands. In this case, the freshwater sediment

underlying marine sediment indicates coseismic subsidence. Conversely, marine sediments sharply underlying freshwater sediment indicate coseismic uplift.

This study investigates the Quaternary geomorphology and active tectonics of the Katalla River Valley to determine the history of earthquakes and the geomorphic response to them. Previous work in the Katalla River Valley shows that coseismic uplift during large-scale Aleutian megathrust earthquakes is sometimes greater than interseismic subsidence. This differs from most of the coast of northeast Gulf of Alaska. For example, the Copper River Delta to the west and the Puffy Slough to the east both undergo net tectonic subsidence.

Katalla is located along the coast of the Gulf of Alaska (Figure 1), between the Copper River Delta and the Bering Glacier. Mountains that contain faulted and folded rocks of the Yakutat terrane bound the Katalla River Valley (Taliaferro, 1932; Bruhn *et al.*, 2004). The Don Miller Hills rise above the eastern side of the valley. The western side of the Katalla River Valley is bordered by an unnamed mountain that contains a large syncline and by Ragged Mountain, which is underlain by rocks of the Yakutat terrane and the Orca Group. The Orca Group belongs to the edge of the North American Plate and is thrust over the Yakutat terrane along the Ragged Mountain fault (Taliaferro, 1932; Winkler and Plafker, 1983). Therefore, the Ragged Mountain fault accommodated convergence between the Yakutat terrane and North America.

The Yakutat terrane is presently accreting to and subducting beneath North America at roughly the rate of the Pacific plate (Elliot *et al.*, 2010). Large-scale earthquakes such as the Good Friday Earthquake are recorded in the stratigraphy along the coast of southeastern Alaska and are attributed to the Aleutian Subduction Zone and

the Yakutat- North American convergence (Hamilton *et al.*, 2005; Hamilton and Shennan, 2005; Carver and Plafker, 2008; Shennan *et al.*, 2009).

Holocene uplift events documented in the Katalla River Valley correlate well with megathrust events found elsewhere in the Gulf of Alaska (Shennan *et al.*, 2013 [in press]), but there does not appear to be net subsidence in the valley, which is unusual for this part of coastal Alaska. The geomorphology and elevation of Katalla suggest net uplift over time as well as shoreline progradation with each subsequent uplift event (Richards, 2000). Net uplift may be related to a structure that acts independently of the Aleutian megathrust. There is one documented uplift event at 500 BP, which does not correlate with a known megathrust event (Bruhn and Shennan, pers. comm. 2010).
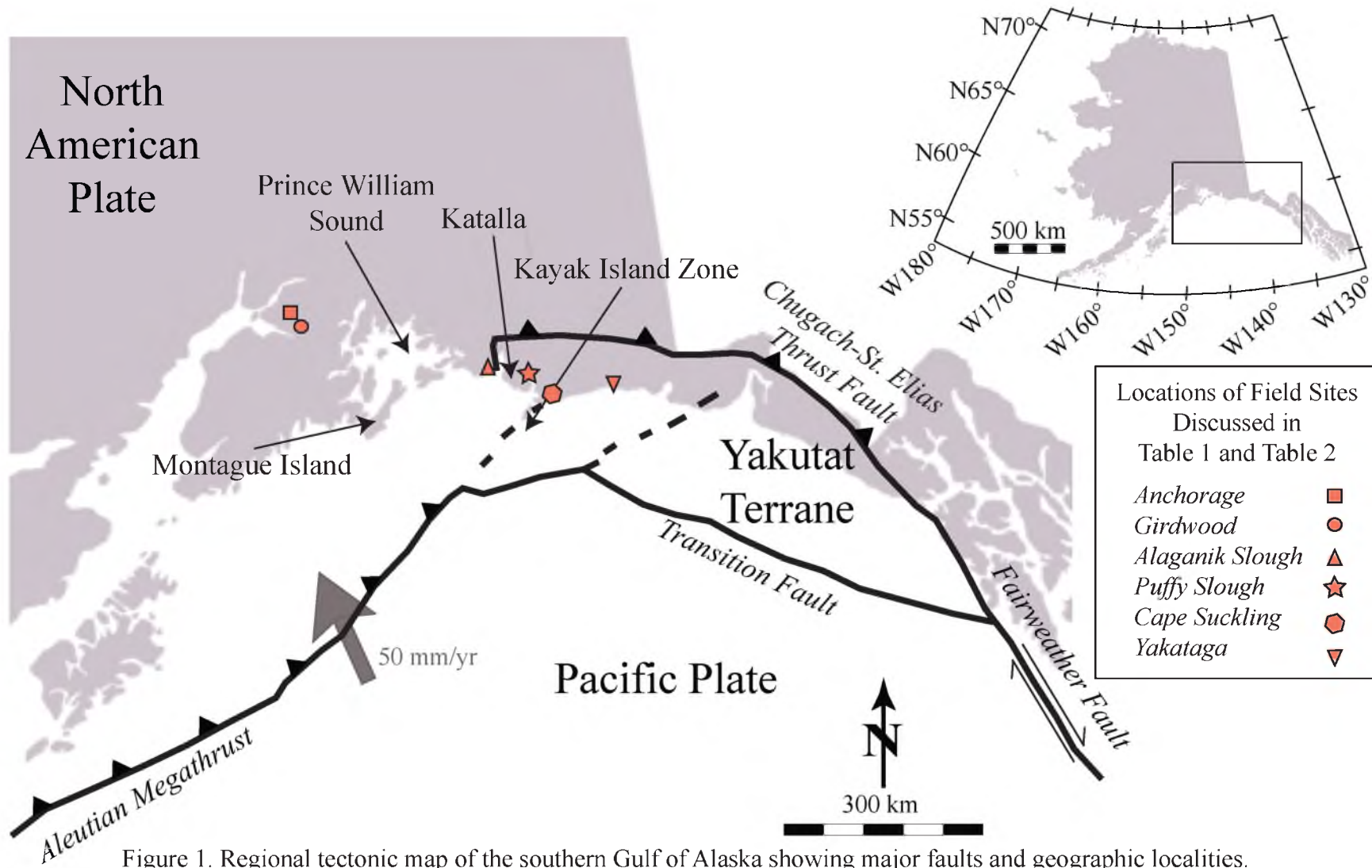
Figure 1. Regional tectonic map of the southern Gulf of Alaska showing major faults and geographic localities. Figure adapted from Bruhn *et al.* (2004).

SW   NE

INTERSEISMIC

Aleutian Trench

Uplift

Subsidence

Pacific Plate

North American Plate

Locked Fault

COSEISMIC

Tsunami generated

Uplift

Subsidence

Rupture
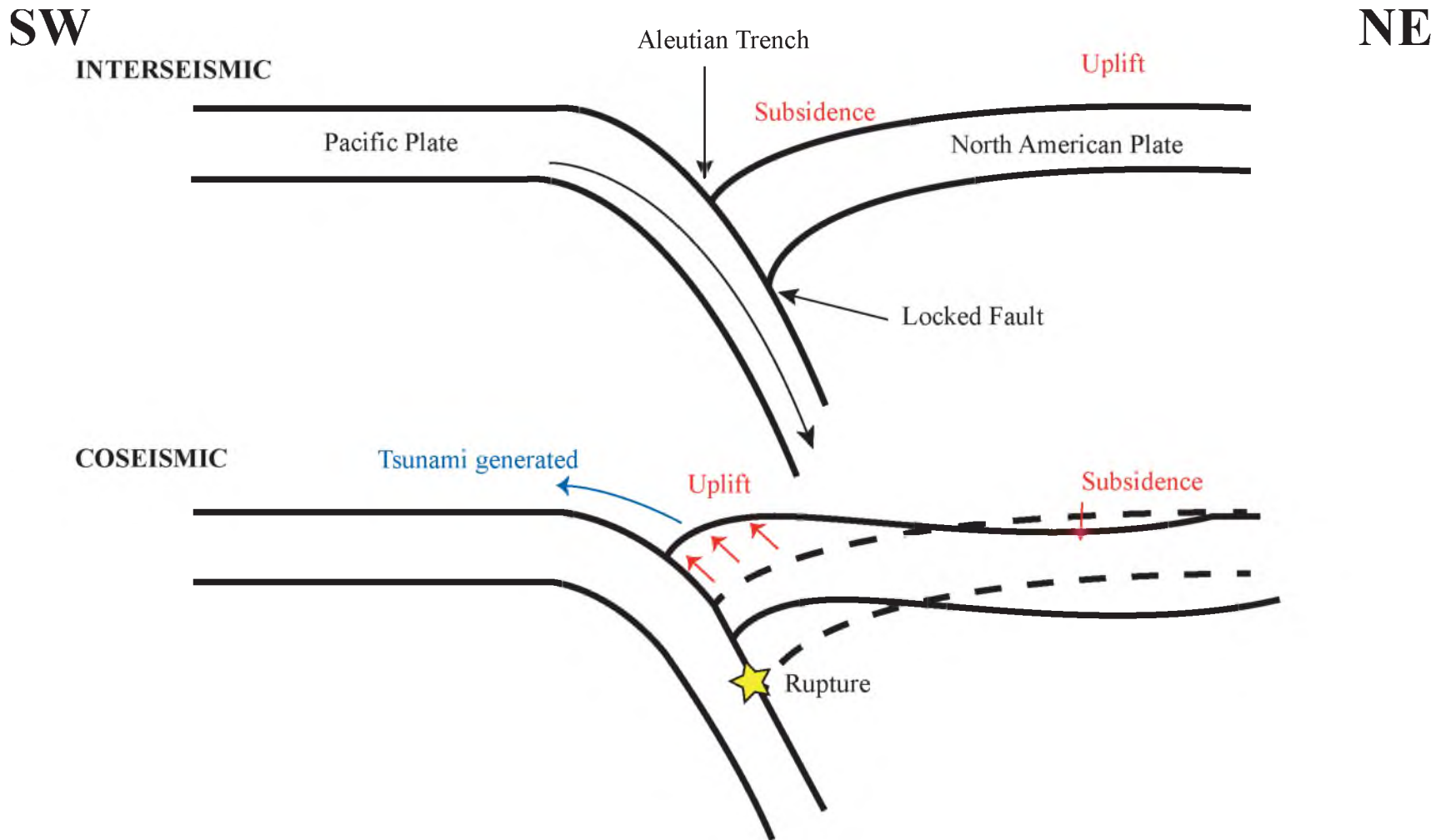
Figure 2. Schematic diagram illustrating how the Pacific plate and North American plate behave interseismically and coseismically. Between earthquakes, strain accumulates on the locked fault. The area closest to the trench subsides, and the area away from the trench bulges. During rupture, the strain is released and the area closest to the trench abruptly uplifts, while the area away from the trench subsides. Tsunamis may be generated due to the abrupt uplift.

CHAPTER 2

GEOLOGIC SETTING

2.1 Regional Tectonics

The Katalla River Valley lies adjacent to the boundary of the Yakutat terrane with the North American plate (Figure 1). The Yakutat terrane is accreting to and subducting beneath the North American plate at a velocity of 50.3 +/- 0.8 mm/yr relative to stable North America (Elliot *et al.*, 2010). The Yakutat terrane is bound to the east by the Fairweather transform fault, to the north by the Chugach-St. Elias thrust fault, and to the west and south by the Transition fault (Plafker, 1994). The Yakutat terrane has been moving northward along the Fairweather transform fault since the middle Eocene from what is now present-day British Columbia (Bruns, 1983). The terrane has been accreting to North America since the late Miocene (Plafker, 1987).

The Fairweather transform fault is a right-lateral strike-slip fault that connects to the Queen Charlotte fault system (Plafker, 1994). The most recent large earthquake on the fault occurred in 1958, and resulted in a dextral slip of up to 3.5 m (Gawthrop *et al.*, 1973). The Chugach-St. Elias thrust fault is the exposed suture between Yakutat terrane sediments and North America. Oceanic crust from the Yakutat terrane shallowly subduct beneath the fault, while the overlying sediments are accreted (Bruhn *et al.*, 2004). The

Transition fault separates the Yakutat terrane from the Pacific plate. The fault may accommodate left-lateral strike-slip motion (Christeson *et al.*, 2010) and/or convergent motion (Elliot *et al.*, 2010) between the Pacific plate and Yakutat terrane.

The Pacific plate is subducting beneath the North American plate via the Aleutian megathrust at a rate of 50.9 mm/year, which is slightly faster than the Yakutat terrane, likely due to difference in convergence style (Elliot *et al.*, 2010). The last seismic event along the Aleutian Megathrust occurred in 1964; it was an Mw 9.2 event that initiated under the Prince William Sound. The event caused deformation along much of the Alaskan coast—as far east as the Bering Glacier (Plafker, 1965). At least four other megathrust earthquakes have occurred in southeastern Alaska at 900 BP, 1500 BP, 2100 BP, and 2600 BP (Table 1) (Hamilton *et al.*, 2005; Hamilton and Shennan, 2005; Carver and Plafker, 2008; Shennan *et al.*, 2009).

Within the Yakutat terrane are other, small tectonic zones in addition to the three bounding faults: the Pamplona Structural zone and the Kayak Island zone, and foreland folds and thrust faults related to the Chugach-St. Elias fault (Bruhn *et al.*, 2004). The Pamplona zone fold and thrust belt is the active deformation front of the Yakutat-North American collision (Worthington *et al.*, 2010). The Kayak Island Zone, situated north west of the Pamplona zone, may be the modern eastern extension of the Aleutian megathrust (Chapman *et al.*, 2011). The Pamplona zone also is the boundary between the active fold and thrust belt and the 'western syntaxis'. The western syntaxis is the manifestation of the corner geometry of the obliquely converging Yakutat terrane (Bruhn *et al.*, 2004; Chapman *et al.*, 2011). The complexly folded rocks in and around Katalla are part of the western syntaxis.

2.2 Local Tectonics

The most prominent structural feature in the Katalla River Valley is the Ragged Mountain fault (Figure 3). The Ragged Mountain fault strikes north and extends for nearly 30 km. The fault is described as both a thrust fault and a normal fault (Tysdal, 1976; Winkler and Plafker, 1993; Richards, 2000) because the fault places older strata on younger but the surface expression of the fault suggests normal displacement. The Ragged Mountain fault is the contact between the Paleogene Orca Group and the Eocene Stillwater Formation (Figure 4). Although the Orca Group originates from the Prince William terrane—which accreted to North America prior to the arrival of the Yakutat terrane—the Stillwater Formation was transported atop the Yakutat terrane (Winkler and Plafker, 1993; Plafker *et al.*, 1994). The Ragged Mountain fault represents a suture between the North American plate and the Yakutat terrane, and thus was interpreted to be a thrust fault that originated as part of the Chugach St. Elias fault (Bruhn *et al.*, 2004). However, the Ragged Mountain fault is marked by a Quaternary scarp that is uphill facing, indicating extension. Therefore, Tysdal (1976) interpreted it to be a re-activated thrust fault that is backsliding, and referred to it as a low-angle normal fault. Bruhn (pers. comm., 2012) posited that it is instead the surface expression of fault propagation folding: the upward facing scarp represents the dip slip of bedding in the limb of the fold.

Other tectonic structures mapped in the Katalla River Valley are poorly understood. The Clear Creek fault is concealed but is mapped because of the juxtaposition of two different rock units: the sedimentary Poul Creek Formation from the late Tertiary and the Stillwater Formation from the early Tertiary (Winkler and Plafker, 1993). The Redwood fault, in the Don Miller Hills on the eastern side of the valley, is

inferred to account for juxtaposition of three different rock units along its length: the

Tokun Formation, the Stillwater Formation, and the Poul Creek Formation (Martin, 1908;

Winkler and Plafker, 1993). Many smaller faults and complex structures in the Don

Miller Hills are attributed to second-phase folding during oblique convergence

(Taliaferro, 1932; Bruhn *et al.*, 2004).

2.3 Bedrock/Stratigraphy

The bedrock geology of the Katalla River Valley is relatively simple (Figure 4).

The footwall of the Ragged Mountain fault comprises Stillwater Formation, a dark

siltstone from the Eocene. The Stillwater Formation is tilted to a near vertical dip and

strikes roughly NNE with few exceptions. The Eocene to Miocene Orca Group is an

accretionary complex consisting of conglomerates, sandstones, and volcanic rocks from

the Prince William terrane. Ragged Mountain, on the western side of the valley, is

composed of these three components of the Orca Group. The Poul Creek Formation

occurs in the hills in the central part of the valley as well as the Don Miller Hills on the

eastern edge of the valley, and it may underlie part of the valley. The Poul Creek

Formation is also Eocene to Miocene in age, and the outcrops are deepwater shales and

sandstones. The Tokun Formation crops out at the northernmost and southernmost ends

of the valley. It is Eocene in age and comprises siltstones interbedded with sandstones.

The outcrops of the Tokun Formation are severely folded and faulted (Winkler and

Plafker, 1993). The rest of the valley is filled with Quaternary sediments that will be

discussed in further detail in the Results section of this thesis.

2.4 Geomorpholgy/Quaternary Geology of Katalla River Valley

Previous geomorphology studies of the Katalla River Valley investigated the glacial history (Fleisher *et al.*, 1999), mapped the Quaternary deposits (Kachadoorian, 1960; Winkler and Plafker, 1993) and analyzed the Holocene deposits (Sirkin and Tuthill, 1971; Richards, 2000).

Fleisher and others (1999) found well-rounded exotic boulders in Katalla Bay, and glacial till in the valley and on the flanks of Ragged Mountain and glacial silt in the valley. They concluded that glaciers advanced to the coast as recently as ~10,000 years ago (Fleisher, 1999; Richards, 2000).

The most conspicuous feature of the valley is the series of dark cuspate, ridges separated by marshes (Figure 3). The ridges are made of well-sorted sand (Sirkin and Tuthill, 1971; Richards, 2000) and gradually increase in elevation up the valley (Richards, 2000). The fill between each ridge is a freshwater peat marsh.

Sirkin and Tuthill (1971) interpreted the ridges to be storm berms—ridges that build up in high water events at the most landward side of the beach. In order for the berms to be rebuilt further down the valley as the elevation data suggest, Richards (2000) hypothesized that the valley is uplifted during great megathrust earthquakes. The shoreline then moves seaward and a new berm begins to form. The freshwater marshes atop the marine sediment are also interpreted to form after the beach is raised above sea level.

Plafker (1965) documented coseismic uplift of the Katalla River Valley following the 1964 Good Friday Earthquake. He found that the coastline near the Katalla River Valley was uplifted nearly 2 m and comparison of historical photos to the present show
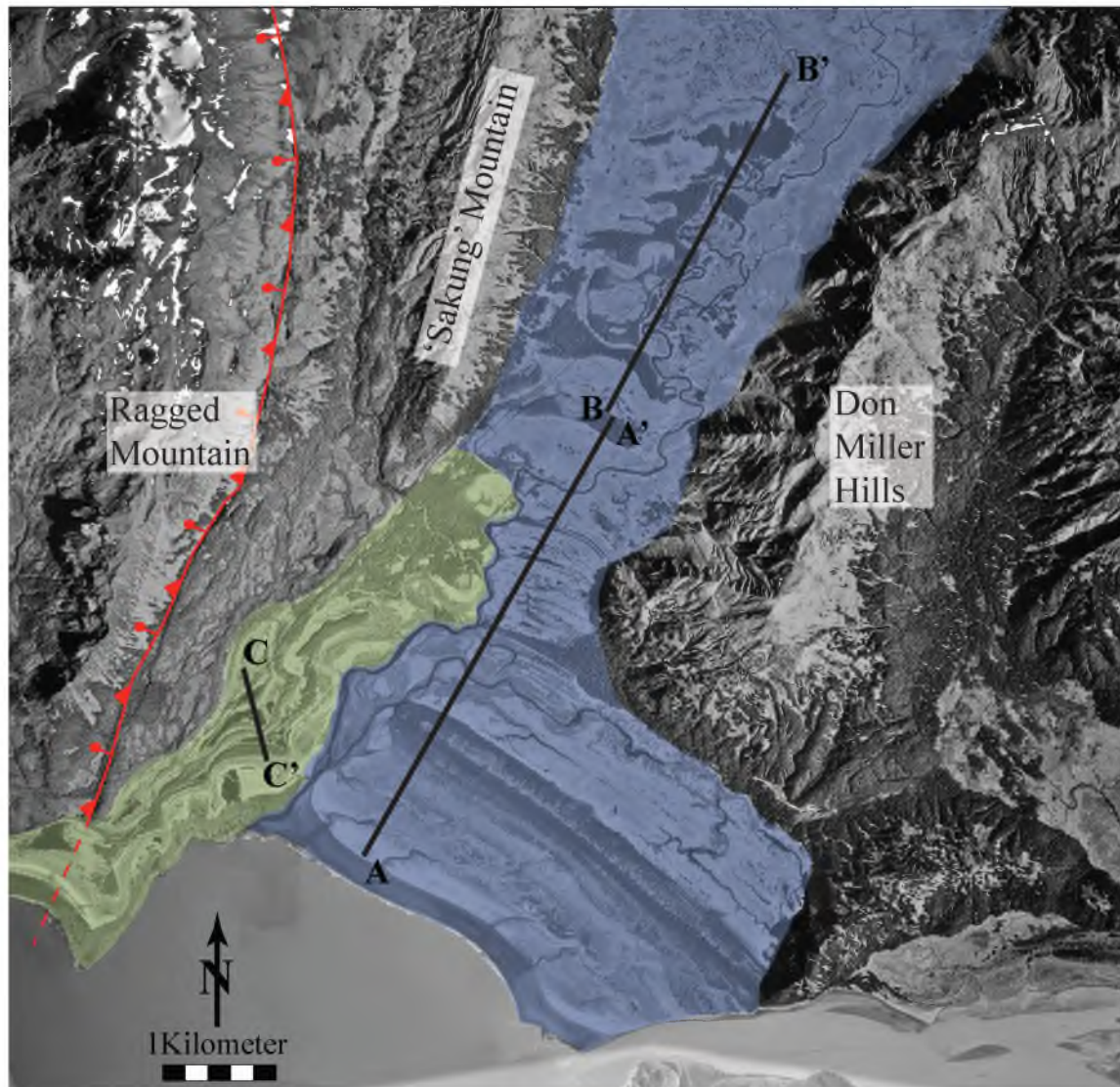
the shoreline moved at least a kilometer seaward. An uplift event documented in a lower marsh was dated at 500 BP (R. Bruhn and I. Shennan, 2011 pers. comm.). This date does not correlate with any known megathrust event (Table 1). Thus, it is possible that there is some other control on the tectonic geomorphology of the valley besides the Aleutian Megathrust.

Richards' study (2000) showed that the valley not only undergoes coseismic uplift but interseismic subsidence as well. This was based on drowned trees found in the marshes between the spruce deposits. Richards concluded from the elevations of the berms, however, that the valley experiences net tectonic uplift. Although the valley probably experienced isostatic rebound after disappearance of the glaciers, a simple one-dimensional isostatic rebound model demonstrates that the berms presumably formed after isostatic rebound following retreat of the glaciers from the valley (Richards, 2000).

Sinuous terrace-like features are located west of the Katalla River on the Ragged Mountain piedmont (Figure 3). The eastern edge of each terrace is lined with spruce and hemlock-covered ridges. Previous mapping of this side of the valley describes the deposits as marine or glacial terraces, unconsolidated sedimentary material, or swamp deposits (Kachadoorian, 1960; Winkler and Plafker, 1993). The terraces gain elevation from the Katalla River toward Ragged Mountain, and each terrace is 2-5 m higher than the one below it. This step-like pattern indicates that the terraces may be tectonically derived (Figure 5).

Table 1. Ages of megathrust events recorded in cores throughout the southern Alaska Coast (Hamilton *et al.*, 2005; Hamilton and Shennan, 2005; Carver and Plafker, 2008; Shennan *et al.*, 2009) and Katalla. Locations shown in Figure 1.

Megathrust Event	Anchorage	Girdwood	Alaganik Slough	Puffy Slough	Cape Suckling	Yakataga	Katalla
1964	X	X	X	X	X	X	X
500 BP							X
900 BP	X	X	X	X	X	X	X
1500 BP	X	X	X				X
2100 BP	X	X	X				X
2600 BP	X	X	X				X

Figure 3. Katalla area highlighting the Ragged Mountain piedmont (green) and the Katalla River Valley (blue). Cross sections are shown in Figures 22a and 22b.

Photo credit: US Forest Service (early 2000s)

Figure 4. Geologic map of the Katalla River Valley, Ragged Mountain, and Don Miller Hills (adapted from Winkler and Plafker, 1993).

Legend

Quaternary

Qs	Surficial Deposits (Holocene)
Qb	Beach Deposits (Holocene)
Ql	Lagoon Deposits (Holocene)
Qt	Talus Deposits (Holocene)

Tertiary

Tr	Redwood Formation (Pliocene to Oligocene)
Tps	Poul Creek Formation (Miocene to Eocene)
Tt	Tokun Formation (Eocene)
Tk	Kulthieth Formation (Eocene)
Ts	Stillwater Formation (Eocene)

Orca Group (Eocene to Paleocene)

Tos	Sedimentary Rocks
Tov	Volcanic Rocks
Tovs	Sedimentary and Volcanic Rocks

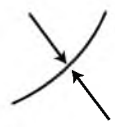Thrust fault with normal-sense reactivation
Barbs and balls and sticks on the hangingwall block
Dashed where inferred

Fault with no known sense of displacement
Dashed where inferred.

Anticline   Syncline

Tovs

Tos

Qs

Tov

Tos

Ragged Mountain Fault

Ts

Qt

Clear Creek Fault

Ts

Tps

Qb

Ql

Qb

N

5 kilometers

Tt

Katalla River

Qs

Tps

Tps

Tt

Redwood Fault

Tk

Bering Lake

Tr

Qs

Pacific Ocean
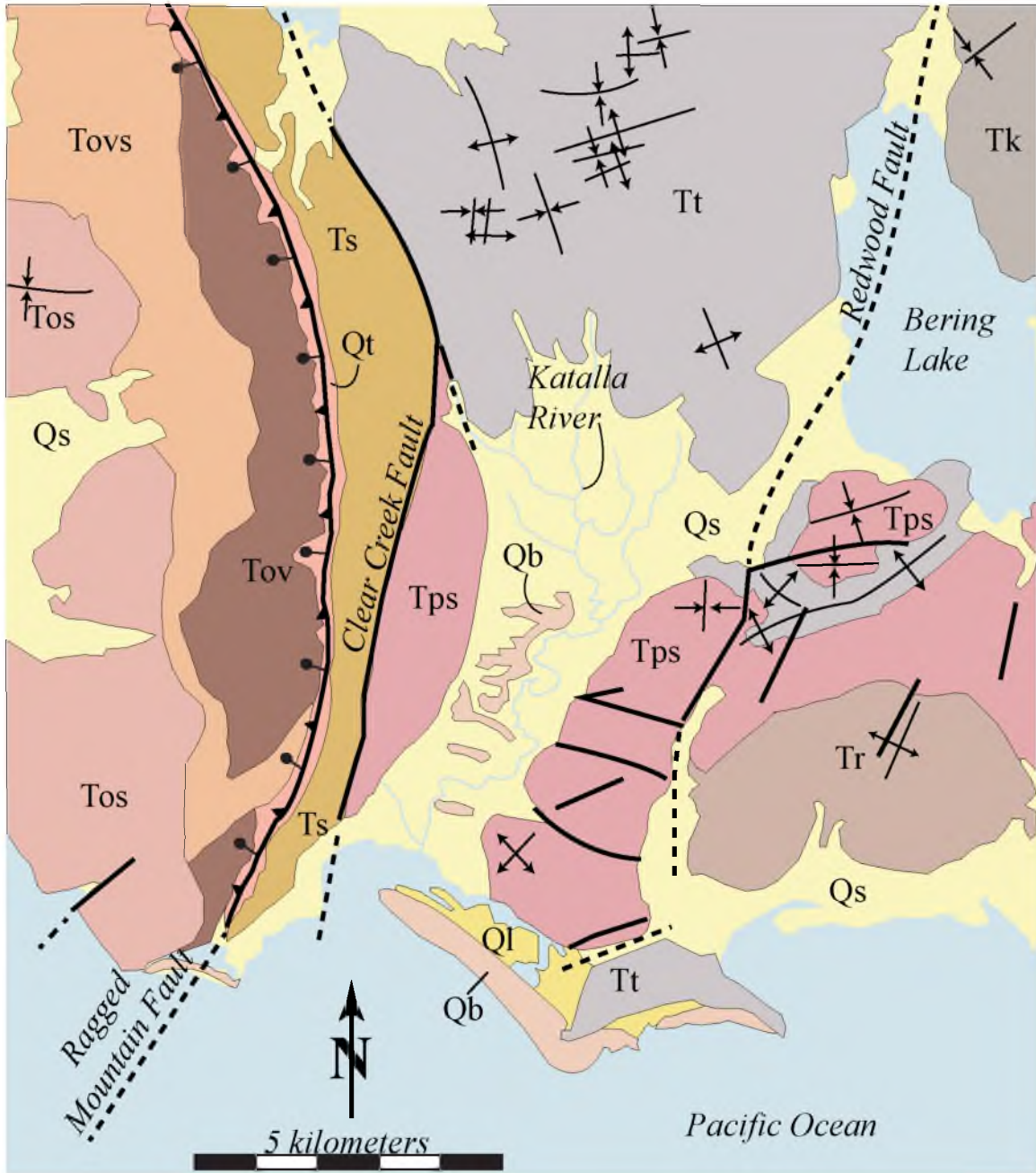
Figure 5. Hillshade images and profiles of the Ragged Mountain piedmont demonstrating important topographic features. a) Hillshade image of the terraces on Ragged Mountain piedmont. Box in top image is the more detailed section shown in bottom figure. Terraces are labeled in yellow, ridges in white. Cross sections A-A', B-B', C-C', D-D' and E-E' shown in Figures b, c, and d. b) Topographic profile of Ragged Mountain and the piedmont. Important geographic features are noted. c) Topographic profiles of the Ragged Mountain Piedmont from south (B-B') to north (D-D'). Important topographic features are noted. All three profiles are the same scale with ~9x vertical exaggeration. d) Topographic profile of Ridge 2 on the Ragged Mountain Piedmont (35x vertical exaggeration). Note the seaward side of the berm is steeper than the landward side. There is ~2 m difference in height of the seaward side to the landward side. This ridge profile is typical of those elsewhere on the piedmont.
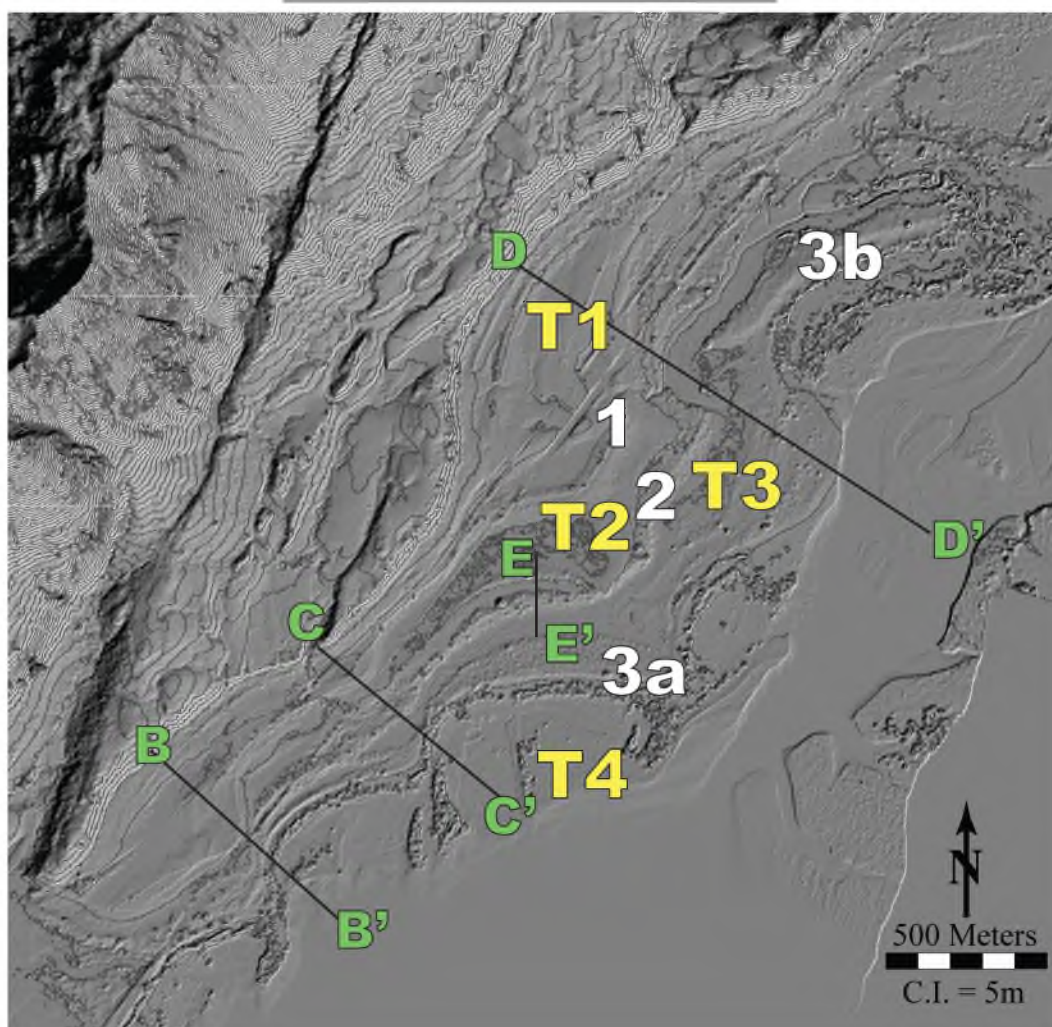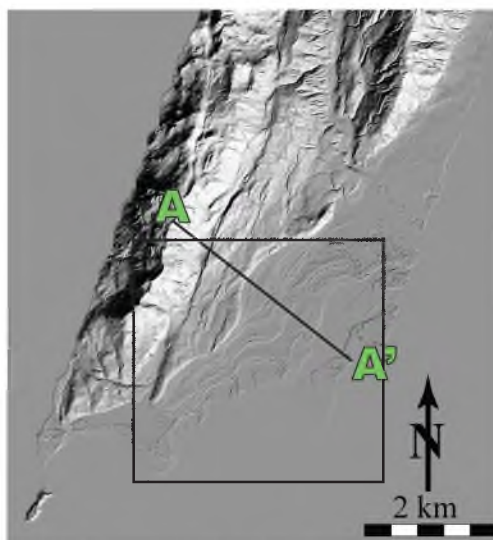
a)
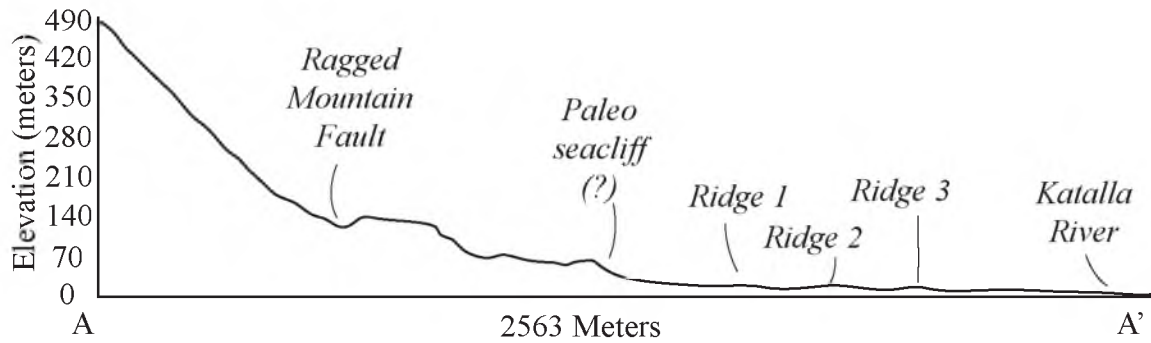
b)
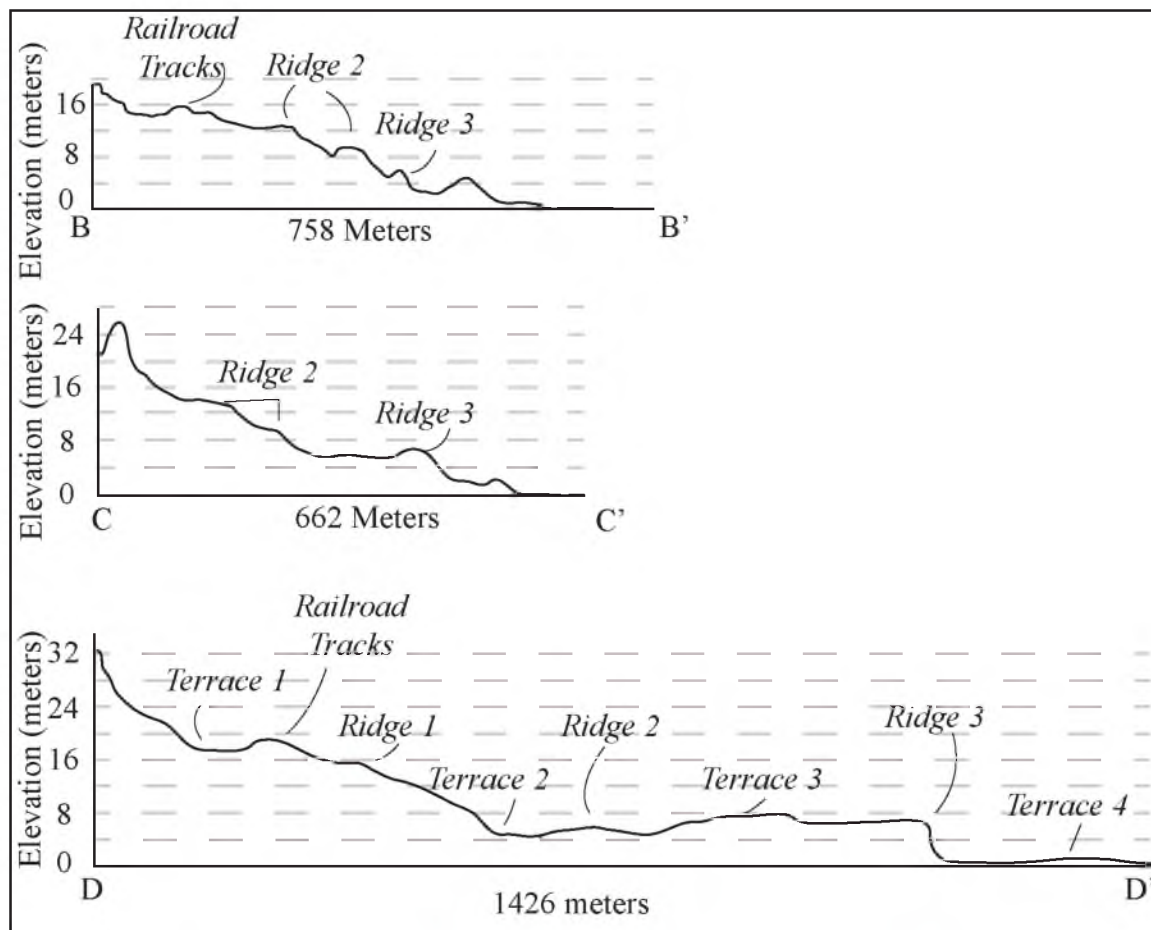
c)
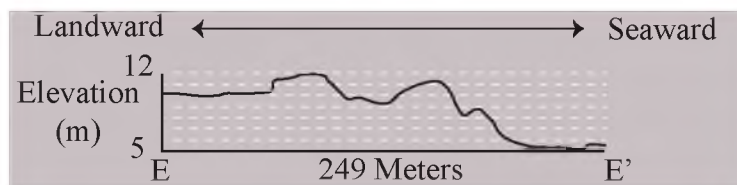
d)

Figure 5 continued

CHAPTER 3

METHODS

A preliminary geomorphic mapping exercise using air photos as well as digital elevation data was completed prior to the field season in order to better understand the local geomorphology and to accurately choose locations to study while out in the field (Figure 6).

3.1 Fieldwork

In August of 2011, the author along with colleagues from the University of Utah, Durham University, University of Texas at El Paso, and the Alaska Division of Geological and Geophysical Surveys flew into the abandoned town site of Katalla, Alaska, where we spent eight days in the field. Access to geologic features within and adjacent to the town site was by foot, while a boat with an outboard jet unit was used to gain access into the valley by traveling on the Katalla River. Field localities were located using a handheld GPS unit with horizontal resolution of roughly +/- 15 m, and by reference to aerial photographs.

One objective of the field study was to confirm interpretations of geomorphic features observed on aerial photography and revealed by a high-resolution Digital

Elevation Model (DEM) acquired by Light Designation and Ranging (LIDAR). The LIDAR survey was flown in August of 2005 by the National Center for Airborne Laser Mapping as part of the St. Elias Erosion and Tectonics Project (STEEP). The data were postprocessed to refine geographic positioning and to filter out the effects of vegetation. The resulting bare earth DEM (Figure 6) has a posting of 1 m, and a vertical accuracy of ~20 cm. Additional information concerning the surveying equipment and acquisition parameters is in the Appendix.

The second objective was to document the Quaternary stratigraphy at several sites in the Katalla Valley and on the piedmont of Ragged Mountain to search for evidence of depositional environments, evidence for abrupt transitions from marine to nonmarine deposition that reflect vertical changes in elevation caused by earthquakes, and to obtain samples of the strata for analysis of depositional environment and radiocarbon dating. Field sites are shown in Figure 7. A hand auger and core barrels of 25 mm and 50 mm diameter were used to collect samples over a depth range of several meters in marshes. Fifteen core samples were obtained, with 13 of the 15 sampling sites located in the Katalla Valley and the remainder from the piedmont of Ragged Mountain at the Katalla town site. Several additional duplicate core samples were also obtained. Three additional stratigraphic samples were obtained by driving split-halves of PVC pipe and a rectangular box sampler into the wall of cut banks along the Katalla River. The stratigraphy of each core and river cut bank was described in the field, with emphasis on identifying sharp contacts between possible marine deposits and overlying peat. Samples that included the interval spanning ~10 cm on either side of the contact were collected for analysis of diatom assemblages, and radiocarbon dating of peat.

Soil pits were dug by hand in five ridges located in the Katalla Valley and on the piedmont of Ragged Mountain. The composition and grain size of the deposits were noted to aid in identifying the origin of the ridges, and also to compare with similar samples described by Richards (2000) and Sirkin and Tuthill (1971). A comparison of our field sites and those of Richards and Sirkin and Tuthill is in the Appendix.

General geologic and geomorphic features were also noted while in the field. The locations of glacial erratics were recorded, as well as the compositions of clasts that may be the remnant of a former moraine located on the beach south of the Katalla town site. Additionally, cores were taken of trees in order to determine a minimum age of former marine beach ridges. The diameters of most trees were larger than the corer (>30 cm), so determining a maximum age of the trees proved to be difficult. Felled trees were also encountered in the field, both near the Katalla town site and as far north as Ridge E, indicating that the current trees on some ridges are second growth.

3.2 Lab Work

Radiocarbon dating of peat fragments was done using Accelerator Mass Spectrometry by Beta Analytic, Inc. Organic material for dating was separated by hand from bulk peat, and included blade-like leaves and Sphagnum moss. Samples were collected from the base of the peat, and 2 cm above the base. These included samples from Core 3, Core 7, Core 10, Core 11, Core 14, and Core 15 (see Figures 7b and 7c). The dates of the original set of samples were partly "reversed", that is, in all but two of the cores, the samples above the base of the peat appeared to be older than the samples taken at the base. Further examination by Dr. Shennan of Durham University identified

intense rootlet penetration of the *in situ* material as well as reworked organics, which is most likely what gave the false dates. A second round of samples were chosen following careful examination under a microscope to ensure a lack of rootlets penetrating the sample. These samples were submitted and the resulting ages were arranged in the proper stratigraphic order (Table 2). An organic sample from a core collected in Katalla Slough in 2007 by Dr. Bruhn and Dr. Shennan was also dated to confirm a previously obtained age for the base of a peat at that locality.

Dr. Shennan examined the diatoms in the sand and silt horizons to establish if they are marine or freshwater species. He also determined where along the beach profile the diatoms lived based on unique characteristics in their morphology using the techniques outlined by Palmer and Abbot (1986). These include counting frequency of each diatom taxon and placing it in a halobian category, and plotting the frequency/core-depth relationship for each category. A halobian classification divides the diatoms into categories of salt tolerance, which ideally gives a depositional environment. The Hemphill-Haley (1993) classification scheme designates five halobian classifications. For example, taxa falling into the polyhalobous classification occur in >30‰ salinity and are marine in origin. The Hemphill-Haley classification scheme distinguishes diatoms that are marine, brackish, low-salinity stimulated, low-salinity tolerant, and saltwater-intolerant (Hemphill-Haley, 1993).

3.3 Mapping

ITT Visual Information Solutions © ENvironment for Visualizing Images (ENVI) software was used to create shaded relief images and contour maps using the 1 m posted

LIDAR DEM, a 30 m posted Advanced Spaceborne Thermal Emission and Reflection

radiometer (ASTER) Global Digital Elevation Model (GDEM) and a 30 m posted Shuttle

Radar Topography Mission (SRTM). The latest version of the ASTER GDEM was

released in 2009 and is a product of the Ministry of Economy, Trade, and Industry of

Japan (METI) and the National Aeronautics and Space Administration (NASA) (ASTER

GDEM data courtesy of NASA). The SRTM data were released in 2003 and are also a

product of NASA (data courtesy of the USGS). The LIDAR data were used to make a

geomorphic map of the Ragged Mountain piedmont. The LIDAR DEM revealed details

of the geomorphology that were not present on earlier images and air photos because of

thick vegetation. LIDAR sensors record multiple returns of a single laser pulse, and

typically the last return represents the terrain, or bare-earth. This greatly differs from the

SRTM and GDEM because the vegetation can be filtered out after acquisition. Katalla is

densely vegetated, so the LIDAR DEM greatly aided the geomorphic mapping.

Depositional features that were never before mapped such as tree-lined ridges and

uplifted coast were plotted, in addition to known features such as rivers, alluvial fans and

marshes (Figure 6).

Elevation data from the LIDAR DEM were compared to Richards' (2000) GPS

elevations (appendix). Richards' GPS measurements are spot elevations and are not

representative of the entire marsh or ridge surveyed. They do, however, have very high

precision and accuracy. The vertical precision of the GPS elevations is <10 cm, which

falls within the LIDAR margin of accuracy, about 20 cm. The vertical precision of the

GDEM and SRTM is much coarser—on the order of meters—therefore, these data were

not extensively used to compare elevations throughout the valley.

Various geomorphic features such as marshes, terraces, ridges, cliff features, and possible paleo-shorelines were correlated across the Katalla River using contour maps of the valley and terraces as well as high-resolution orthophotos. Elevation data, radiocarbon dates, and previous maps were also used to correlate features. The stratigraphy of the ridges east of the river was compared to the stratigraphy recorded by Sirkin and Tuthill (1971), despite their lack of exact location: unfortunately, Sirkin and Tuthill (1971) failed to indicate where along the marsh or ridge their samples were taken. The geomorphic, depositional, and stratigraphic relationships were used to create a series of paleogeomorphic/paleogeographic maps. These maps represent the Katalla River Valley as it may have appeared just before and just after a known megathrust event. The maps will be discussed further in the following sections.

3.4 Historical Archive Search

An historical archive search of Katalla circa 1900-1910 was undertaken for two reasons. The first was to determine how much, if any, the citizens of Katalla changed the landscape as they built multiple railroads, sea breaks, docks, and buildings. The second reason was to understand the short-term effects of the rapid uplift in 1964. What is known about Katalla prior to the Good Friday Earthquake is based upon photos and maps made while the town was thriving. A review of newspapers, photos, and survey maps provided information on the town site that is mostly not available in the scientific literature. It was apparent in the field how quickly the town of Katalla had deteriorated since it was abandoned in the early twentieth century. All that remains are a few foundations, jetty pilings, and railroad beds that are overgrown by trees and brush. This area of Alaska

receives nearly 220 cm of precipitation per year (Boggs, 2000), resulting in rapid growth and decay of vegetation. For example, the 10+ m high trees that we cored were only a few decades old.

Figure 6. Geomorphic map of the Ragged Mountain piedmont over LIDAR DEM hillshade image. Shaded relief LIDAR DEM created with artificial illumination from the southeast. The area in the black circle is the trapazoidal ridge constructed to hold the town of Katalla's reservoir. The area in the black rectangle on Ragged Mountain is shown in greater detail in Figure 13b.

Legend

Quaternary

■ Ocean/Rivers/Lakes/Ponds

Qb Beach

Qut Uplifted Subtidal Terrace

Qbf Boulders

Ql Landslide

Qaf Alluvial Fan

Marsh

Qm

Youngest ←———→ Oldest

Ridge

Qr

Youngest ←———→ Oldest

Man Made Feature

Ragged Mountain Thrust Fault
(with probable extension)

Paleo Sea Cliffs

Glacial Deltas/Channels

Qaf
Qm
Qr
Qaf
Qm
Qr
Ql
Qr
Qut
Qut
Qr
Qb
Qaf
Qm
Lake Kahuntla
Qb
KatallaBay
Palm Point
Qbf
Whale Island
Pacific Ocean
Katalla River

N
1 Kilometer
C.I. = 5m

Figure 7. Aerial photos of the Katalla Valley showing the names of ridges and marshes in the valley and on the Ragged Mountain piedmont. a) Overview photo. Ridges are in white and marshes are in yellow. The orange circle represents the location of the shell bed found by Richards (2000). Areas in black rectangles are shown in greater detail in b and c. b) Location of field sites in Katalla River Valley. Ridge names are in white, marshes are in yellow, core sites in red, and soil pits in blue. c) Location of field sites on the Ragged Mountain piedmont. Ridge names are in white, terrace names in yellow, core sites in red, soil pits in blue, and bedrock outcrop in green.

Photo credit: US Forest Service (early 2000s)
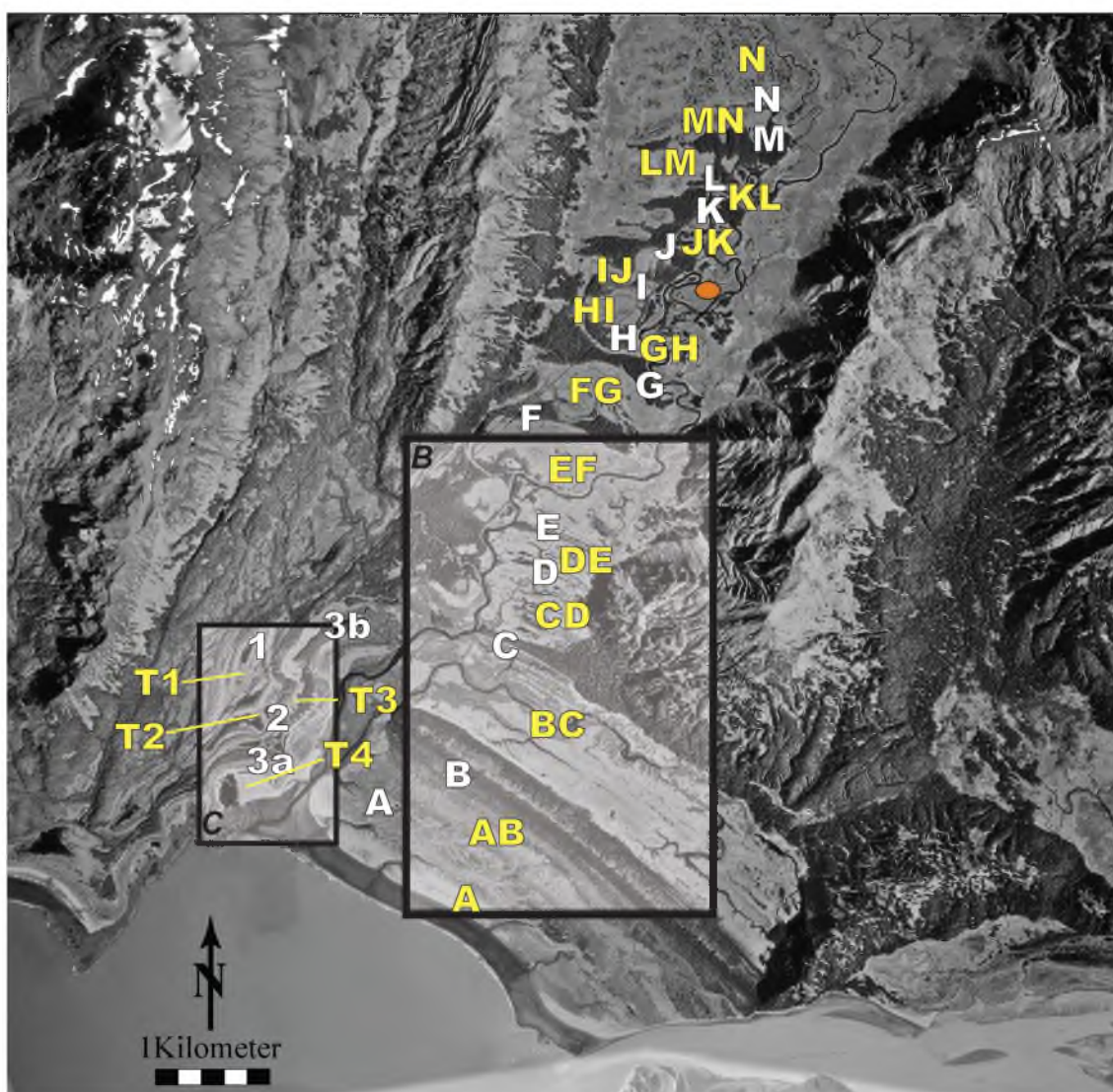
a)
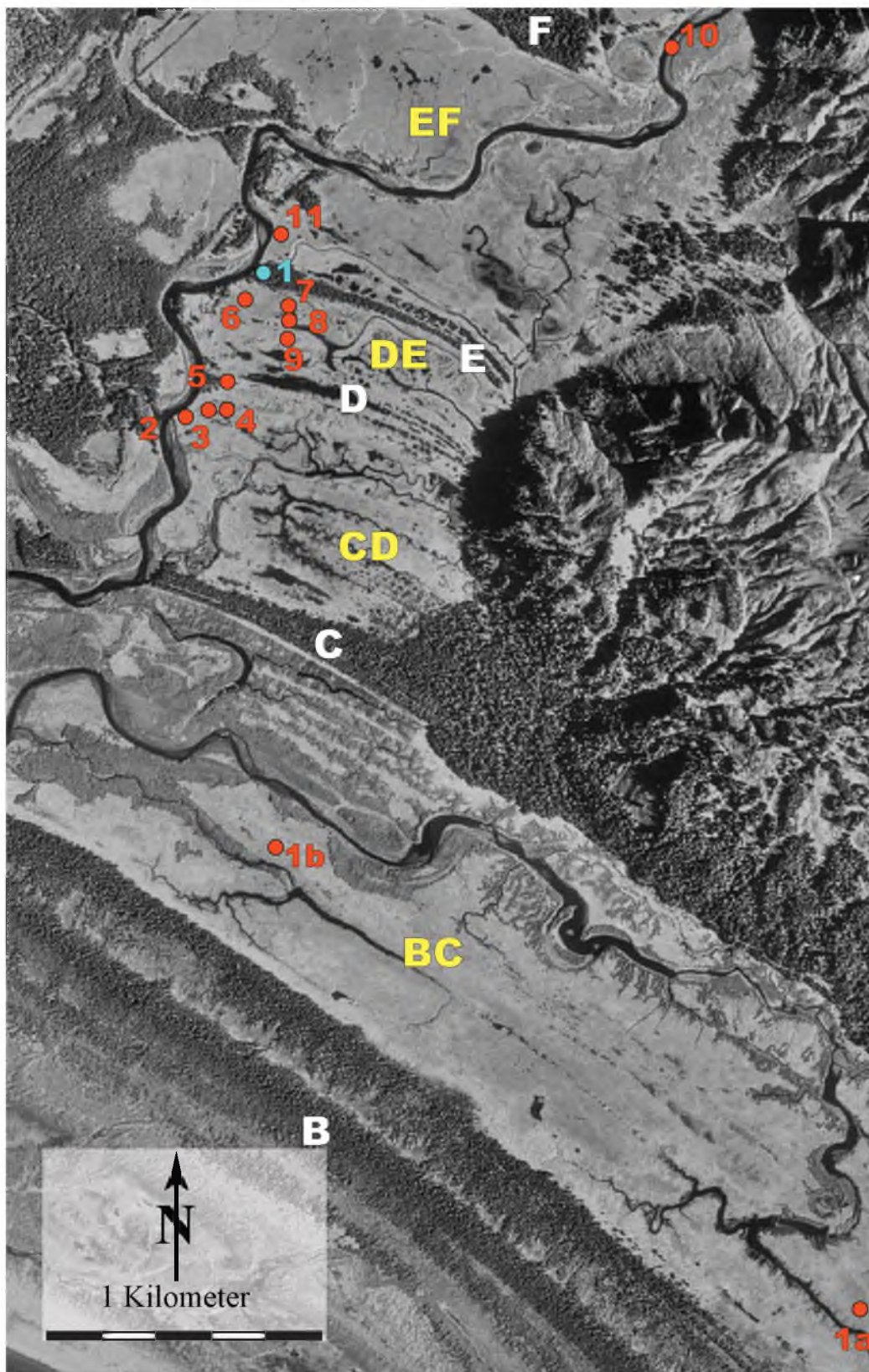
b)

Figure 7 continued
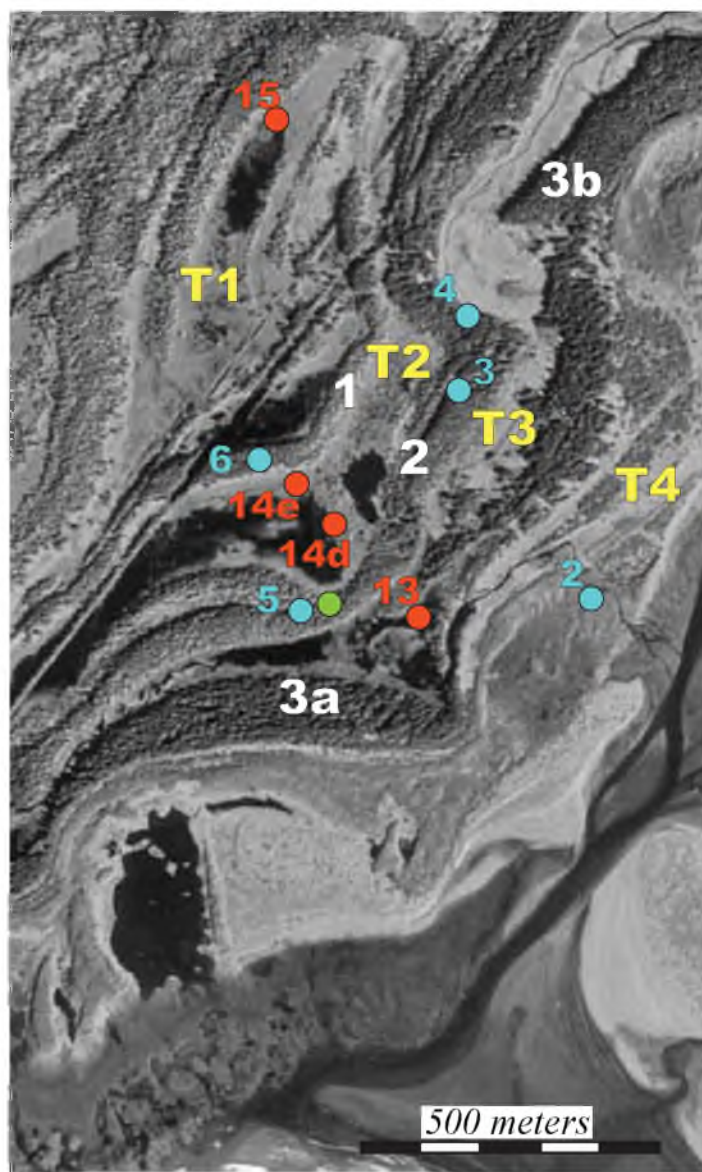
c)

Figure 7 continued

Table 2. Radiocarbon dates from samples taken from cores in 2007 and 2011.

Location	Core sampled	Radiocarbon age±1σBP	Calibrated age, 95% probability range
Marsh BC	[1]Core 1a	510-310 BP	510-310 BP
	[1]Core 1b	550-500 BP	550-500 BP
Ridge C			
Marsh CD	[2]Core 2	1410-1360 BP	1340-1510
		540-520 BP	630-510 BP
	[3]Core 3	730-680 BP	740-660 BP
		730-690 BP	760-680 BP
Marsh DE	[2]Core 6	1160-1210 BP	910-850 BP
		1170-1220 BP	790-690 BP
		1060-980 BP	1120-960 BP
	[4]Core7	430-0 BP	430-0 BP
		310-0 BP	310 BP- 1950 AD
	[2]Core 8	1260-1170 BP	1270-1080 BP
Marsh EF	[3]Core 10	1700-1610 BP	1720-1560 BP
		2000-1950 BP	2060-1900 BP
		2060-1990 BP	2120-1950 BP
		2340-2210 BP	2350-2160 BP
	[3]Core 11	260-20 BP	270-10 BP
		760-700 BP	790-690 BP
		920-800 BP	930-790 BP
Terrace 2	[4]Core 14	2950-2860 BP	2960-2850 BP
		2950-2870 BP	2970-2850 BP
Terrace 1	[3]Core 15	2290-22120 BP	2300-2060 BP
		780-730 BP	790-690 BP
		1530-1420 BP	1540-1410 BP

[1]Dated in 2007 and 2012
[2]Dated in 2012
[3]Dated in 2011 and 2012
[4]Dated in 2011

CHAPTER 4

RESULTS

The Katalla River Valley is located on the coast of Alaska, roughly 35 km

southeast of Prince William Sound (Figure 1). The Katalla River is a meandering river

that runs from the northern end of the valley and drains into the Pacific Ocean. The

northern portion of the river currently flows down the eastern side of the valley, although

remnant meander scars and oxbow lakes indicate it previously flowed through other parts

of the valley. Small tributaries that drain the Don Miller Hills, Ragged Mountain, and the

hills to the north feed the Katalla River. 'Sakung Mountain' is the informal name of the

unnamed mountain east of Ragged Mountain and west of the Katalla River. Clear Creek

runs south between Ragged Mountain and 'Sakung Mountain' before turning sharply to

the east around 'Sakung Mountain' into the Katalla River. The following sections first

describe the Ragged Mountain piedmont followed by the Katalla River Valley (see

Figure 3 for locations).

4.1 Ragged Mountain Piedmont

The piedmont of Ragged Mountain is a terraced slope that rises above the western

side of the Katalla River mouth and bay (Figure 3). Four terraces step sequentially

upwards and inland between the coast and an elevation of ~18 m (Figure 5). Each terrace

is several kilometers long and up to several hundred meters wide, covered by marshes

and small ponds and bordered by narrow cuspate ridges with thick growths of Sitka

spruce and hemlock. The ridges sit atop small cliffs eroded into bedrock at several

localities. Some, but perhaps not all, of the forest is secondary growth as a result of

extensive logging and deforestation of the lower slopes of Ragged Mountain during

building of the town and port of Katalla, including construction of two narrow gauge

railroad lines (Janson, 1975).

The scarps shown in Figure 8 were observed in the LIDAR hillshade images as

long, sinuous lineaments with high relief. These scarps separate some of the terraces on

the piedmont. Their relative ages are based on elevation. A relatively smooth and gently

sloping surface located higher up on the lower flank of Ragged Mountain may also be a

remnant planation surface (Figure 6, Figure 8). Its origin remains speculative because it

was not visited in the field.

The lowest terrace, Terrace 4, is a compound feature that is a wave cut platform

cutting across steeply dipping sedimentary strata of the Stillwater Formation, and a

former tidal slough that is now a freshwater marsh. This terrace formed when tidal lands

were uplifted relative to sea level during the Good Friday Earthquake (Plafker, 1965).

Historical maps of the Katalla town site and port together with vintage aerial photographs

allow precise mapping of the uplifted terrain on the high resolution LIDAR DEM. Parts

of the terrace are still flooded during high tides and winter storms. The western side of

the terrace is bounded by a cuspate shoreline marked by forested ridges, Ridges 3a and

3b, ~2-4 m higher than Terrace 4. Terrace 3 is partly bordered by Ridges 3a and 3b to the

east, and is followed inland by Terrace 2 and Terrace 1, which are occupied by marshes and ponds located at elevations of ~12 m and ~17 m, respectively (Figure 5). The margins of each terrace are sinuous to cuspate shaped forested ridges. The linear segment of the trapezoidal ridge (Figure 6) separating Terrace 2 and Terrace 1 just east of the railroad track beds is not natural, and reflects construction of a small dam that impounded the town site's reservoir.

The four terraces were previously interpreted as uplifted marine platforms, fluvial terraces, and/or glacial abrasion platforms (Kachadoorian 1960; Winkler and Plafker, 1992; Richards, 2000). Although there is no question that Terrace 4 originated by coseismic uplift of the shore zone in 1964, the origins of the other three terraces are less certain. The stratigraphy of the terraces was investigated by hand driven coring in the marshes and excavation of small soil pits on the ridges. Sample sites are shown on Figure 7c and the stratigraphy is summarized in Figure 9. Soil pits dug into ridges revealed gravel and sand with the exception of Pit 6, which is located on part of the embankment that impounded the town's reservoir. The densely packed gravel and clay encountered in that pit may be impermeable fill in the reservoir dam. Gravel and sand in soil pits 5a and 5b directly overlie bedrock of the Stillwater Formation and sit on top of a small cliff at the western edge of Terrace 2. This feature is presumably a relic sea cliff based on the sinuous shape of the terrace margin and the shape of the overlying ridge with gravel and sand that is typical of beach berms in this area.

Cores obtained from the marshes penetrated modern peat overlying gravel, sand or both, with the exception of localities 14 on Terrace 2 and 15 on Terrace 1 (Figure 9). Cores from the marsh on Terrace 3 consisted of mud with rootlets and mud over peat

beneath the sand. Five cores from the marsh on Terrace 2 encountered bedrock directly beneath the peat. The similar depths of refusal in Terrace 2 suggest the presence of a continuous rocky platform at ~1.3 m depth, rather than several dispersed boulders separated by sand and gravel. Core site 15 was located just east of a pond on the surface of Terrace 1 and coring recovered ~1.75 m of organic peat, lake mud, and herbaceous material overlying sand. The thick organic section may reflect the growth and accumulation of vegetation over time as the pond expanded and contracted. Radiocarbon dating was performed on several samples of peat obtained during coring, and revealed age of formation of peat on Terrace 2 to be ~2900 BP and the lake mud on Terrace 1 to be about 2100 BP (Figure 9 and Table 2).

Boulders are located both in the terrace marshes and along the modern coast (Richards, 2000). Individual boulders with diameters in excess of several meters are in the marshes on all the terraces except Terrace 3. The largest boulder on Terrace 4 was 5.8 m and located just inland from the coast above the high tide mark (Figure 10a). A slightly smaller boulder is located on Terrace 2 (Figure 10b). A block of limestone or marble (Richards, 2000) that is 4-5m in length and width is located on Terrace 1. These boulders are little rounded, and the limestone block was not derived from the Orca Group nor Tertiary rocks of the Yakutat Terrane. Smaller boulders in the marshes on Terrace 4 ranged from 0.5 m 3.5 m in diameter (Appendix).

Fields of boulders are distributed over the active shore zone and adjacent edge of Terrace 4 (Figure 11). These boulder fields have little topographic relief and no discernible shape to aid in interpretation of their origin. The field of boulders exposed along the coast south and southeast of Lake Kahuntla (Figure 6) are exposed at moderate

to low tide and are partly rounded by wave action. The rocks are blocks of sandstone, volcanic breccia, granite, granodiorite, schist, granitic gneiss, and quartzite. The granitic and gneissic rocks are exotic blocks that, like the limestone on Terrace 1, are derived from outcrops in the eastern Chugach Mountains and did not originate in the mountains surrounding the Katalla Valley (Appendix).

Historical photographs of the waterfront at the town site of Katalla also reveal many rounded boulders and cobbles exposed at low tide along the western edge of the Katalla River mouth and bay. These boulders are now partly to totally covered by soil and vegetation on Terrace 1 following uplift relative to sea level during the earthquake in 1964.

The huge and isolated boulders located in the marshes must be glacial erratics deposited by glaciers circa 10 ka. The origin of the boulder fields is more difficult to ascertain given the lack of form and topographic relief. Some of the boulders along the coast southeast of Lake Kahuntla may be from a large jetty or 'sea wall' that was built out from the point into the mouth of Katalla Bay for protection from ships. The jetty was built using rocks from a nearby quarry but was destroyed by severe storms shortly after it was completed (*Katalla Herald*, 1907; Janson, 1975). However, the many exotic blocks of plutonic and metamorphic rock suggest that glaciers transported the rocks southwards out of the Chugach Mountains. If the concentrated boulder deposit formed as a moraine then it, like the man-made jetty, was totally destroyed by wave action. An alternative process is ice rafting of boulders along the coast to form a concentrated field of drop stones, which were then partly rounded by wave action when uplifted through wave base.

Other remnant glacial features are located on Ragged Mountain. Possible glacial deltas and outwash channels are shown in Figure 6. The deltas are broad, relatively flat surfaces on the piedmont at the end of a glacial-cut, U-shaped valley. The channels are located on the western side of 'Sakung Mountain'. They were interpreted as such because of the way they cut across the mountain, as opposed to flowing down perpendicular to the valley as on the eastern side of 'Sakung Mountain'. These remnant channels and deltas were only observed on the LIDAR, and not visited in the field. Therefore, other origins are possible.

Streams, creeks, lakes, and ponds are on all four terraces as well as farther up on the Ragged Mountain (Figure 6). The lakes and ponds form in the lowest parts of the marsh, but appear to be ephemeral. Maps and vintage aerial photos show the locations and shapes changing through time. The pond on Palm Point as well as the largest pond on Terrace 2 are man-made features remnant of Katalla Town (Figure 6). The streams on the terraces serve to transport water throughout the marshes and to and from different terrace levels. Many streams on Ragged Mountain, however, are entrenched which indicates a relative drop in base level. When there is a drop in base level, a stream or river is no longer at equilibrium. To accommodate this change, the stream will incise its streambed (Keller and Pinter, 1996). This is most obvious on streams highlighted on Ragged Mountain, but also occurs on the Clear Creek Fan and in the Katalla River (Figure 6). Although the Katalla River is a meandering river, it is also relatively incised in its channel. According to Richards' (2000) GPS elevations, the Katalla River level is anywhere from 2-5 m below the marshes and ridges. The down cutting indicates that the

area underlying these streams and creeks was uplifted relative to the river's base level (Keller and Pinter, 1996).

An unnamed stream on the southern end of Ragged Mountain is not only entrenched, but has an asymmetric transverse channel profile (Figure 12). The riverbank is steeper to the south, and there is a small terrace on the northern bank. This geomorphology may indicate a tilting toward the south (Keller and Pinter, 1996). However, there is not enough evidence to show whether tilting affected only the Ragged Mountain block or the entire region underlying the Ragged Mountain piedmont and the Katalla River Valley.

The Ragged Mountain fault was not directly observed in the field, but LIDAR data were used to make hillshade images. These high-resolution images show the fault in very fine detail and display features related to the fault. The fault is ~30 km long, runs roughly parallel to the Katalla River Valley, and dips to the west (Figures 3 and 4). Three point solutions calculated from the LIDAR data and field observations by Tysdal *et al.* (1976) yield dips less than 10°. On the southern end, the fault scarp appears just north of Lake Kahuntla. The scarp height is as much as 40 m over a distance as little as 26 m. The height may be even greater, but talus and landslide debris fill the depression at the foot of the scarp and likely obscure its true height.

The fault scarp appears to end at Lake Kahuntla although there is evidence that it is buried in lake sediment and may extend off the coast. LIDAR data show a slight increase in elevation toward the east across Lake Kahuntla, which is consistent with the scarp morphology on Ragged Mountain. The increase is only on the order of centimeters,

and occurs in and around vegetation that did not get filtered out of the LIDAR data. Therefore the increase may just be an artifact of the postprocessed data.

Although the scarp appears to indicate normal offset, the bedrock geology suggests otherwise. The Katalla Valley is in a convergent zone as opposed to an extensional setting. The juxtaposition of older rocks on top of younger rocks also implies a thrusting relationship (Winkler, 1993, Plafker, 1994). However, the scarp itself is clearly extensional (Figure 13a). The convex and uphill facing characteristics of the fault indicate that the Orca Group in the hanging wall moved westward relative to the Stillwater Formation in the footwall. Offset of landslide deposits emplaced after glacial retreat records normal-sense movement across the fault since about 10 ka (Figure 13b). Tysdal *et al.* (1976) measured trees and soil profiles on landslides transected by the fault and determined that the fault has not ruptured in the last 100-150 years. There is conflicting evidence concerning large-scale extension verses local extension in the upper plate of the thrust fault. Trenching done along the middle of the Ragged Mountain Fault in the early 2000s showed evidence for reverse fault splays (R. Bruhn, pers. comm., 2013). One hypothesis speculates that as the footwall is thrust beneath the hanging wall, the hanging wall "folds over" the boundary, making the scarp appear to be extensional. However, one would expect some evidence of the thrust boundary below—or in this case east of—the extensional scarp. There is no evidence for a thrust fault east of the Ragged Mountain fault scarp. The offset landslide combined with the lack of thrusting evidence leads to the conclusion that the Ragged Mountain fault is extensional.

The vertical offset of the Ragged Mountain fault scarp is as much as 20 m. This gives a rudimentary rate of vertical movement along the fault of 20 m per 10,000 years or

2 mm per year. Tysdal *et al.* (1976) estimated 180 m of horizontal displacement over the last 12,000 years or 15 mm per year, which is a reasonable heave estimate if the dip of the fault is truly less than 10°. The mechanism for extensional movement is poorly understood; however, it is possible the mountain block is sliding back in response to uplift in the valley.

No other faults mapped by Winkler and Plafker (1993) (Figure 4, this publication) were examined in the field or on the LIDAR. Paleogeographic analysis determined that there is no offset along the terraces on the Ragged Mountain piedmont, indicating that the Clear Creek fault has not ruptured in the last 7000 years.

4.2 Katalla River Valley

The Katalla River Valley refers to the entire area between the Don Miller Hills and 'Sackung' Mountain as well as the region east of the Katalla River mouth and bay (Figure 3). The Katalla River Valley consists mainly of freshwater marshes separated by elevated ridges and ranges in elevation from sea level to ~20 m above sea level. The ridges range from >500 m wide to <10 m, and are covered in Sitka spruce and hemlocks. The freshwater marshes are several kilometers wide and are drained by the Katalla River. Many small lakes and ponds also cover the marshes. The ridges in the southern half of the valley are arcuate in shape and are roughly parallel to the present-day shoreline. The northern ridges are primarily on the western side of the valley and become less cuspate to the north. Large, abandoned meanders cutting through these ridges indicate that the Katalla River reworked them at some time.

There are many abandoned channels and oxbow lakes on the marshes in the Katalla River Valley, as well as many small ponds connected by streams in the northern part of the valley. Landslides and alluvial fans rim the valley where the marshes meet the Don Miller Hills, 'Sakung Mountain' and the hills to the north. These sediment inputs may affect the elevations of the marshes and the rivers, as well as the stratigraphy. Alluvium sourced from these mountains is easily reworked by streams flowing through the marshes toward the Katalla River, and is considered when discussing the depositional setting below (see Figure 14 for locations). Richards (2000) interpreted the lower ridges in the Katalla River Valley as remnant beach berms based on their stratigraphy. However the profile of the ridges do not resemble modern-day beach berms. The ridges are much broader and more symmetrical. For example, Ridge B is greater than 500 m wide and is about 5 m high from base to crest. The commonly accepted definition of a berm, however, is a sand body that runs parallel to the shoreline and has a more steeply dipping seaward slope than landward slope. Berms are also generally no higher than one meter (Jensen 2009).

For the purposes of this section, the term berm will be used to describe an elevated ridge that was deposited as either a series of amalgamated beach berms, spits, or barrier bars. The specific origin of each ridge cannot be conclusively determined without an in-depth study of the sedimentary structures within the ridge.

4.2.1 Coast to Ridge C (Figure 15)

The lowest marshes, Marsh A and Marsh AB, are heavily influenced by the Pacific Ocean and are likely brackish marshes. No field investigations were done of these

marshes, but historical maps and studies show that they were uplifted from below sea level during the 1964 earthquake. Ridge A was described by Richards (2000) as sand and gravel. Ridge B has a composition similar to A. Both Richards (2000) and Sirkin and Tuthill (1971) interpreted these ridges to be either a spit or berm that was later uplifted to become a ridge.

Marsh BC was cored in 2007 (Cores 1a and 1b). Each core contains sand sharply overlain by peat. The peat layer is overlain by silt and clay, which is sharply overlain by modern peat. The lowest contacts between the sand and peat were sampled for diatom and radiocarbon analysis (I. Shennan, pers. comm., 2012). Sirkin and Tuthill (1971) described a core from this marsh containing beach sand overlain by sedge peat. Diatoms in the lowest sands indicate that Marsh BC was a tidal inlet or brackish marsh prior to being uplifted above sea level around 500 BP. Gradual subsidence followed the uplift event, giving way to the tidal slough shown in photographs taken prior to 1964 (Alaska Historical Archive). The slough was elevated above sea level in 1964 and is currently a freshwater marsh.

According to Richards (2000), Ridge C is comprised of marine sand deposits. Sirkin and Tuthill (1971) described sand overlain by clay, peat and gravel, and another layer of peat. Ridge C was originally deposited as a sandy spit. After progressive uplift the spit became a storm ridge, protecting Marsh CD to the north. Storm gravels were deposited on top of the spit. Eventually, peat was able to form once Ridge C was no longer being directly hit with storms. Woody peat located in Ridge C was dated at 1230±90 BP (Sirkin and Tuthill, 1971).

4.2.2 Marsh CD to Ridge D (Figure 16)

Three cores—Core 2, Core 3, and Core 4—were removed from Marsh CD. Each core contained two sequences of muddy sand sharply overlain by peat. The lowest contact between sand and peat in Core 2 was extracted for analysis. Marsh CD was uplifted at least three times. The diatoms located in the transition between sand and mud in Core 2 indicates uplift from a beach environment to a tidal slough or brackish marsh around 1500 BP. The first mud-peat couplet represents an abrupt change in environment from marine to freshwater around 700 BP. The mud overlying the peat in each core represents a gradual sea level rise. This is likely due to local subsidence. The second sharp contact of peat indicates Marsh CD was once again uplifted above sea level, allowing a freshwater environment to form. The data taken by Sirkin and Tuthill (1971) also agree with this interpretation.

Core 5 was taken in Ridge D. The core consisted of sand overlain by clay topped by peaty topsoil. No samples were taken from this core. The description of Ridge D by Richards is similar to ours, but Sirkin and Tuthill (1971) described it slightly differently. Their data show peat intermixed with sand and gravel at the base, overlain by clay and gravel. The gravel is overlain by peat and muskeg. The differences in observations are likely due the location of the cores and pits. Our data come from the crest of the ridge, but different sediment would be observed if the pit were located on the seaward or landward side of the ridge. All of the observations support the interpretation that the ridge was formed by marine influences—similar to Ridges A, B, and C. It likely started out as a spit or sand bar, and after an uplift event became a storm berm. A later uplift event placed it above storm levels, and it was able to support freshwater flora.

4.2.3 Marsh DE to Ridge E (Figure 17)

Four cores were taken from Marsh DE. In general, all of the cores contain sand overlain by mud and clay, sharply overlain by peat. All four cores were taken out of the field for further analysis. Diatom analysis of the sand-mud contact shows a transition from lagoon deposits to intertidal deposits. Sirkin and Tuthill (1971) observed similar stratification. They described silty clay overlain by peat. Similar to Marsh CD, Marsh DE was a prograding shoreline that underwent abrupt transitions, most likely due to uplift events. Subsidence around 1100 BP caused the transition from a lagoon to intertidal slough. The intertidal deposits were abruptly uplifted to a freshwater marsh ~900 BP. The interbedded peat and clay in Core 8 may represent a time of migration of the tidal inlet or freshwater ponds.

A soil pit was dug into Ridge E. The pit contains laminated sand overlain by pebbles and clay, which is in turn overlain by gravel, sand, and sandy soil topped with peat. Richards (2000) observed sand and gravel in Ridge E. Sirkin and Tuthill (1971) recorded gravel interspersed with thin clay and organics, overlain by peat. The differences in these data are also due to do the location of the pits. Ridge E is an uplifted beach berm.

4.2.4 Marsh EF to Ridge F (Figure 18)

Two cores were taken in Marsh EF. Each core contains some sand overlain by interbedded peat and mud. Marsh EF is a tidal slough that was uplifted enabling freshwater peat to form around 2600 BP. The area subsequently underwent gradual subsidence followed by another uplift event around 2100 BP. The alternating layers of

peat and mud and muddy peat suggest that there were alternating periods of seawater and freshwater dominance. Overbank flooding of either the Katalla River or the Katalla Bay is also a possibility. The peat on top shows that the area remained above seawater influence since around 900 BP. Both cores were taken out of the field for further diatom and radiocarbon analysis.

Sirkin and Tuthill (1971) also observed sand, clay, and peat in Marsh EF. They observed a much thicker layer of modern peat, but their core likely came from the marsh itself whereas our cores came from the riverbank and the river. The age of formation of this peat is ~3510 BP, much older than any of the 2007 and 2010 samples. It is difficult to determine whether or not this is the true age of the peat, or if it is due to the relatively primitive dating methods at the time. In 1971, radiocarbon dates were determined using bulk samples. Older organic material may have washed into this peat layer at the time of deposition, causing it to appear much older than it actually is.

The ridges and marshes north of Marsh EF were not examined in the 2010 field season, and therefore, data from Richards (2000) and Sirkin and Tuthill (1971) are used exclusively to determine paleo-environments.

Ridge F is comprised of fluvial, marine, or glacial gravel (Sirkin and Tuthill, 1971). Richards (2000) interpreted it to be deposited by melt water from the Stellar and Bering Glacier.

4.2.5 Marsh FG to Marsh IJ (Figure 19)

Marsh FG is composed of peat with grey clay and sand at the base, overlain by muskeg (Sirkin and Tuthill, 1971). The grey clay and sand most likely indicate a tidal

slough environment, overlain by a freshwater environment. It is unclear whether or not the boundary is sharp, so it is not possible to infer an abrupt uplift event at this location. Another interpretation is that the sand may be from a freshwater lake or pond in the marsh, and Marsh FG was not below sea level at the time of deposition. A conclusive interpretation cannot be made without analysis of the diatoms in the sand. The depositional environment of Marsh FG determines that of Ridge F. That is, if Marsh FG was below sea level at some point, then Ridge F was likely deposited as a sand bar and/or storm berm. However, if Marsh FG was never below sea level, then Ridge F represents reworked river and glacial gravels.

Ridge G is also composed of possible fluvial, marine, or glacial gravel (Sirkin and Tuthill, 1971; Richards, 2000). Marsh GH was not studied.

Ridge H comprises thinly bedded gravel and fine-grained sand. Marsh HI is mostly peat with gravel at the base (Sirkin and Tuthill, 1971). The gravel at the base of the peat may be fluvial, marine, or glacial in origin (Richards, 2000), and radiocarbon dating shows the peat was formed ~4000 BP (Sirkin and Tuthill, 1971). As with the previous marshes, it is uncertain if this is the correct age or not. The geomorphology of the marshes and ridges in the northern part of the valley clearly changed with the migration of the Katalla River, so it is difficult to infer any specific depositional setting.

Ridge I is made primarily of muskeg (Sirkin and Tuthill, 1971). A mud layer with articulated shells is located east of Ridge I in the Katalla River (Richards, 2000). The shells are marine in origin, likely subtidal to intertidal (A. A. Ekdale, pers. comm. 2012), and deposited ~7000 BP (Richards, 2000). Marsh IJ is similar to Marsh HI—gravels at the base of peat (Sirkin and Tuthill, 1971). Origin of Ridge I cannot easily be determined

based on stratigraphy, but is likely the same as Ridge H. The presence of marine shells suggests that Marsh HI and Marsh IJ were below sea level at some time, and the gravels may possibly be marine in origin. If sea level was as far north as Marsh IJ, then Marsh FG and Marsh GH were under water at that time as well.

4.2.6 Ridge J to Ridge L (Figure 20)

Ridge J contains alternating seams of gravel and sand followed by modern peat (Sirkin and Tuthill, 1971). Richards (2000) interprets Ridge J to be glacial outwash or reworked till. Sirkin and Tuthill (1971) observed interbedded marine clay and shells, overlain by sand, gravel, and peat. Radiocarbon dating of shells in Marsh JK indicates they were deposited around 7000 BP (Sirkin and Tuthill, 1971). However, Sirkin and Tuthill (1971) also claim that the peat began forming ~10,700 BP and the clay gave an age of ~14,000 BP. The age of the shells is likely the more accurate because it was determined using only shell material rather than bulk sediment. It is also similar in age to the shells found and dated by Richards (2000). The apparent ages of the peat and marsh are likely due to older material being washed in at the time of deposition.

Richards (2000) interpreted Ridge K to be possible glacial outwash or reworked till. Marsh KL is composed of interbedded sand and gravel overlain by clay. The clay is overlain by muskeg (Sirkin and Tuthill, 1971). Sirkin and Tuthill (1971) interpreted the first layer of gravel to be fluvial, and the second layer of sand to be marine. This marsh has a relatively high amount of gravel, and was likely heavily influenced by glacial outwash or alluvium from Clear Creek. Ridges north of Marsh KL are oriented roughly north to south at a high angle to ridges farther south. It is possible they were not

deposited as separate ridges, but as a hooked spit. A hooked spit is one that forms parallel to the bay, as opposed to forming across the bay mouth. As sediment was being deposited into the Katalla Bay by Clear Creek, a delta formed. Wave action from the southeast eventually transported the sediment north in a spit parallel to the valley walls. Similar processes were observed in Washington, Germany, the Netherlands, and Massachusetts among others (Hine, 1979; van Heteren *et al.*, 2006; Lindhorst *et al.*, 2010; R. Bruhn, 2012 pers. comm.). Later, the Katalla River slightly reworked the spit, evidenced by the meander scars in these marshes. According to Sirkin and Tuthill (1971), Ridge L is similar in composition to Ridge J.

4.2.7 Marsh LM to Marsh N (Figure 21)

The core from Marsh LM contains peat with gravel at the base overlain by sand, which is in turn overlain by muskeg. The peat apparently began forming around 2400 BP, according to radiocarbon dating by Sirkin and Tuthill (1971) but given the age of the shells in marshes further south, the peat is likely much older. The origin of this marsh is interpreted to be similar to Marsh KL.

Richards (2000) interpreted Ridge M as possible glacial outwash or reworked till. Marsh MN was not studied. Ridge N is the northernmost ridge and was interpreted to be a reworked gravel bar or glacial outwash (Sirkin and Tuthill, 1971; Richards, 2000). Marsh N contains sandy peat with sand at the base. The sandy peat is overlain by a variety of herbaceous peat. Radiocarbon dating of the peat shows it is 6500 years old. This is a reasonable age of formation of this peat for this location, but based on the inaccuracies at other locations, this date may also be due to contamination (Sirkin and

Tuthill, 1971). The sand at the base of this deposit suggests that there was possibly a marine influence as far north as Marsh N.

Richards (2000) interpreted the ridges north of HI to be of glacial or fluvial origin. However, the presence of possible marine clay indicates that sea level may have reached as far north as Marsh N. Therefore, we propose that these ridges are marine in origin, but there are two possible depositional interpretations. The first is that they were originally deposited with cuspate shapes similar to Ridges A through H. The Katalla River subsequently meandered through the northern half of the valley, reworking and redepositing the sediments in linear ridges. The second alternative is that these northern ridges were all deposited as part of a hooked spit system that originated from the Clear Creek delta.

Figures 22a and 22b are provided to summarize the stratigraphic descriptions discussed above and show how the stratigraphy of the marshes and ridges change or stay the same from the lowest elevations to the highest. In general, the marshes consist of sand or mud overlain by peat, and the ridges are gravel or sand and occasionally are overlain by peat. This pattern suggests the ridge-marsh sequences were each deposited in a similar way. The paleogeography discussed below explores the deposition of the ridges and marshes in more detail.

The geomorphic observations and geochronologic data are used to reconstruct the paleogeography and tectonic history of the Katalla area. These new data, when combined with data and results from earlier studies (Plafker, 1965; Karachadoorian, 1960; Sirkin and Tuthill, 1971; Richards, 2000), allow us to develop a series of paleogeographic maps showing the evolution of the Katalla Valley and coast during the last 7000 years.

4.3 Relationship between Ragged Mountain Piedmont and

Katalla River Valley

The marshes and ridges of the Ragged Mountain piedmont and Katalla River Valley are similar both in shape and underlying stratigraphy. The ridges are former beach berms and coastal spits that were shaped by wave action and long-shore currents. Evidence for foreshore to beach deposition include the sinuous to cuspate forms of the ridges in map view, relatively narrow widths to lengths of the berms, modest topographic relief, and the underlying sorted deposits of sand, pebbles, and gravel.

The berms are correlated between the piedmont and valley using similarity in elevation and shape, new constraints on age from radiocarbon dating, and the spatial alignment of ridges where projected across the Katalla River. The high quality and sub-meter vertical resolution of the LIDAR DEM when combined with Richards (2000) high-resolution GPS station elevation measurements from the valley floor greatly enhances our ability to correlate ridges from the piedmont to the valley east of the Katalla River.

The lowest two ridges are easily correlated across the valley on shape alone, but Ridge 1 was more difficult to match. Correlation of Ridge 2 with Ridge C requires Ridge 1 to have formed prior to Ridge C. Lake sediments on Terrace 1 were apparently formed ~2100 BP, similar to the age of the second peat horizon in Marsh EF. However, the sand in Terrace 1 was not necessarily deposited in a marine environment, so the terrace may have been above sea level prior to the mud formation. The elevation of Ridge 1 suggests that it corresponds to ridges in the northern part of the Katalla River Valley. The northernmost constraint is Ridge I, which contains shells dated at 7000 BP, nearly 5000

years older than the lake mud. Ridge 1 is likely to correlate with Ridge F, G, H, or I, but a more precise correlation is not possible (Figure 23).

The interpretation is that each berm was deposited by wave action and then abandoned when the coast prograded seaward and relative sea level dropped. At some localities, two or more berms either merge together or bifurcate by several meters to tens of meters. These berm complexes are roughly the same age and may represent a series of both shallow foreshore and shoreline berms that were partly merged during storms. The berms on the piedmont were deposited along the edges of wave-cut and/or glacially abraded platforms that are partly bounded by sea cliffs up to several meters high. The platforms, some of which are cut into bedrock, probably became the sites of small sloughs prior to emergence above high-high tide following uplift.

The berms in the valley developed as the shoreline prograded southward during infilling of the estuary. The berms are separated by marshes underlain by marine and fluvial deposits, with intercalated peat layers. Old meander scars and oxbow lakes in the northern part of the valley mark localities where estuary fill was eroded and reworked by the river prior to establishment of its present course. Alluvial fans and landslides fringe the margins of the river valley; the largest fan is located at the mouth of Clear Creek (Figure 6). Clear Creek supplied sediment that partly filled the estuary as the coast migrated southward. Some of this sediment presumably formed a sharply hooked spit that extended along the western side of the estuary, and was subsequently reworked by waves and fluvial processes.

4.4 Relationship to Known Megathrust Events

The radiocarbon dates were most useful when relating the history and geomorphology of the Katalla area to known megathrust events. Previous studies show that there were at least five megathrust events along the eastern portion of the Aleutian Subduction zone—1964, 900 BP, 1500 BP, 2100 BP, and 2600 BP (Hamilton *et al.*, 2005; Hamilton and Shennan, 2005; Carver and Plafker, 2008; Shennan *et al.*, 2009). The Katalla Valley was also uplifted during these megathrust events, as evidenced by the radiocarbon dates taken from the field in 2011 (Table 2).

The deformation caused by the Good Friday Earthquake was documented in field studies immediately following the earthquake. The Katalla area was uplifted as much as 2 m during this event. (Plafker,1965).

Cores taken from Marshes CD, DE, and EF were uplifted ~930-790 BP. This corresponds with megathrust events documented by mapping and coring of marshes at Anchorage, Girdwood, Alaganik Slough, Turnagain Arm, Puffy Slough, Cape Suckling, and Yakataga (see Figure 1 for locations). Marsh CD was also uplifted ~1510-1340 BP, at the same time sites in Anchorage, Girdwood, Alaganik Slough, and Turnagain Arm were coseismically uplifted or subsided. Marsh EF was uplifted ~2120-1950 BP and ~2650-2350 BP. This roughly corresponds to uplift events documented in Cook Inlet and Turnagain Arm (Hamilton *et al.*, 2005; Hamilton and Shennan, 2005; Carver and Plafker, 2008; Shennan, 2008; Shennan *et al.*, 2009). The timing of uplift events at Katalla show that this area was uplifted by the same megathrust events recorded elsewhere in southern Alaska (Table 1).

4.5 Evidence for a 500 BP event

One documented uplift event in Katalla does not correlate with a known Holocene earthquake. Marsh BC was cored in 2007 and the contact was dated at ~550-500 BP. No other field sites along the southeastern coast of Alaska were uplifted at that time. The samples were dated again in 2011 to confirm the results. This anomalous date suggests that there is a local structure that moved at least somewhat independently of megathrust events underneath the Katalla Valley. The structure must be relatively small because it did not affect Puffy Slough, eight kilometers to the east, or Alaganik Slough, 60 km to the west (Figure 1). It is possible that this structure ruptured more than once prior to 500 BP, but the evidence of uplift may be masked by younger and larger megathrust events.

4.6 Paleogeographic Reconstructions

The geomorphology of the Katalla area, along with the stratigraphy of the cores and dates of uplift, were used to reconstruct the geography since ~7000 BP when the shoreline was located near the head of the valley based upon the presence of marine mollusk shells (Richards, 2000). A series of paleogeographic maps help to visualize the change, which leads to understanding the structural forces working on the valley.

4.6.1 1964-Present

The Good Friday Earthquake not only changed the elevation of the landscape but also altered the geomorphology and vegetation (Boggs, 2000). The extent of uplift in the region can be inferred from the distribution of "uplifted marshes" in Figure 24.

The geomorphology surrounding Katalla includes landforms associated with alluvial fans, landslides, boulder fields, lakes, streams, and faults (Figure 25). Marsh deposits cover former alluvial floodplains and marine terraces that are separated by former beach ridges. The relative age of the terraces and ridges are shown by shades of brown and green, respectively, with the lightest color being the youngest, and the darkest being the oldest. The tidal range in the area can be as much as 6 m, and tidal influence extends far up the Katalla River (NOAA).

The geomorphology map is used as a base for the paleogeographic reconstructions. Much can be ascertained about the depositional environments in Katalla by highlighting depositional features and vegetation. Pre-1964 documents provide an historic reference that is useful when evaluating geomorphic changes due to uplift and human influence.

4.6.2 1900-1964: The Katalla Case Study

The town of Katalla was founded in the early twentieth century in response to a coal discovery north of the valley (Janson, 1975). Two competing railroad companies brought in many workers in the hopes of reaching the coal first. In its prime, 1907-1908, the town of Katalla had about 5,000 residents. During this time, the landscape was well documented by town site engineers, geologists, photographers, and journalists. These historical records illustrate precisely how the region looked prior to the 1964 earthquake. They also record human alteration of the landscape.

The most noticeable difference of the Katalla Valley from pre-1964 to now is the location of the coastline and the tidal influence (Figure 26). The coast on the western side

of the Katalla Bay moved by as much as 400 m to the east, and the shore in front of

Ridge B prograded nearly 900 m south since the Good Friday Earthquake. The mouth of

the Katalla River used to be a large bay. Records show that the bay was deep enough to

land ships until 1899, when an earthquake uplifted the landscape. The only major

earthquake that occurred at this time was the 1899 Cape Yakataga Earthquake. Although

most scientific records do not show the deformation front to reach as far north and west

as Katalla, it is mentioned in an issue of the Katalla Herald (Janson, 1975). Historic maps

and photographs also show that Marsh BC was a tidal slough, although presently it is a

freshwater marsh (Figure 26). There was also a tidal inlet between Ridges 1 and 2 on the

Ragged Mountain piedmont that is now a freshwater marsh. These changes show that

coseismic uplift causes rapid progradation of the coast, and an accelerated change from

brackish water to freshwater environments. There are currently no tidal sloughs or inlets

in Katalla, despite their presence prior to 1964. This is likely because interseismic

subsidence has not yet allowed low-lying areas of the Katalla Valley to be inundated with

seawater. Although coseismic uplift exceeds interseismic subsidence in Katalla,

subsidence is documented in cores up valley. Some interseismic subsidence is necessary

for the formation of tidal sloughs and inlets. There is no evidence of movement across the

Ragged Mountain fault during the 1964 earthquake.

Figure 27 is an idealized cross section of an uplifted berm/marsh sequence from

Boggs (2000). The cross sections illustrate how much the vegetation is affected by a

large-scale megathrust event over time. Uplift immediately creates new surface area for

freshwater and saltwater-tolerant plants to inhabit. It also allows some types of soils and

sediments to drain, enabling less water-dependent plants to take root. Interseismic subsidence has the opposite effect on the flora.

The following paleogeographic reconstructions are presented from oldest to youngest in order to visualize how the coastline prograded south through time.

4.6.3 10000 BP-2100 BP

Glaciers in the Katalla area retreated ~10,000 BP (Fleisher, 1999). During the advance and retreat of the glaciers, a broad, flat platform was cut into the Stillwater Formation and possibly the Poul Creek Formation on the eastern side of the valley. Outwash channels were carved into the western side of 'Sakung Mountain' and glacial deltas were deposited between Ragged Mountain and 'Sakung Mountain'. The Pacific Ocean may have reached as far north as the head of the valley following glacial retreat. Once megathrust event cycles began, relative sea level dropped and continued to drop since. The presence of marine mollusks near Ridge I indicate that tidal influence reached at least as far north as that ridge. There are three possible interpretations of deposition in the northern Katalla Valley. The first, proposed by Richards (2000), is that ridges are remnant glacial till that was reworked by the Katalla River. The second is that ridges were marine in origin and were deposited parallel to the present-day shoreline, and were subsequently reworked by the Katalla River. The third is that they were all of the same ridge system that formed on a hooked spit (Figure 28a). There is no way to tell whether the last two hypotheses are correct without a thorough stratigraphic analysis. The first hypothesis is unlikely though, based on the marine shells far north in the valley.

Between 7000 BP and 2600 BP, the valley prograded south, although the exact mechanism for this progradation is unknown. Prior to 2600 BP, the Katalla River was likely an established meandering fluvial system and the ridges and marshes north of Ridge F were above sea level.

Around 2600 BP, a megathrust event elevated Marsh EF above sea level long enough for intertidal peat to form on top of it (Figure 28b). Gradually, sea level rose (Figure 28c), but the area was uplifted again ~2100 BP (Figure 28d). During the times that Marsh EF was above sea level, Ridge E was the active berm. When these areas were submerged, Ridge F was the active berm, and Marsh FG was the back beach. The amount of uplift is difficult to determine, but a minimum can be estimated using the diatoms in the sample. The 2600 BP event caused uplift from an intertidal slough to a freshwater peat marsh. The Good Friday Earthquake in 1964 also uplifted an intertidal feature—the Katalla Slough—to a freshwater peat marsh, and the amount of uplift was 2 m. Two m is a reasonable minimum estimate for amount of uplift during both the 2600 BP event and the 2100 BP event. The amount of subsidence that occurred interseismically was similar since the 2100 BP event lifted the same area as the 2600 BP event. Therefore, net uplift at this time was zero.

4.6.4 1500 BP-900 BP

The 1500 BP megathrust event raised the Katalla Valley above sea level as far south as Marsh CD (Figures 29a and 29b). Ridge C transitioned from a spit to storm ridge, and Marsh CD went from marine to a tidally influenced lagoon or back beach. The amount of uplift caused by this event is difficult to determine, as there is no evidence

how far below sea level Marsh CD was prior to uplift. Between 1270-1080 BP, relative sea level gradually rose, submerging Ridge C and allowing Ridge D to form (Figure 29c). Sea level continued to rise until Ridge E became the active berm, and Marsh EF the lagoon. The gravel in Ridge D was likely sourced from Clear Creek and its fan, and was reworked into the spit. The amount of interseismic subsidence was greater than coseismic uplift during this time period, and therefore net uplift is less than zero.

4.6.5 900 BP- AD 1950 BP

The megathrust event at ~900 BP is the last recorded megathrust event prior to 1964. This large uplift event raised Marshes CD, DE, and EF above sea level (Figure 30a). Marsh CD became either a lagoon or a freshwater marsh at this time; the diatom evidence is not strong either way (Shennan, 2012, pers. comm.). Marshes DE and EF were dominated by freshwater. The amount of uplift was at least 2 m. Sediment from a large landslide or alluvial fan on the Don Miller hills continued to build Ridge C. This spit may have extended much farther to the west than its present-day position. It is clear that the Katalla River transects it now, but the presence of more than one large meander scar suggests that the river travelled around the ridge at some point. After the uplift at 900 BP, Marsh BC was most likely a beach environment. It is also possible that Ridge B even started forming at this time, given the southern protrusion of the Don Miller Hills, but the sea floor may have been too deep for a spit to take hold.

Ridge 3b on the Ragged Mountain piedmont side of the study area was deposited at the same time as Ridge C, and is part of the same spit system. Although there are no stratigraphic data from this ridge, the elevation of the base of the ridge is the same as

Ridge C, and the shape of the two ridges suggests that they were probably connected. Ridge 3b may have extended as far south as Ridge 3a, but the sediment was reworked during the building of Ridge 3a. The trees that "connect" the two ridges are all younger than Katalla Town and the area was below sea level prior to the 1964 earthquake, indicating that these two ridges are not actually connected. This is evidenced in maps and photos made prior to the Good Friday Earthquake. Net uplift during this time period was greater than zero.

The 500 BP event was the last earthquake to uplift Katalla prior to 1964 (Figures 30b and 30c). Between the 900 BP event and the 500 BP event, Marsh BC transitioned from submarine to intertidal, which indicates an interseismic fall in sea level. There is no record in the stratigraphy of this fall, and it may have occurred coseismically during the 900 BP event. Following uplift Ridge B was deposited. Long shore drift from the southeast transported sediment, most likely from the Bering River Delta, toward Katalla. The southernmost point of the Don Miller Hills created a natural barrier and allowed a spit to form off of the point. Storms also contributed to the sediment buildup. Ridge B appears to record two different depositional episodes, as evidenced by the slight drop in topography through the middle of the ridge. This may be due to a change in storm patterns, in sediment supply from the east, or even in sea level. It may also be attributed to the 1899 Cape Yakataga Earthquake. A slight uplift of the area could have lowered the relative sea level, causing a second spit to form just seaward of the first. The 500 BP event also uplifted the seafloor behind the spit to form an intertidal platform to a freshwater marsh. Gradually sea level rose, and the freshwater marsh became a brackish

water-saturated area that was both tidally dominated as well as fluvially dominated by the Pacific Ocean and the Katalla River, respectively (Figure 25).

Prominent currents that travel from southern Alaska contact the western side of the Katalla Bay. This high-energy environment shaped the high-water berms into the scalloped ridges that exist today. The 500 BP event raised Ridge 2 above the high water mark. What was once a platform with a thin beach cover became a tidal inlet, and a new high-water berm formed in front of it. Ridge 3a likely started forming further east than its present position, but intense wave energy coming from the east caused it to be pushed it back to coalesce with the older ridges. The Katalla River may have also played a role in shaping the coastline here. The coastline prior to the 1964 event was scalloped, and also concave toward the south. This suggests that the Katalla River was pushing sediment to the south while the Pacific Ocean was pushing sediment toward the east. It is less apparent further north because the spit protected the area from direct wave action. Between the 500 BP event and the 1964 event, net uplift was zero. However, net uplift between the 500 BP event and the present is at least 2 m.
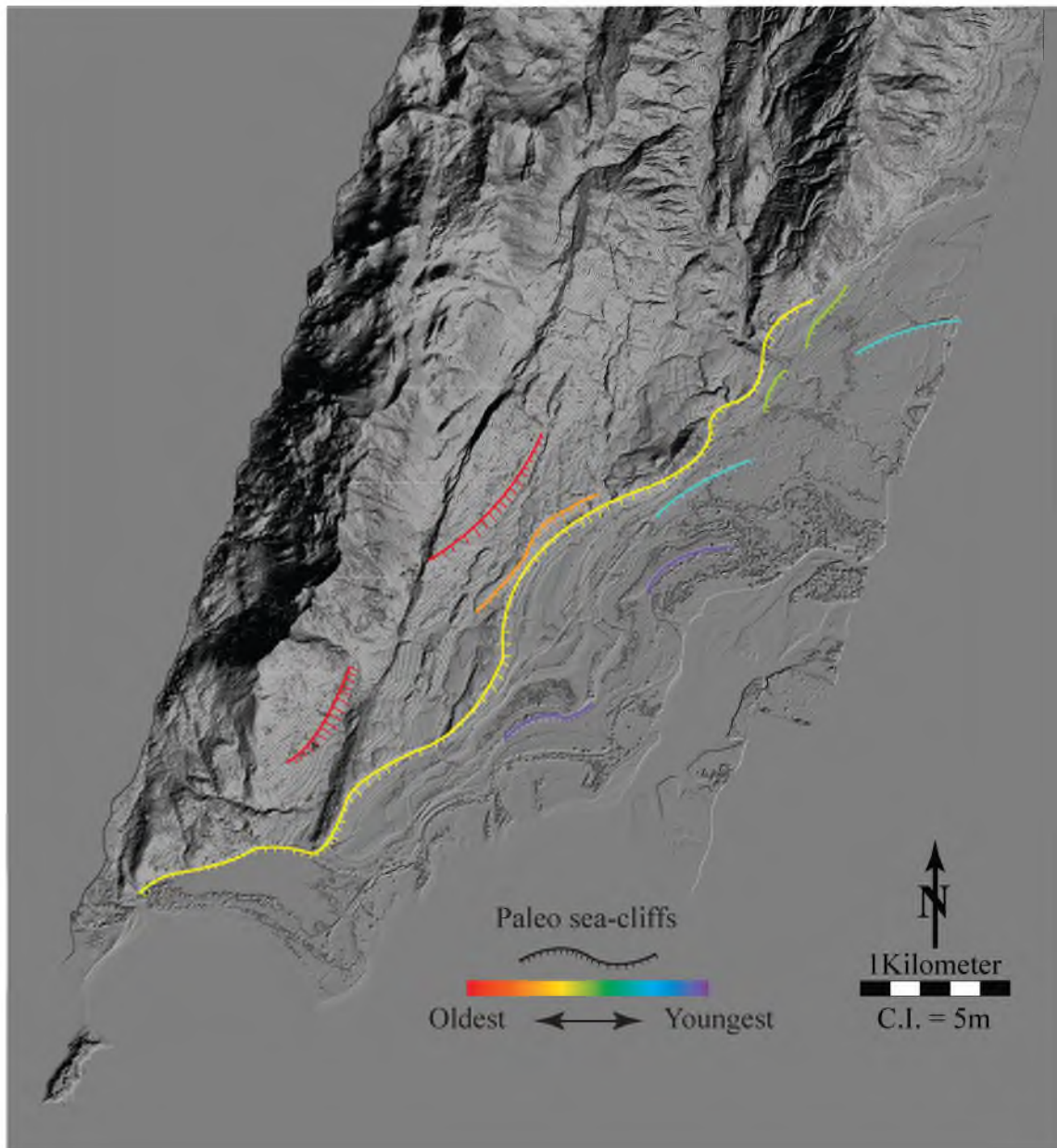
Figure 8. Escarpments interpreted as former sea cliffs cut by wave action following several episodes of uplift along the piedmont of Ragged Mountain. Each sea cliff is cut into a marine shore zone or gentle sloping platform following uplift relative to sea level.

Shaded relief LIDAR DEM created with artificial illumination from the southeast.

Figure 9. Stratigraphy of marshes and ridges of the Ragged Mountain piedmont. Location is shown in Figure 14. Marshes are labeled in yellow, ridges in white, cores in red, and soil pits in blue. Radiocarbon dates of organic material found at important contacts is noted.

Photo credit: US Forest Service (early 2000s)

Pit 2

Gravel

Sand, no depth recorded

13a

Peat

Fine grained sand

Mud with rootlets

13b

Peat

Sand

Mud
Peat

Pit 3

Fining upwards sequence of cobbles and sands

Pit 4

Pebbly gravel

Pits 5a and 5b

Peat

Leached zone

Gravel and sand

Bedrock

14a, 14b, 14c, 14d, 14e

One to 1.5 meters peat

Bedrock

2900 BP

Pit 6

Peat

Densly packed gravels in clay

2100 BP

15

Herbaceous peat

Light brown mud with herbaceous fragments

Grey-green mud with wood and herbaceous fragments

Brown mud with sand lenses

Dark brown mud with herbaceous fragments

Silty sand

Depth below the surface (in cm)

0
50
100
150
200
250
300

15

3b

T1

T3

4

T2

3

6

1

2

14e

14d

5

13

2

3a

T4

N

500 Meters

Legend

Peat

Sand

Gravel

Clay/Silt/Mud

Solid Rock

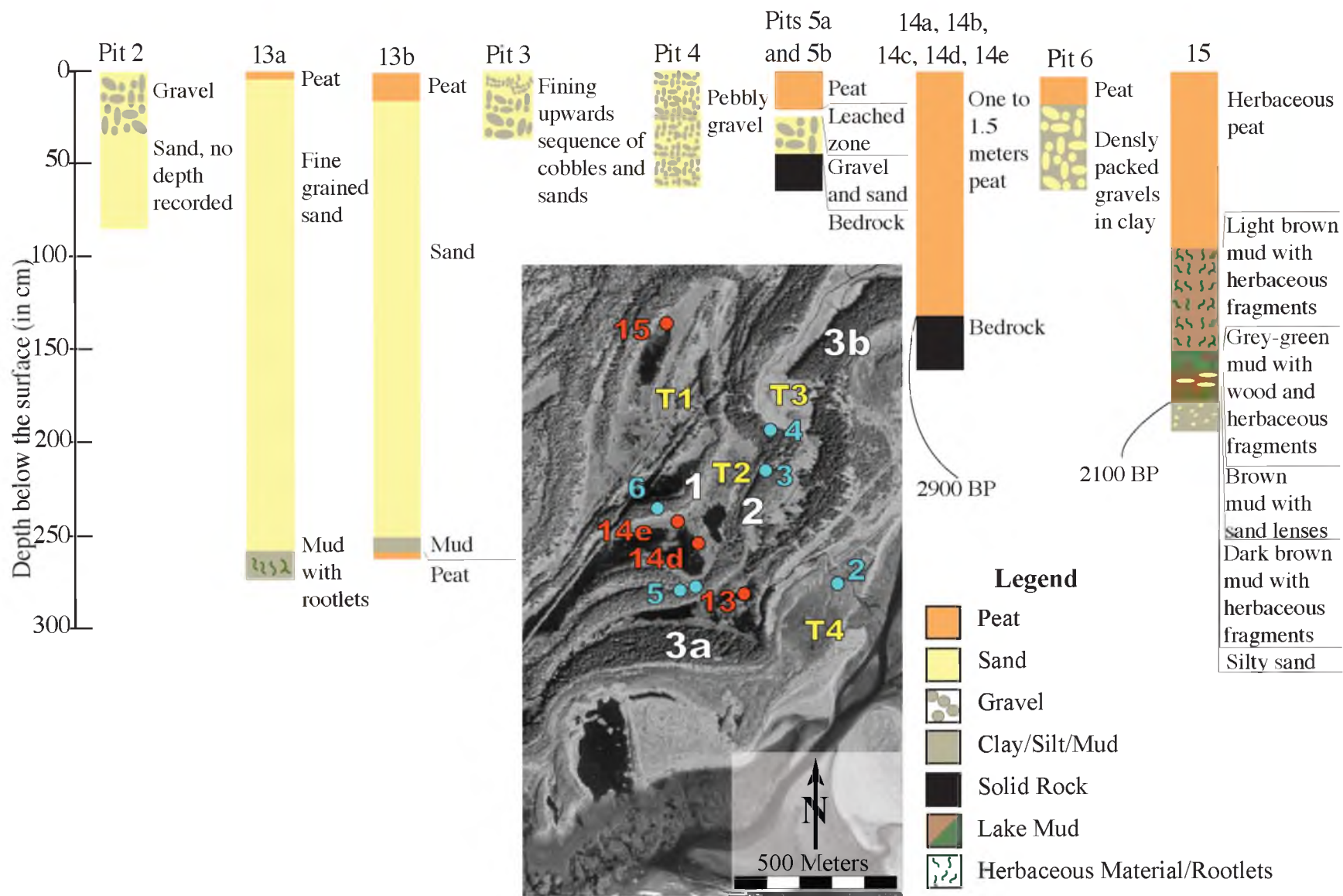Lake Mud

Herbaceous Material/Rootlets

Figure 10. Large boulders found in the field. A) Photo located at 60 11.254 N, 144 31.917 W (Terrace 4). B) Photo located at 60 11.800 N, 144 31.393 W (Terrace 2). Note geologists for scale.
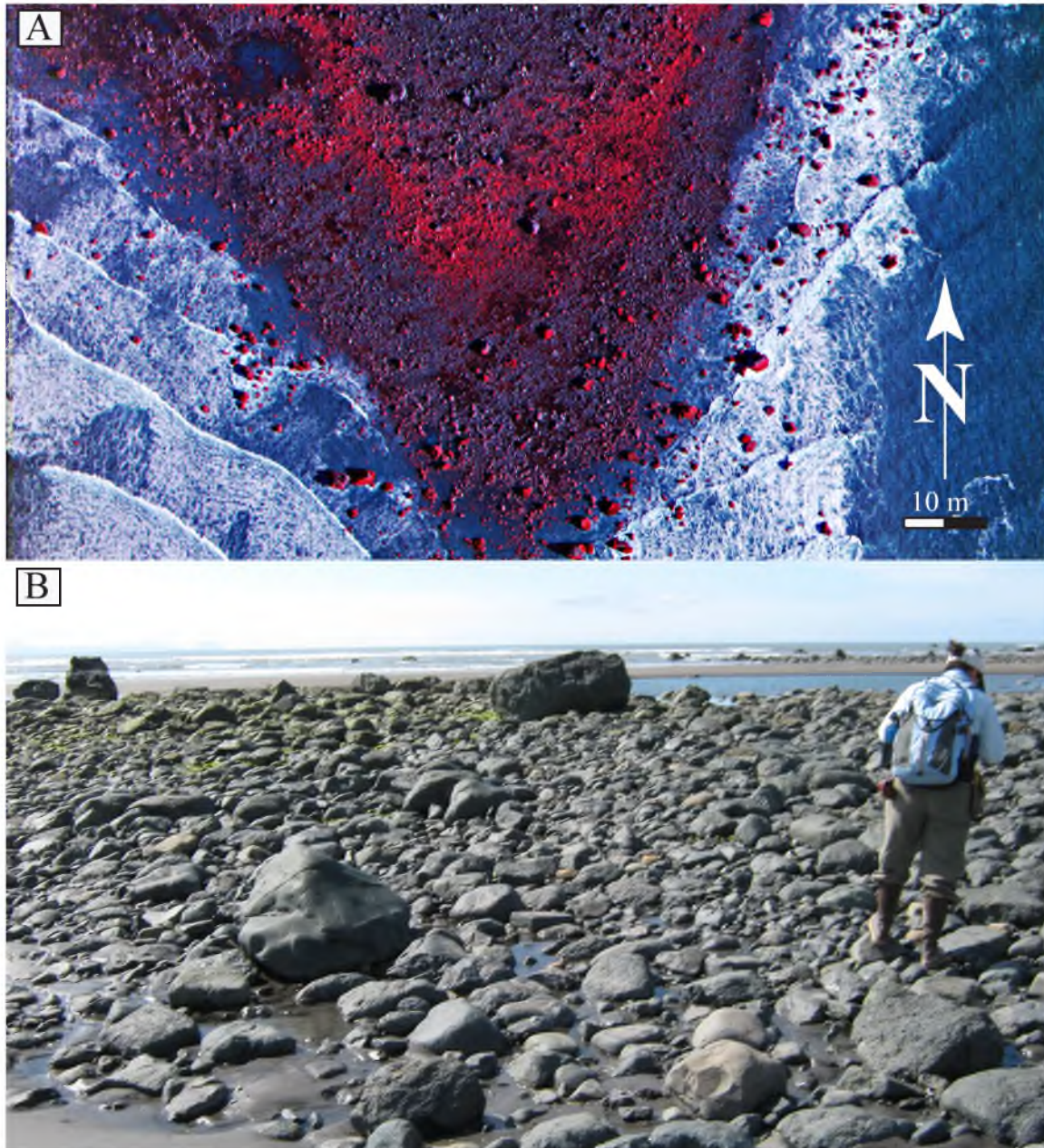
Figure 11. Boulder fields on the Katalla coast. A) Aerial photo of the boulder fields shown on Figure 6. This is a color-infrared image which shows vegetation in red. Most of the boulders seen in this photograph are moss-covered and appear red, although there is some ground vegetation present as well. The blue on either side of the boulder field is the Pacific Ocean with waves breaking on the beach. (Photo credit: National Center for Airborne Laser Mapping (NCALM), 2007). B) The boulder field as seen from the ground, looking south. Note geologist for scale.
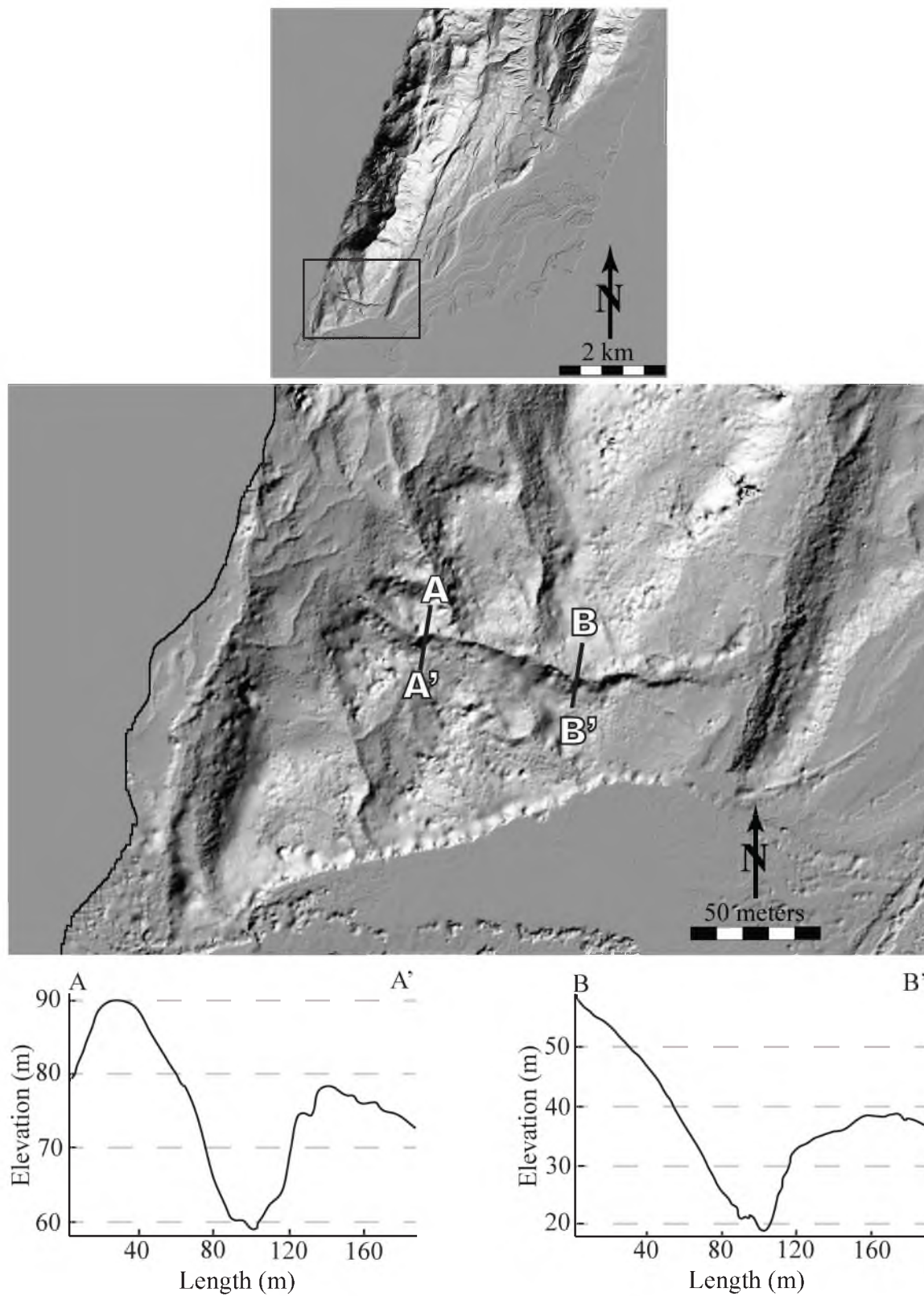
Figure 12. Topographic profiles across a stream on the southern end of Ragged Mountain, location shown in top image by black rectangle (note, 4x vertical exaggeration). The stream bank is slightly steeper to the south, but taller to the north.
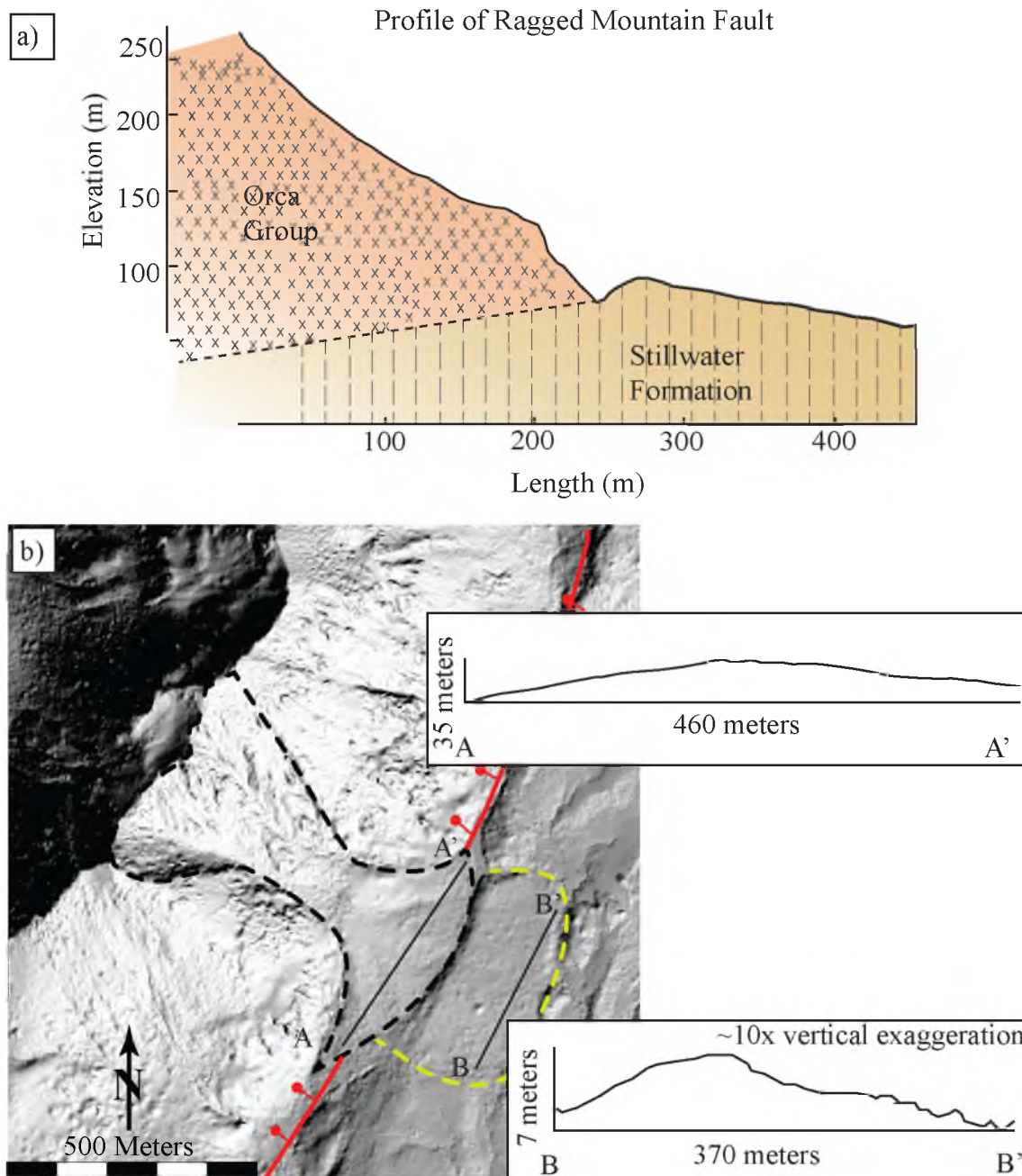
Figure 13. Topographic features of the Ragged Mountain fault. a) Typical cross section of the Ragged Mountain Fault. Older volcanic rocks of the Orca Group overlie younger sedimentary rocks of the Stillwater Formation, indicative of a thrust fault. However, the scarp faces west, or uphill, implying extensional offset. b) Landslide offset by the Ragged Mountain Fault (location shown on Figure 6). The black dashed line shows the position of the present-day landslide and the yellow line shows an older toe of the slide. The two topographic profiles show the convex nature of the landslide (note, B-B' not to scale). This offset indicates the fault has been active since the landslide was first deposited, which was post glacial retreat (10,000 BP).
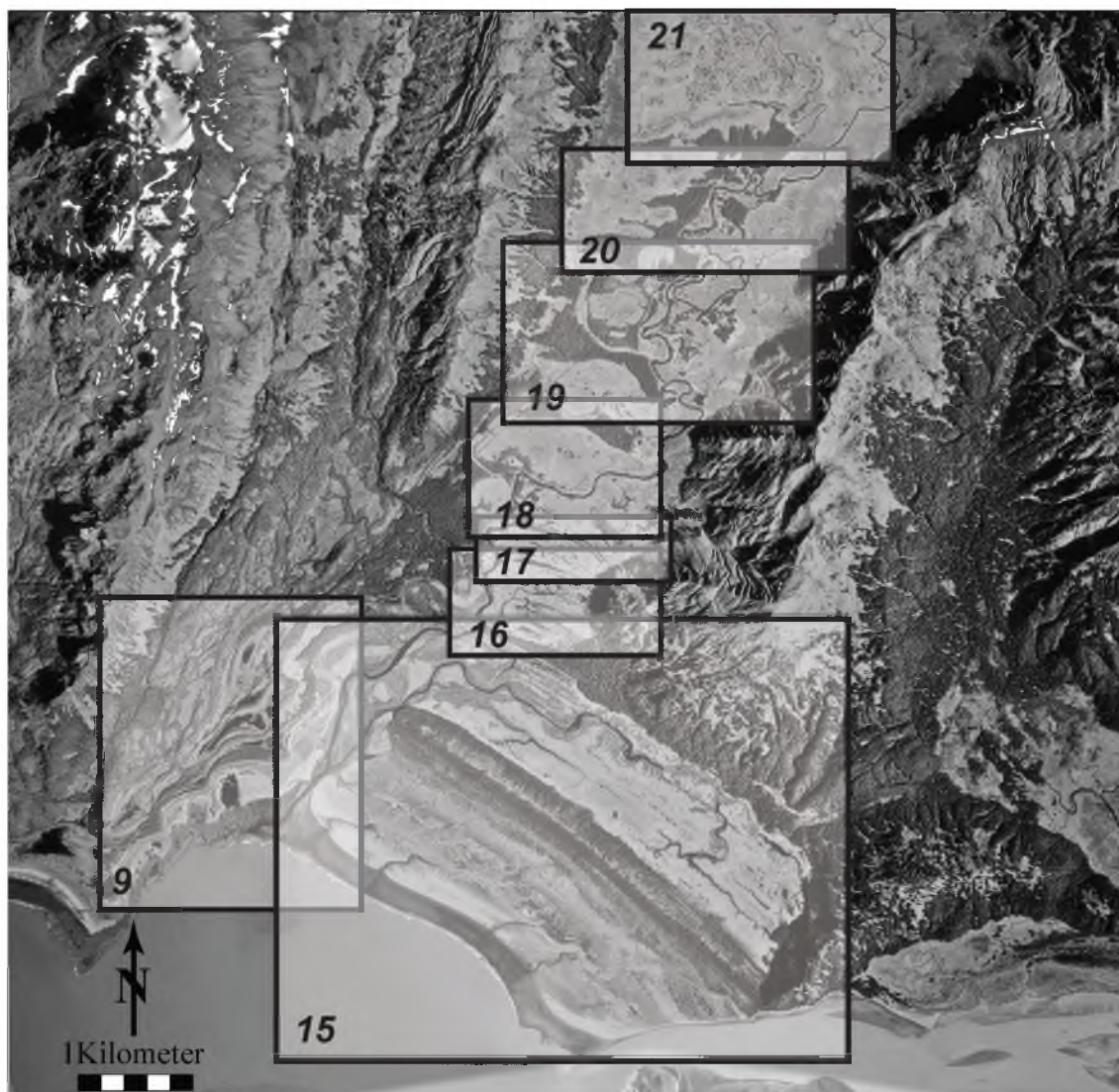
Figure 14. Aerial photo of the Katalla River Valley and the Ragged Mountain Piedmont with rectangles outlining localities of maps and cross sections shown in Figures 9 and 15 through 21.

Photo credit: US Forest Service (early 2000s)

Figure 15. Stratigraphy of marshes and ridges from the Katalla Coast to Ridge C. Location is shown in Figure 14. Marshes are labeled in yellow, ridges in white, and cores in red.

[1]Described by Richards (2000)
[2]Described by Sirkin and Tuthill (1971)

Ridge A[1]

Sand and gravel, no depth recorded

Ridge B[1,2]

Sand and gravel no depth recorded

Marsh BC[2]

Muskeg

Sedge peat

Wood, rooted stumps in underlying beach sand

440 BP[2]

1a

Silty, herbaceous peat

Grey clay silt with rootlets

Sphagnum peat, occasional wood at base, gradational upper contact

Fine unlaminated sand, occasional rootlets in top 5cm extending down from peat

1b

Sphagnum peat

Silt clay with rootlets

Silty, herbaceous peat

Grey, fine sand, oxidized brown 71-81 cm

510-310 BP
550-500 BP

Ridge C[1]

Sand, no depth recorded

Ridge C[2]

Sandy forest peat and sedge peat

Gravel

Grey clay

Wood peat

Grey clay with thin sand seams, scattered wood fragments

Sand

1230 BP[2]

Depth below the surface (in cm)

Legend

Peat
Sand
Gravel
Clay/Silt/Mud
Solid Rock
Lake Mud
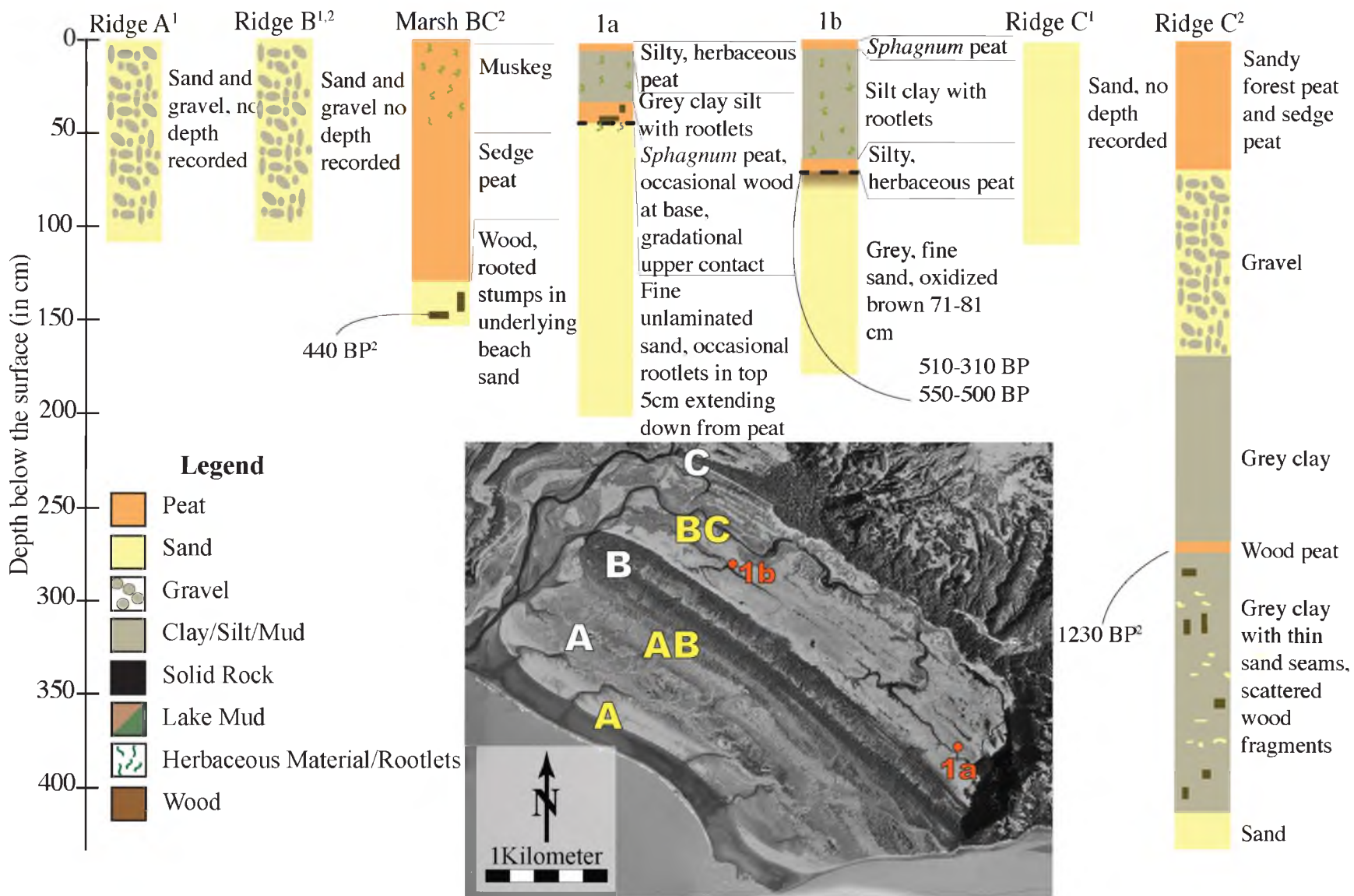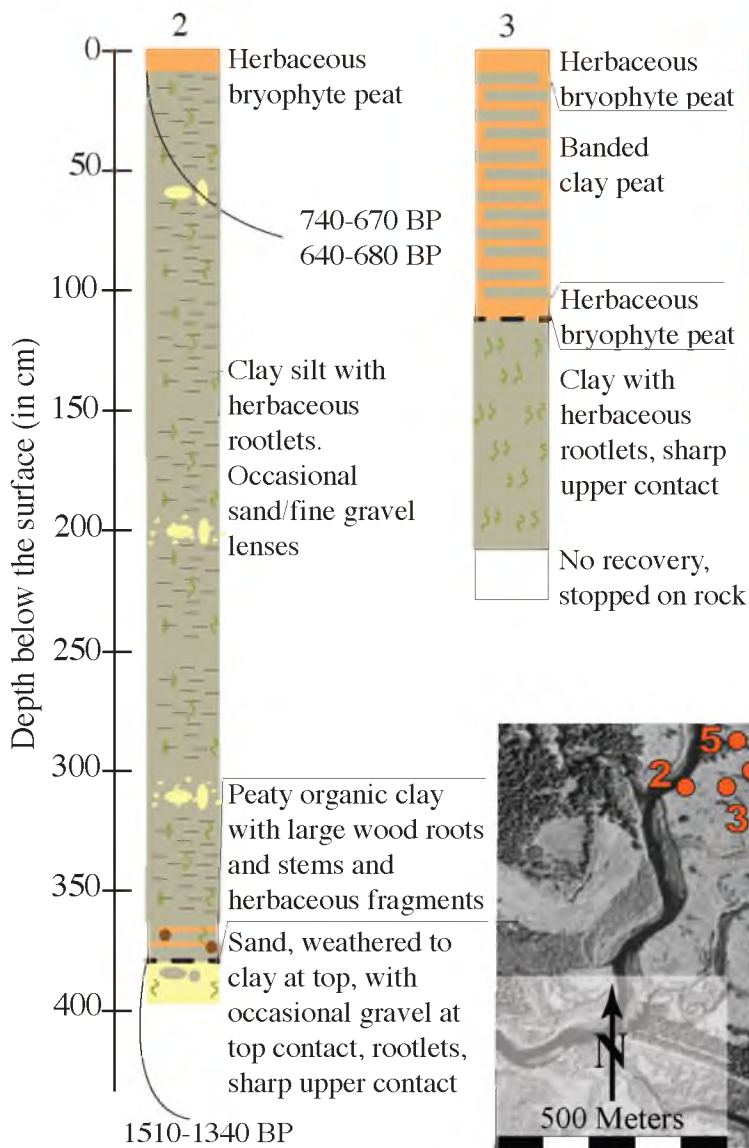Herbaceous Material/Rootlets
Wood

1Kilometer

Figure 16. Stratigraphy of marshes and ridges from Marsh C to Ridge D. Location is shown in Figure 14. See Figure 15 for legend. Marshes are labeled in yellow, ridges in white, and cores in red.

[2]Described by Sirkin and Tuthill (1971)

Depth below the surface (in cm)

2

0 — Herbaceous bryophyte peat

50 —

740-670 BP
640-680 BP

100 —

Clay silt with herbaceous rootlets. Occasional sand/fine gravel lenses

150 —

200 —

250 —

300 —

Peaty organic clay with large wood roots and stems and herbaceous fragments

350 —

Sand, weathered to clay at top, with occasional gravel at top contact, rootlets, sharp upper contact

400 —

1510-1340 BP

3

Herbaceous bryophyte peat

Banded clay peat

Herbaceous bryophyte peat

Clay with herbaceous rootlets, sharp upper contact

No recovery, stopped on rock

4

5
2 4
3

N

500 Meters

Peat

Mud and
peat bands

Peat
Mud

Some
water-saturated
sand

Marsh CD²

Muskeg

Sedge peat

Grey clay,
sand at base

Ridge D²

Muskeg

Sedge peat

Gravel,
sandy at top

Grey clay
Sedge peat,
sand and
gravel at
base

5

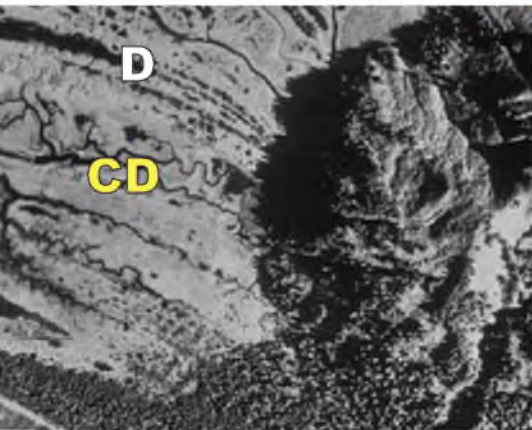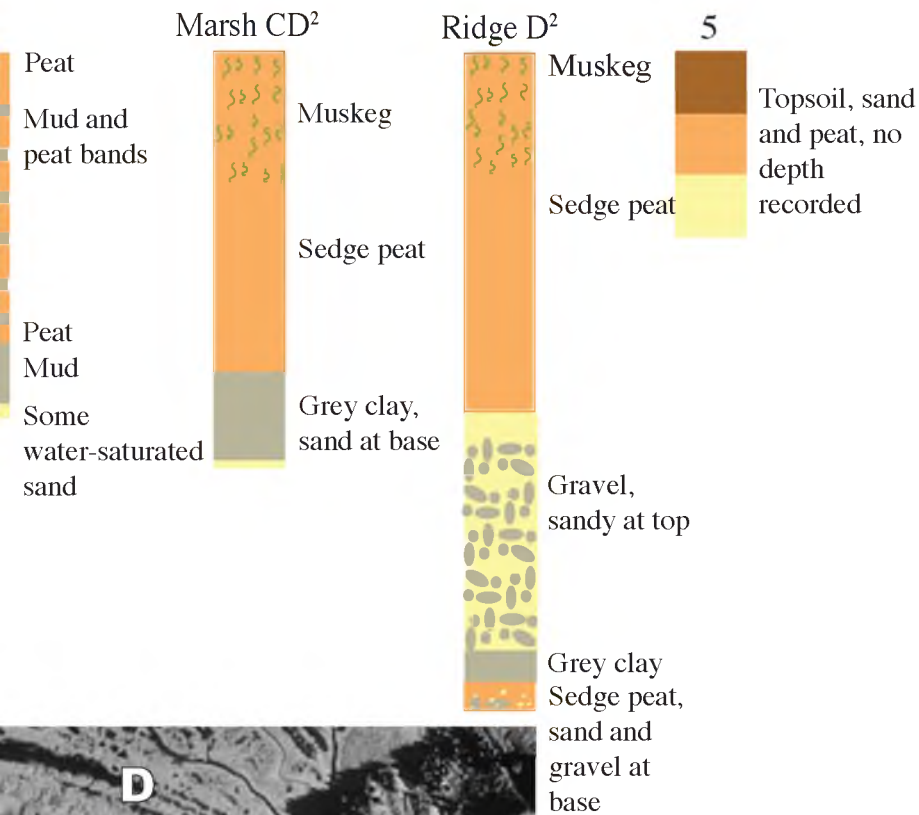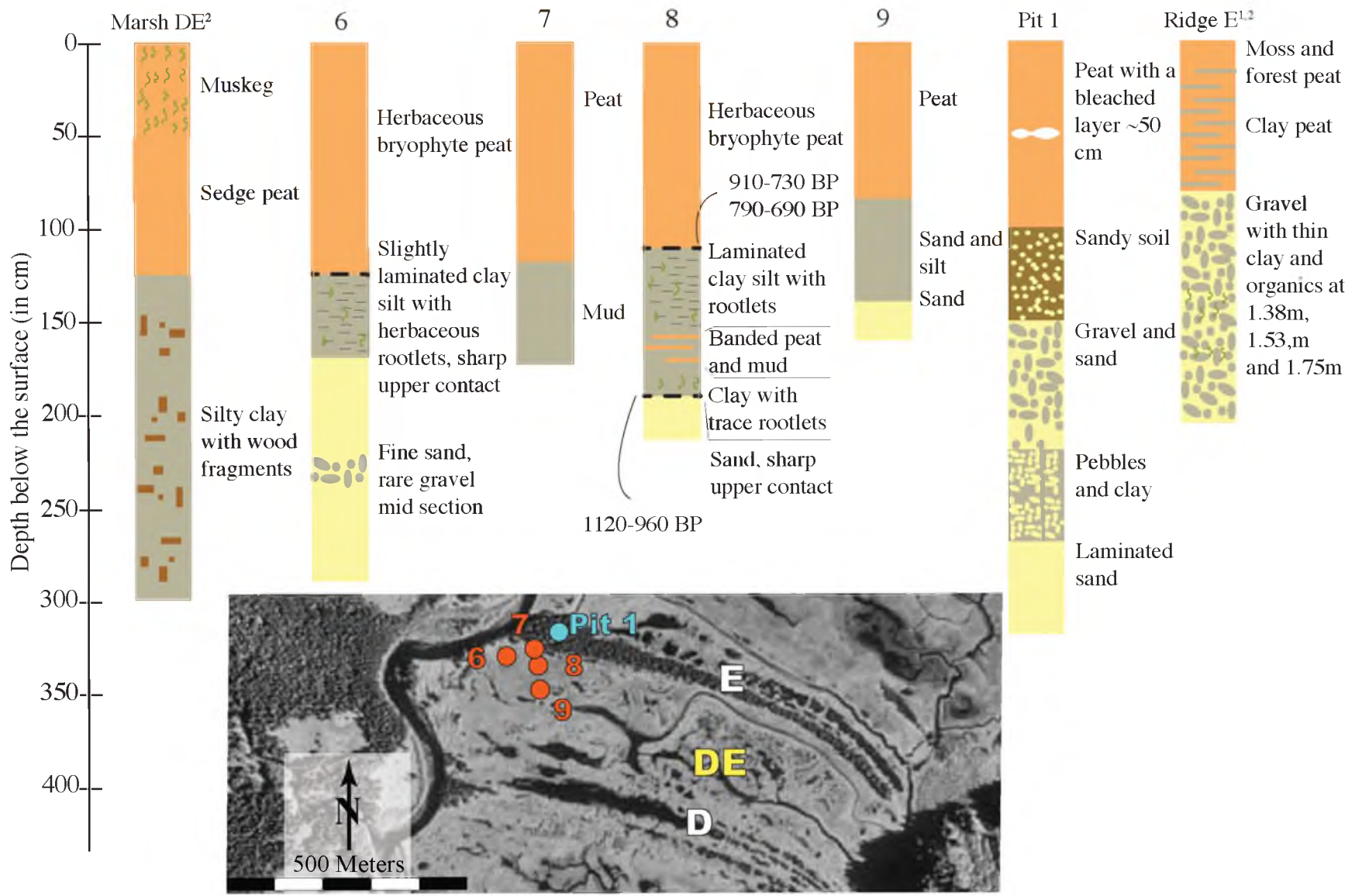Topsoil, sand
and peat, no
depth
recorded

Figure 17. Stratigraphy of marshes and ridges from Marsh DE to Ridge E. Location is shown in Figure 14. See Figure 15 for legend. Marshes are labeled in yellow, ridges in white, soil pits in blue, and cores in red.

[1]Described by Richards (2000)
[2]Described by Sirkin and Tuthill (1971)

Marsh DE[2]
- Muskeg
- Sedge peat
- Silty clay with wood fragments

6
- Herbaceous bryophyte peat
- Slightly laminated clay silt with herbaceous rootlets, sharp upper contact
- Fine sand, rare gravel mid section

7
- Peat
- Mud

8
- Herbaceous bryophyte peat
- 910-730 BP
- 790-690 BP
- Laminated clay silt with rootlets
- Banded peat and mud
- Clay with trace rootlets
- Sand, sharp upper contact
- 1120-960 BP

9
- Peat
- Sand and silt
- Sand

Pit 1
- Peat with a bleached layer ~50 cm
- Sandy soil
- Gravel and sand
- Pebbles and clay
- Laminated sand

Ridge E[1,2]
- Moss and forest peat
- Clay peat
- Gravel with thin clay and organics at 1.38m, 1.53,m and 1.75m

Depth below the surface (in cm)

N

500 Meters

Figure 18. Stratigraphy of marshes and ridges from Marsh EF to Ridge F. Location is shown in Figure 14. See Figure 15 for legend. Marshes are labeled in yellow, ridges in white, and cores in red.

[1]Described by Richards (2000)
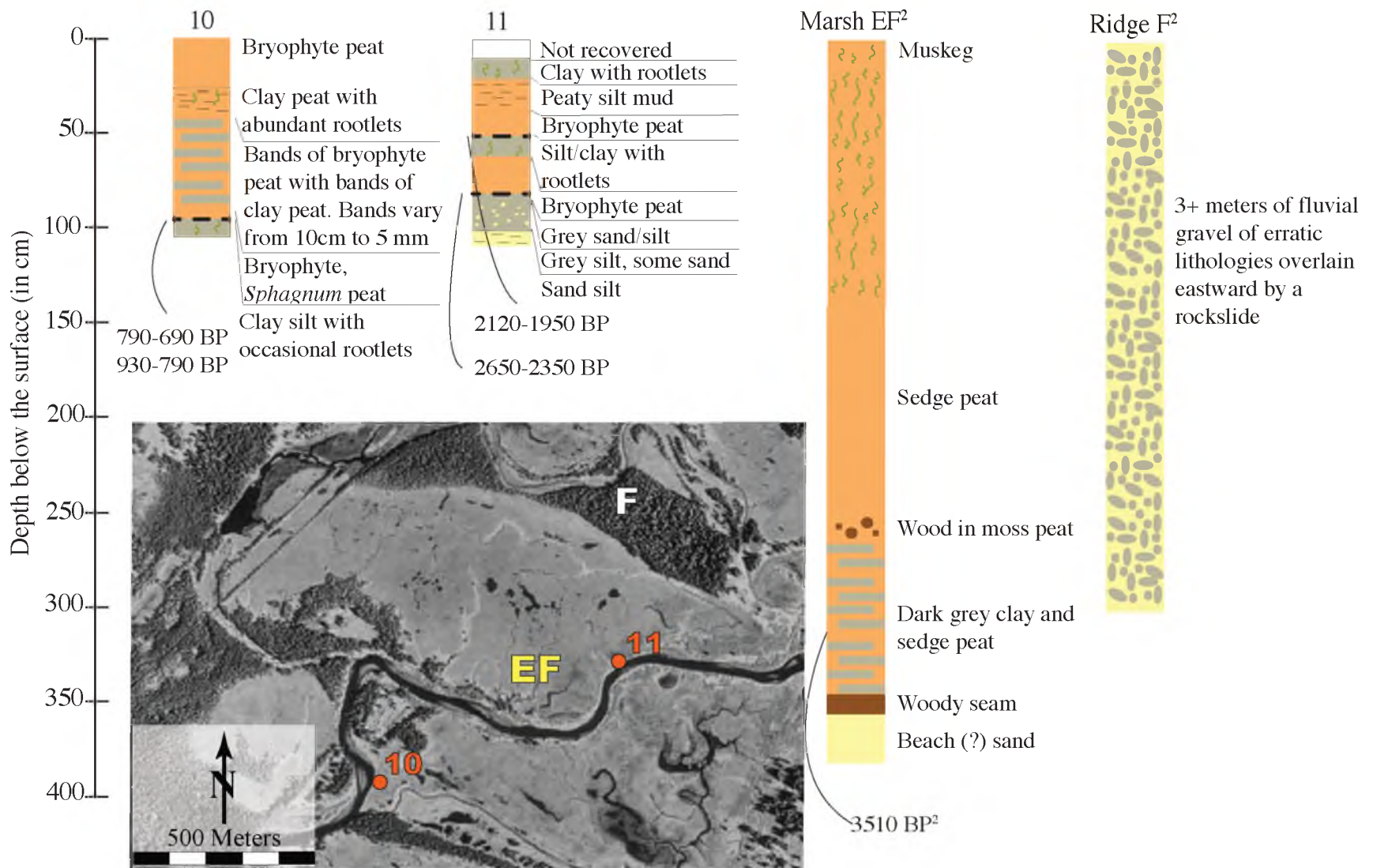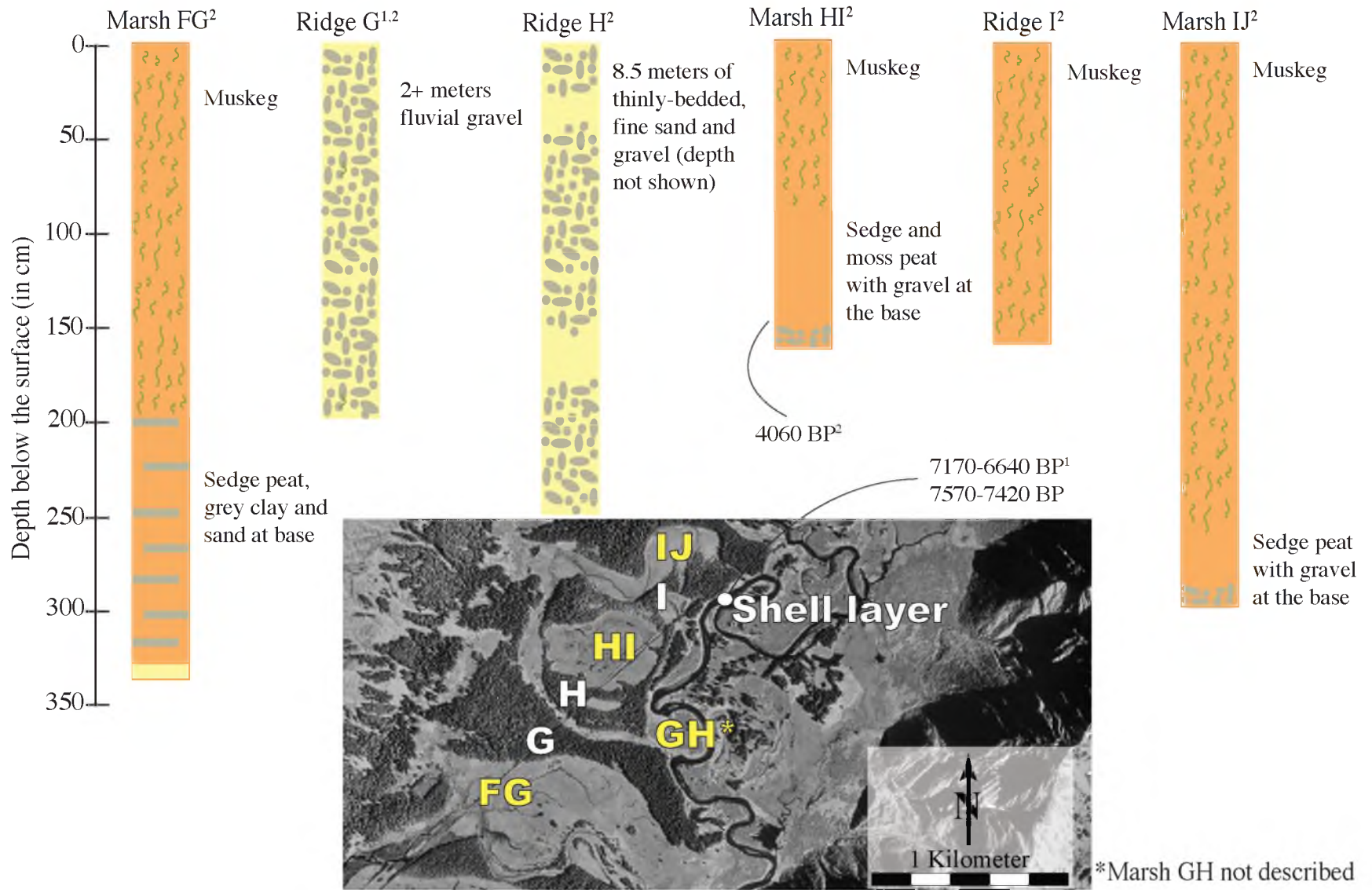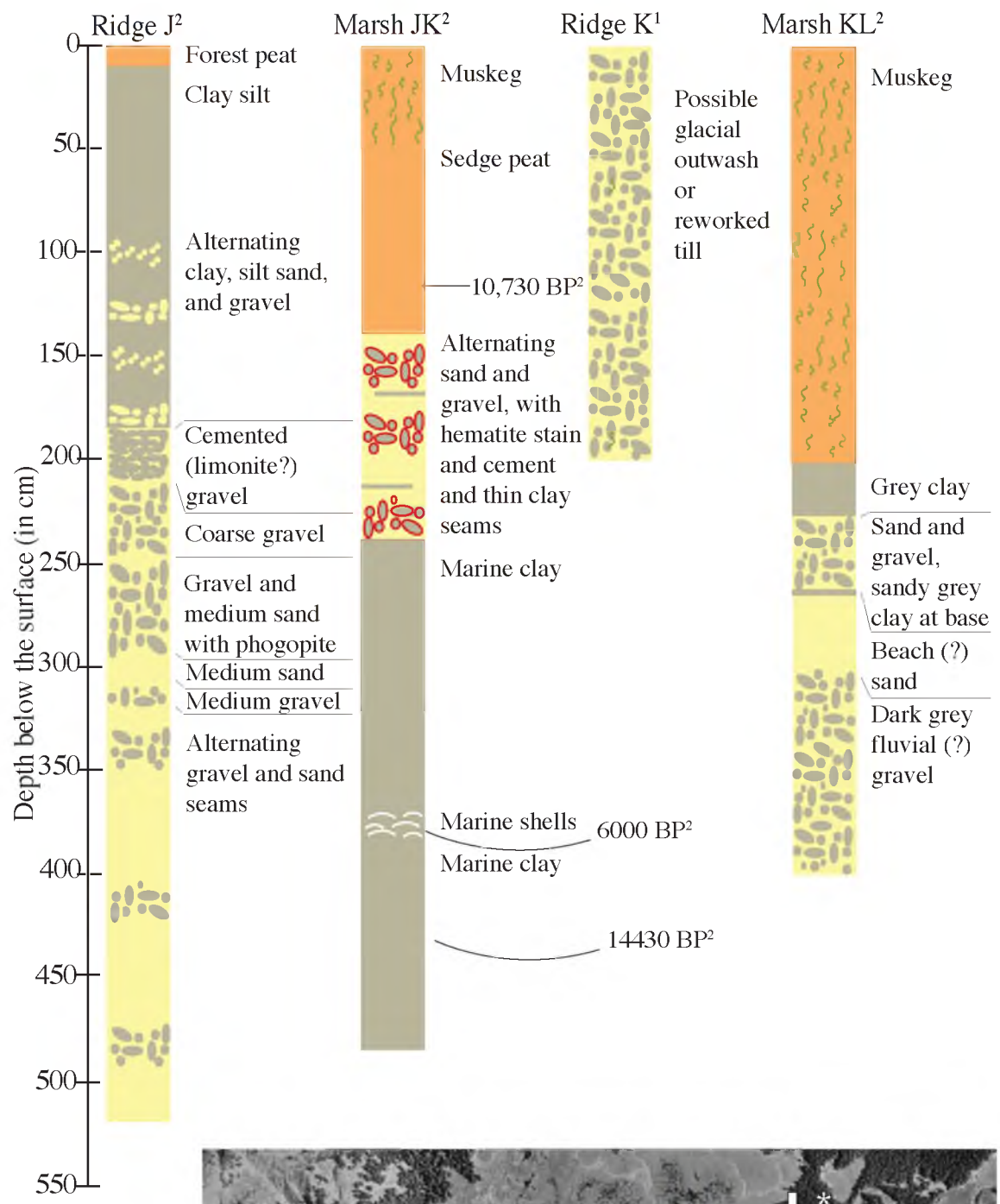[2]Described by Sirkin and Tuthill (1971)

Depth below the surface (in cm)

10

Bryophyte peat

Clay peat with abundant rootlets

Bands of bryophyte peat with bands of clay peat. Bands vary from 10cm to 5 mm

Bryophyte, *Sphagnum* peat

Clay silt with occasional rootlets

790-690 BP
930-790 BP

11

Not recovered
Clay with rootlets
Peaty silt mud
Bryophyte peat
Silt/clay with rootlets
Bryophyte peat
Grey sand/silt
Grey silt, some sand
Sand silt

2120-1950 BP

2650-2350 BP

Marsh EF[2]

Muskeg

Sedge peat

Wood in moss peat

Dark grey clay and sedge peat

Woody seam

Beach (?) sand

3510 BP[2]

Ridge F[2]

3+ meters of fluvial gravel of erratic lithologies overlain eastward by a rockslide
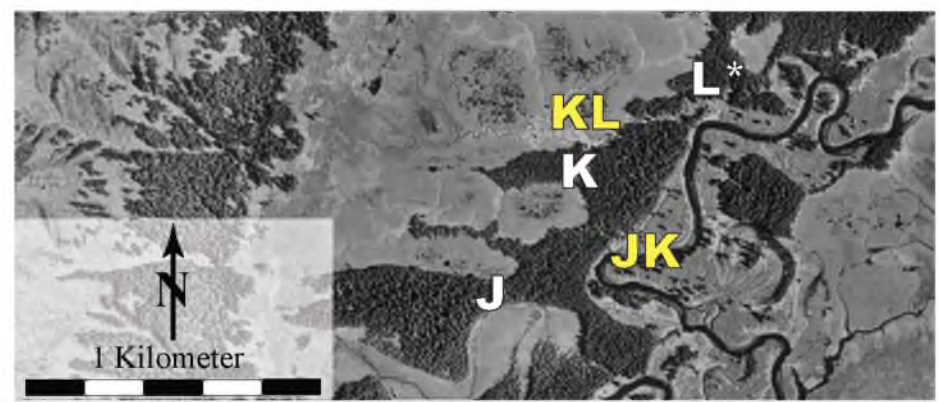
F

EF

11

10

N

500 Meters

80

Figure 19. Stratigraphy of marshes and ridges from Marsh FG to Marsh IJ. Location is shown in Figure 14. See Figure 15 for legend. Marshes are labeled in yellow and ridges in white. All data from Richards (2000) and/or Sirkin and Tuthill (1971).

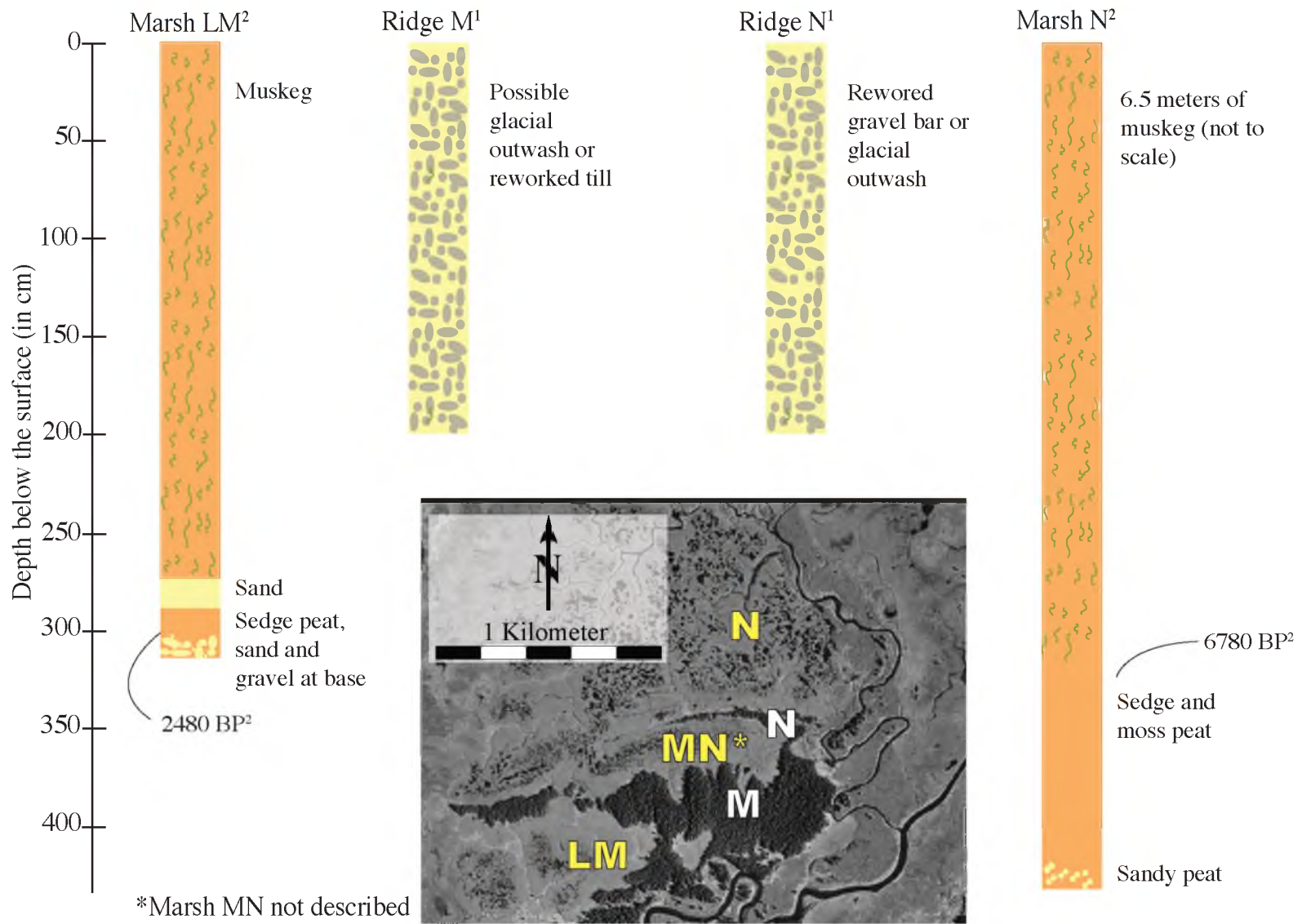[1]Described by Richards (2000)
[2]Described by Sirkin and Tuthill (1971)

Marsh FG[2]

Muskeg

Sedge peat, grey clay and sand at base

Ridge G[1,2]

2+ meters fluvial gravel

Ridge H[2]

8.5 meters of thinly-bedded, fine sand and gravel (depth not shown)

Marsh HI[2]

Muskeg

Sedge and moss peat with gravel at the base

4060 BP[2]

Ridge I[2]

Muskeg

Marsh IJ[2]

Muskeg

Sedge peat with gravel at the base

Depth below the surface (in cm)

0
50
100
150
200
250
300
350

7170-6640 BP[1]
7570-7420 BP

Shell layer

IJ
I
HI
H
GH*
G
FG

1 Kilometer

N

*Marsh GH not described

Figure 20. Stratigraphy of marshes and ridges from Ridge J to Ridge L. Location is shown in Figure 14. See Figure 15 for legend. Marshes are labeled in yellow and ridges in white. All data from Richards (2000) and/or Sirkin and Tuthill (1971).

[1]Described by Richards (2000)
[2]Described by Sirkin and Tuthill (1971)

Ridge J[2]

Forest peat

Clay silt

Alternating clay, silt sand, and gravel

Cemented (limonite?) gravel

Coarse gravel

Gravel and medium sand with phogopite

Medium sand

Medium gravel

Alternating gravel and sand seams

Marsh JK[2]

Muskeg

Sedge peat

10,730 BP[2]

Alternating sand and gravel, with hematite stain and cement and thin clay seams

Marine clay

Marine shells — 6000 BP[2]

Marine clay

14430 BP[2]

Ridge K[1]

Possible glacial outwash or reworked till

Marsh KL[2]

Muskeg

Grey clay

Sand and gravel, sandy grey clay at base

Beach (?) sand

Dark grey fluvial (?) gravel

Depth below the surface (in cm)

*Ridge L not described

N

1 Kilometer

L*

KL

K

JK

J

Figure 21. Stratigraphy of marshes and ridges from Marsh LM to Marsh N. Location is shown in Figure 14. See Figure 15 for legend. Marshes are labeled in yellow and ridges in white. All data from Richards (2000) and/or Sirkin and Tuthill (1971).

[1]Described by Richards (2000)
[2]Described by Sirkin and Tuthill (1971)

Marsh LM²

Muskeg

Sand

Sedge peat,
sand and
gravel at base

2480 BP²

Ridge M¹

Possible
glacial
outwash or
reworked till

Ridge N¹

Rewored
gravel bar or
glacial
outwash

Marsh N²

6.5 meters of
muskeg (not to
scale)

6780 BP²

Sedge and
moss peat

Sandy peat

Depth below the surface (in cm)

1 Kilometer

N

N

MN*

N

M

LM

*Marsh MN not described

86

Figure 22. Composite topographic profiles with stratigraphic sections of the Katalla River Valley and the Ragged Mountain piedmont. a) Cross sections A-A' and B-B' of Katalla Valley (note, ~100x vertical exaggeration). Cross section locations are shown in Figure 3. The stratigraphy of the marshes and ridges is shown as well as horizons corresponding to megathurst events. b) Cross section C-C' of terraces on Ragged Mountain piedmont showing the stratigraphy of the marshes and ridges. Cross section location is shown in Figure 3 (note, ~65x vertical exaggeration).
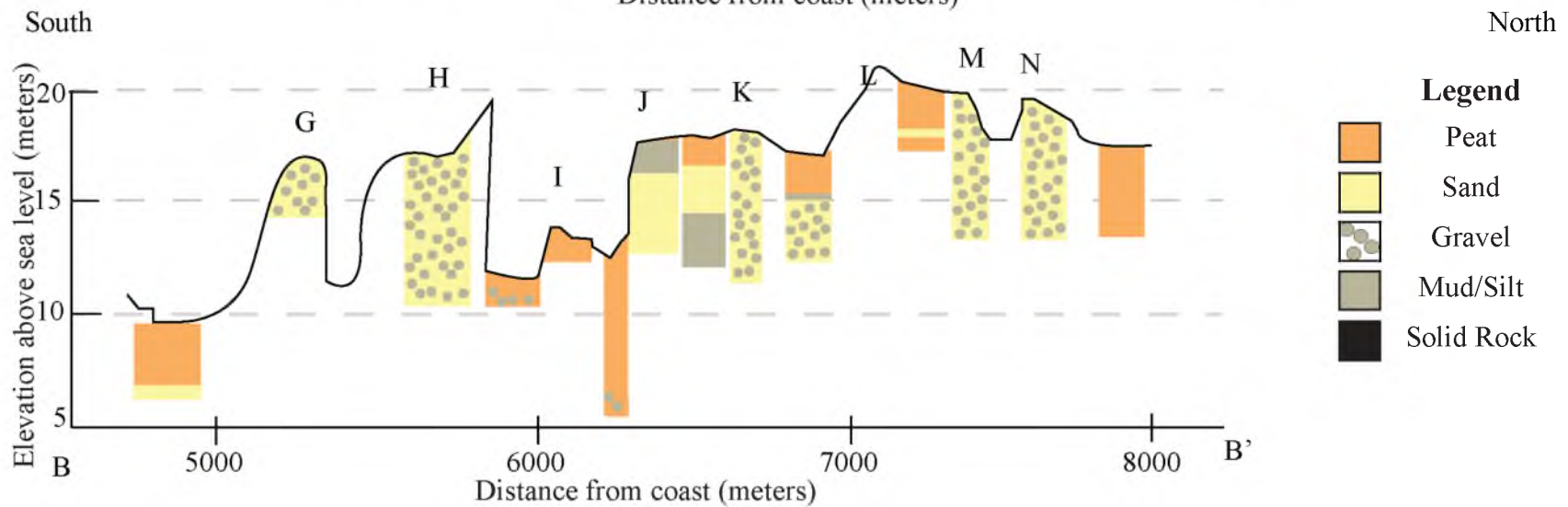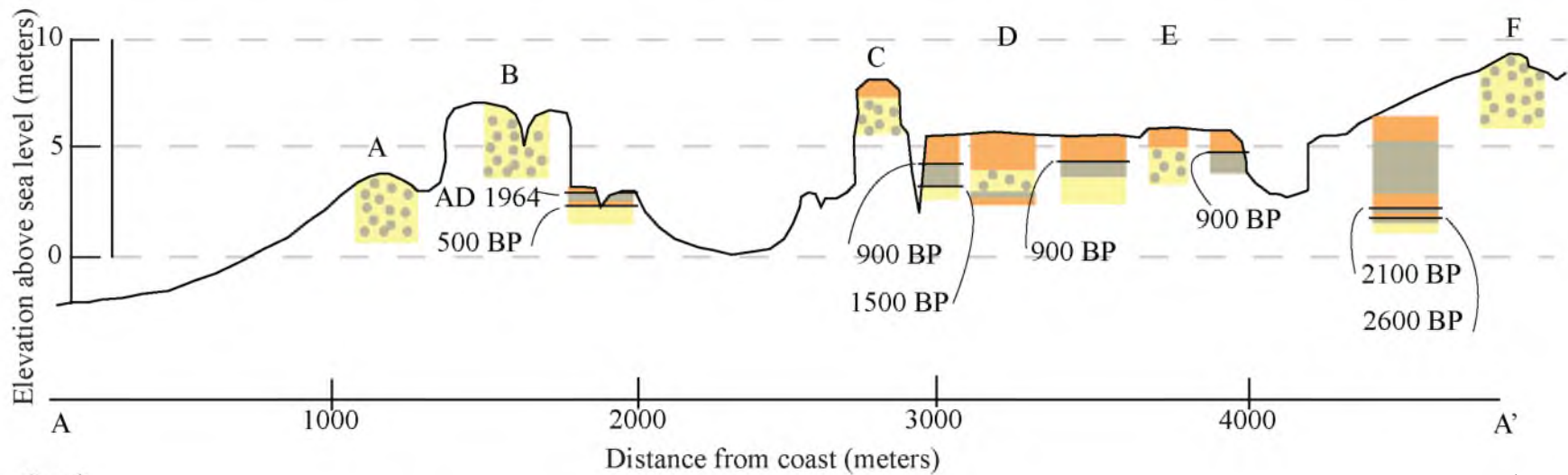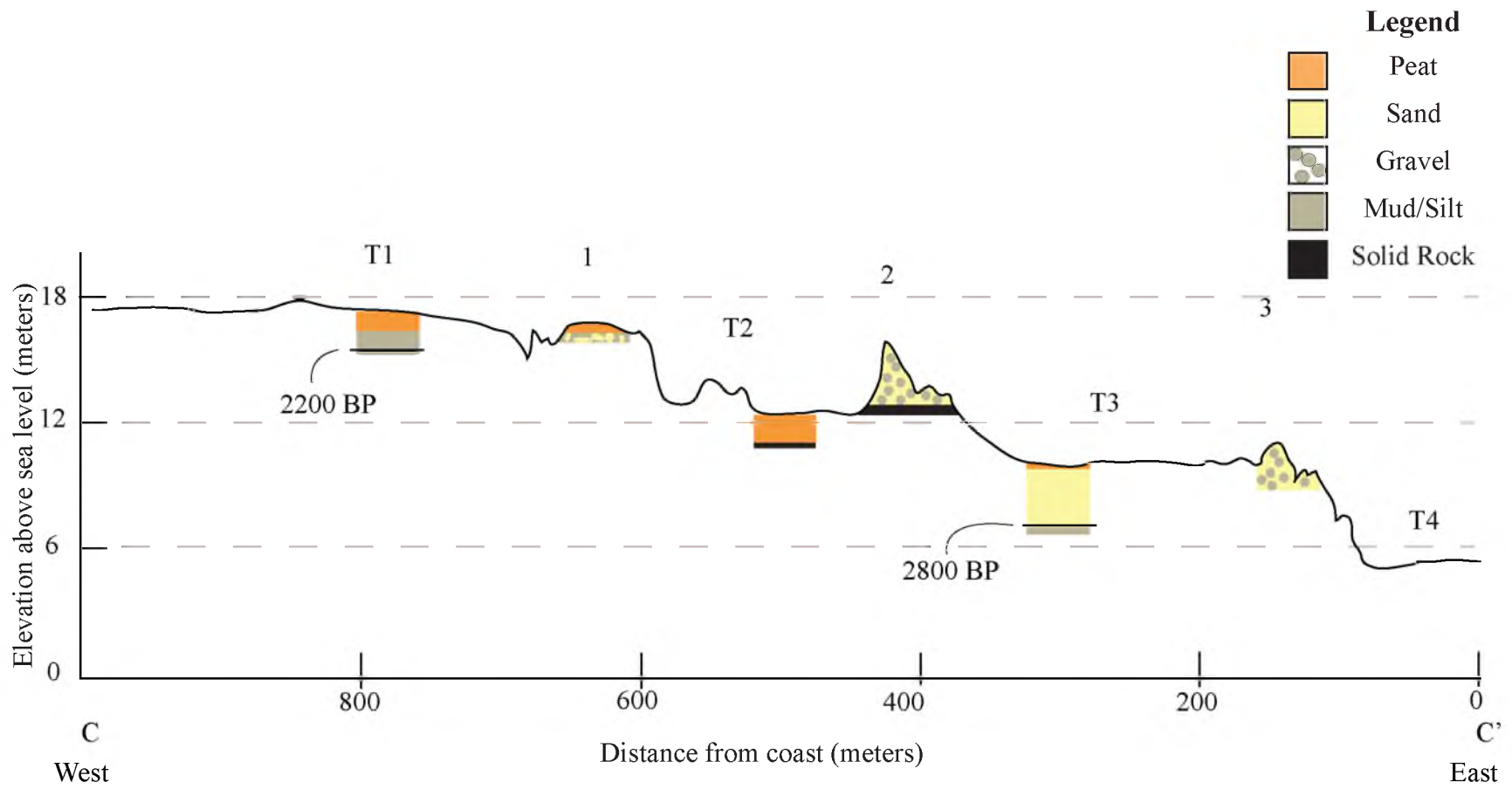
b)

Figure 22 continued
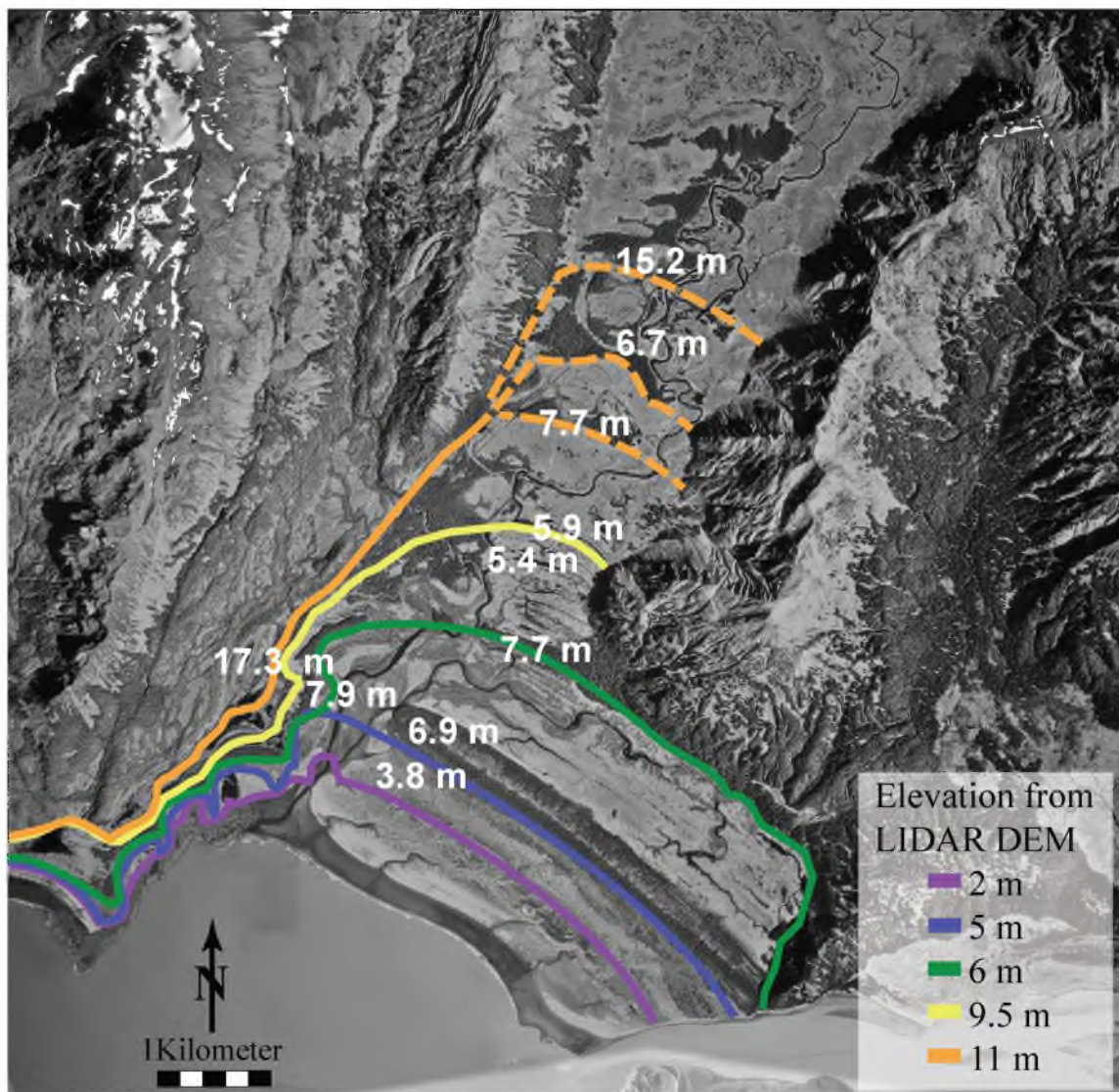
Figure 23. Aerial photo of the Katalla Valley showing spot elevations taken by Richards (2000) in white. Elevations from LIDAR DEM are colored and correlated across the valley. Where the elevations differ, geomorphic features were used to correlate ridges across the valley.

Photo credit: US Forest Service (early 2000s)
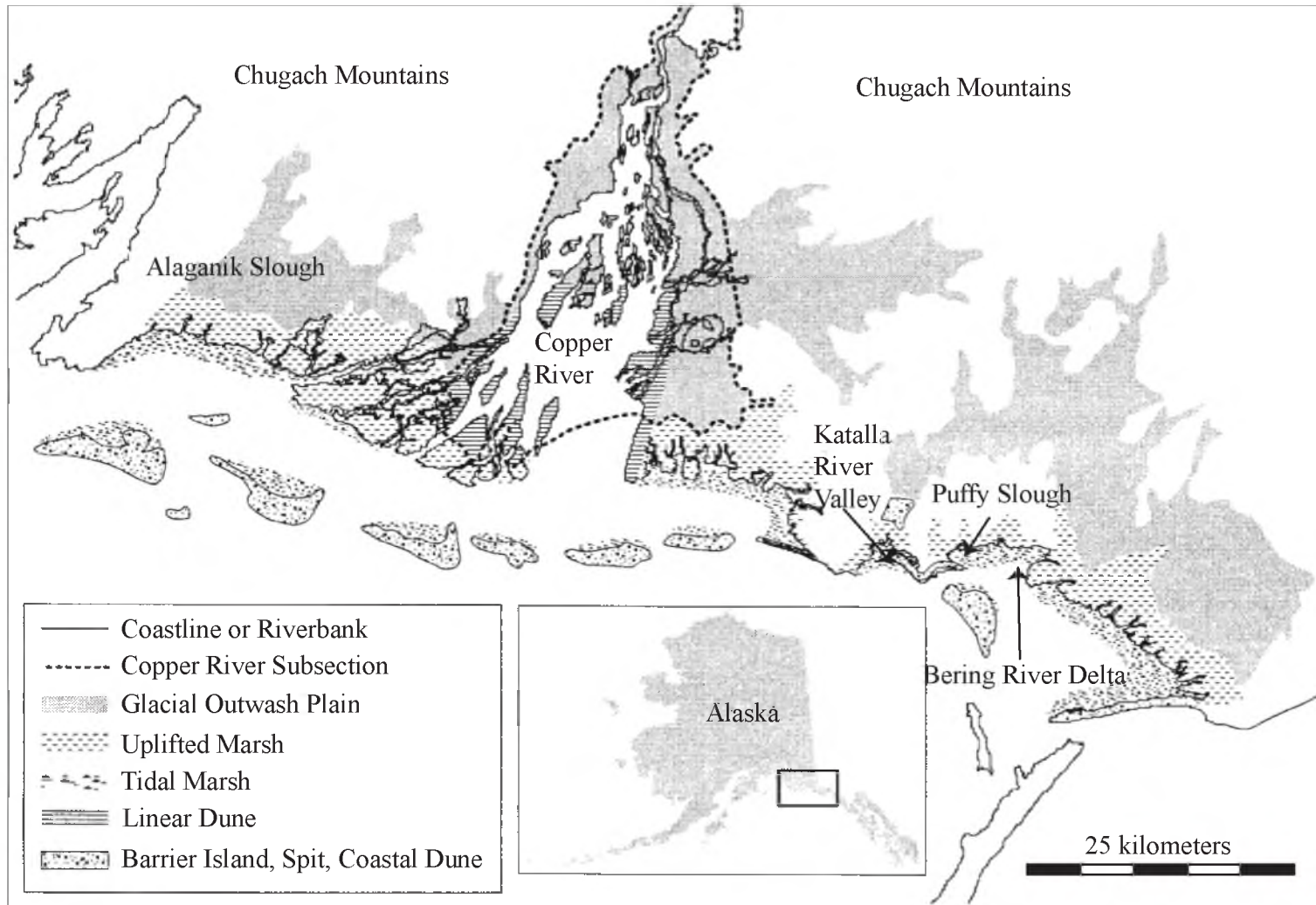
Figure 24. Vegetation map of the region surrounding the Katalla River Valley, showing areas of coseismic uplift during the Good Friday Earthquake (from Boggs, 2000). The Katalla Valley itself comprises mainly uplifted marshes and barrier islands, spits and coastal dunes.

Figure 25. Geomorphic map of the Ragged Mountain piedmont and the Katalla River Valley (adapted from Kachadoorian, 1960).
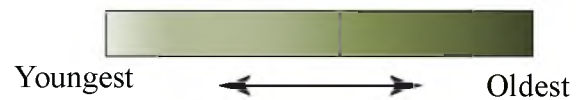
Legend

Rivers/Lakes/Ponds

Beach

Landslide

Alluvial Fan

Bedrock from the Yakutat terrane

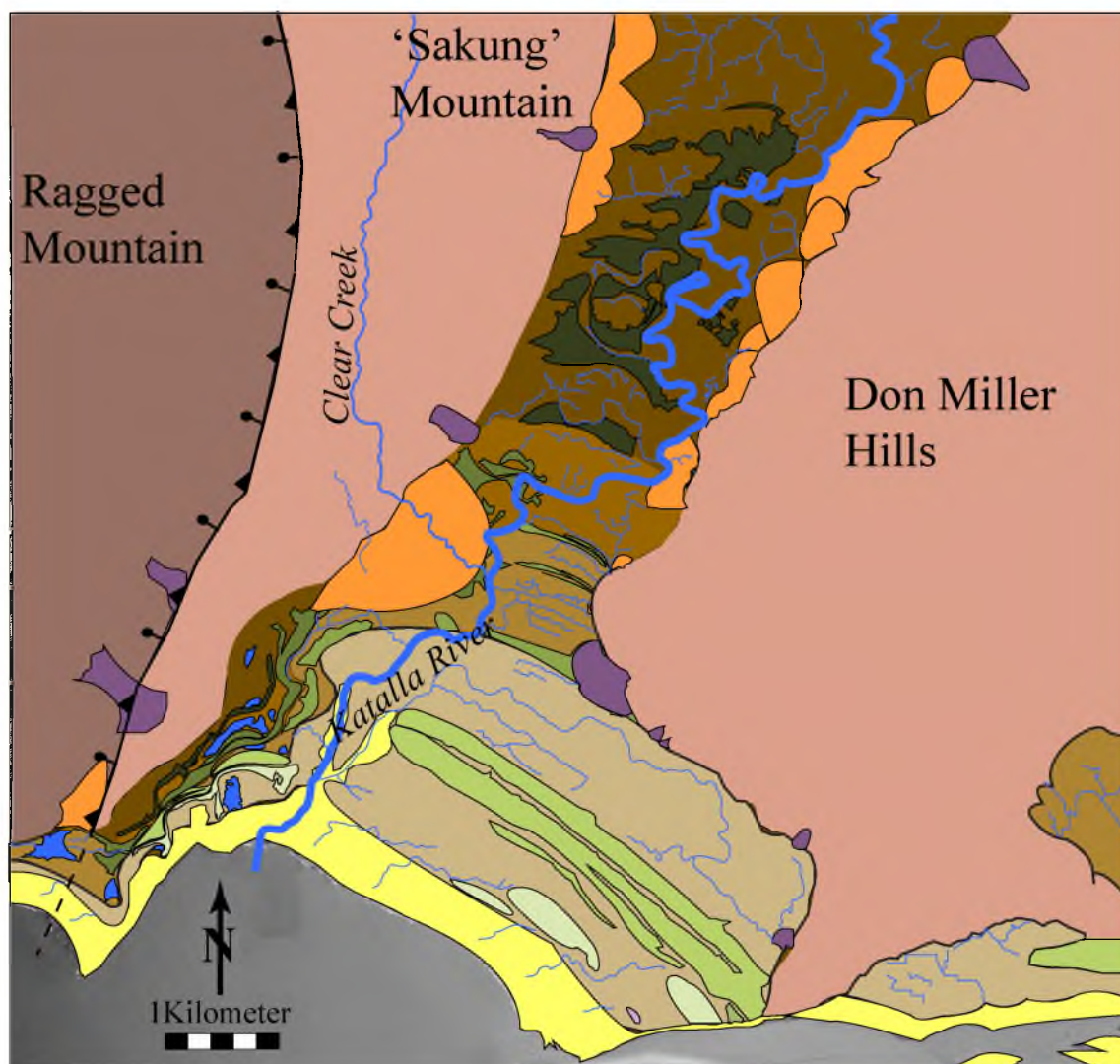Bedrock from Prince William terrane

Freshwater Marsh/Former Slough

Youngest ⟷ Oldest

Tree-lined Ridge/Former Berm

Youngest ⟷ Oldest

Ragged Mountain Thrust Fault
with normal-sense reactivation

Ragged Mountain

'Sakung' Mountain

Clear Creek

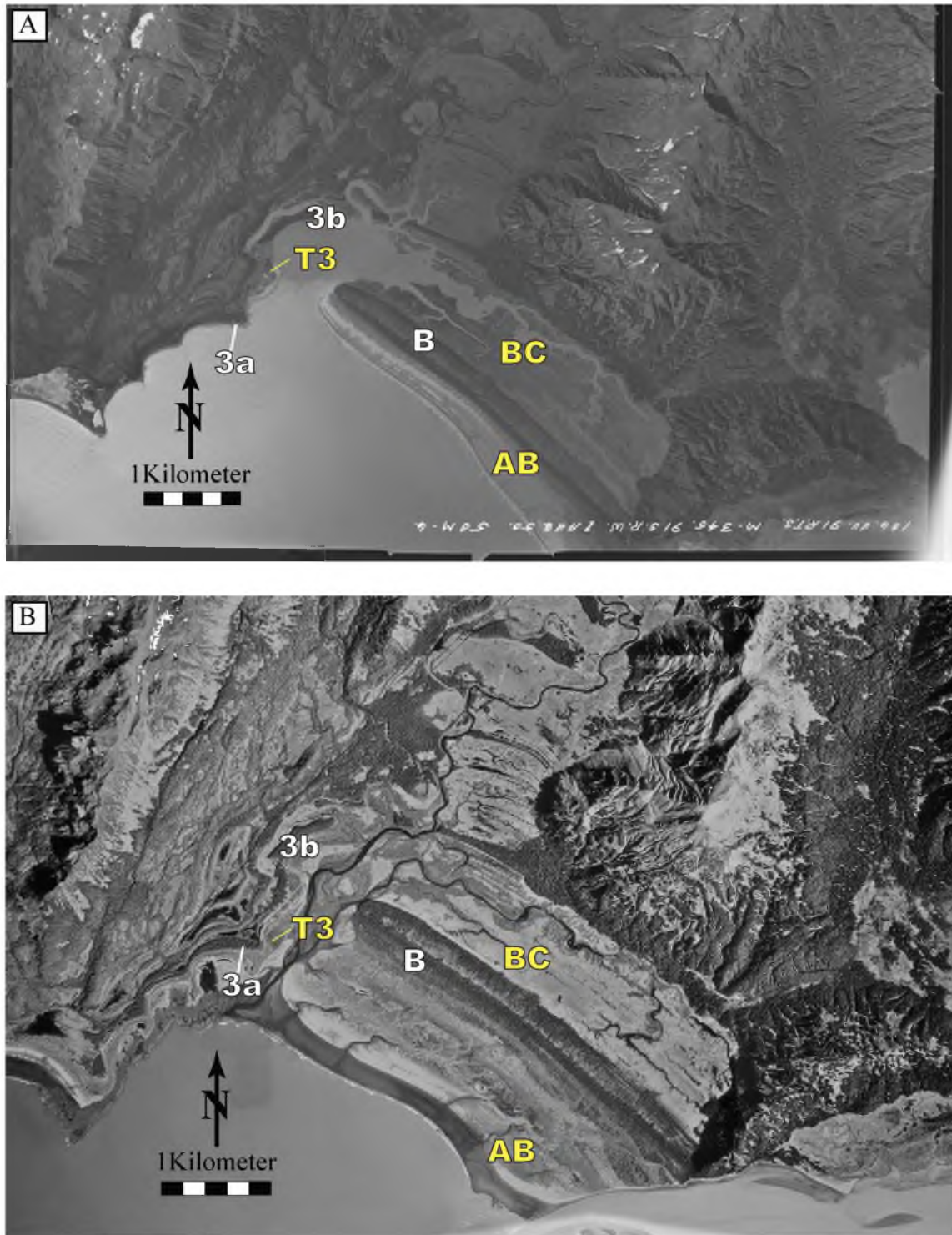Don Miller Hills

Katalla River

N

1 Kilometer

Figure 26. Katalla River Valley and Ragged Mountain before and after the 1964 Good Friday Earthquake. a) Katalla circa 1950 (photo credit: US Geological Survey). Berm B was the active berm in the valley as were Ridges 3a and 3b on the Ragged Mountain piedmont. Marsh BC was a tidal inlet, as was Terrace 3 to the west. b) After the Good Friday Earthquake, the coastline prograded by nearly a kilometer in some places.
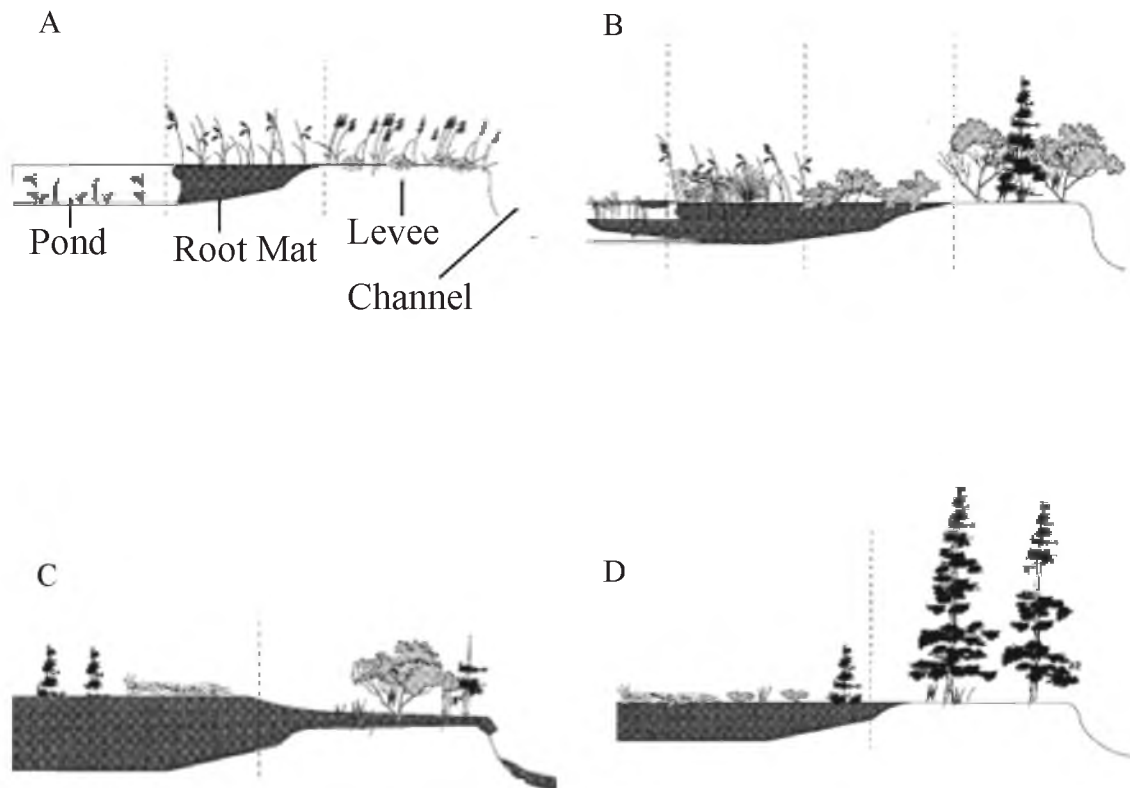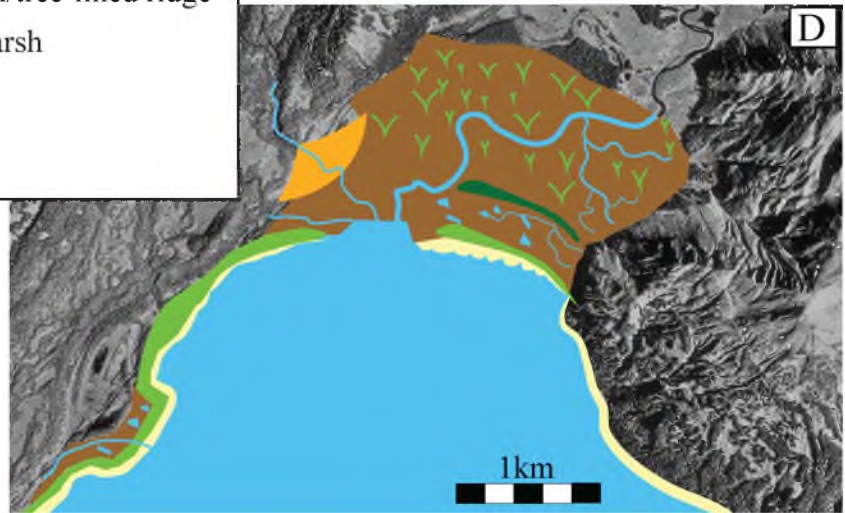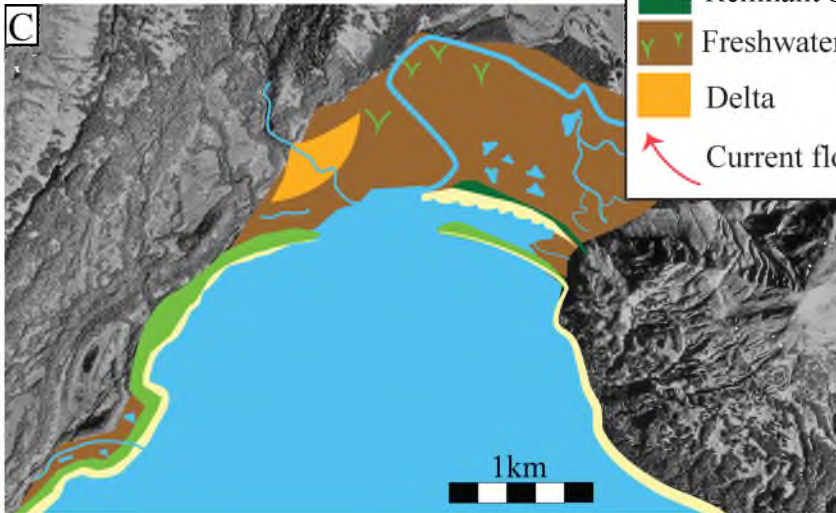
Figure 27. Idealized cross section of vegetation succssion and landform development adapted from Boggs (2000). A) Post-1964 marsh vegetation: Tide tolerant species continue to dominate immediately after the 1964 uplift. Tides no longer flood the ponds or levees. B) Early seral (30 years after uplift): Freshwater-tolerant species (herbs, shrubs and trees) invade the peat and levees. C) Mid seral: Peat continues to fill the ponds, supporting mature peatland communities. Tree and shrub communities dominate the levees. D) Late seral: Peat continues to fill the ponds, and may invade the levees. The peat supports mature peatland communities.

Figure 28. Paleogeographic maps dipicting Katalla from ~7000 BP through time the 2100 BP uplift event. A) Katalla circa 7000 BP. The valley was fully under marine influence, and a possible hooked spit was forming off of Clear Creek Fan. The black rectangle approximates the location of the following maps. B) Katalla after the 2500 BP uplift event. Diatom and stratigraphic data show the development of a freshwater marsh following uplift. C) A relative sea level fall caused a transgression of the previously uplifted marshes prior to the 2100 BP event. D) The 2100 BP uplift had the same effect as the 2500 BP event.

Legend

〰 Rivers and streams

▨ Beach/spit

▨ Active berm

▨ Tidally influenced marsh/slough

▨ Remnant berm/tree-lined ridge

Y Freshwater marsh

▨ Delta

N ↑

1km
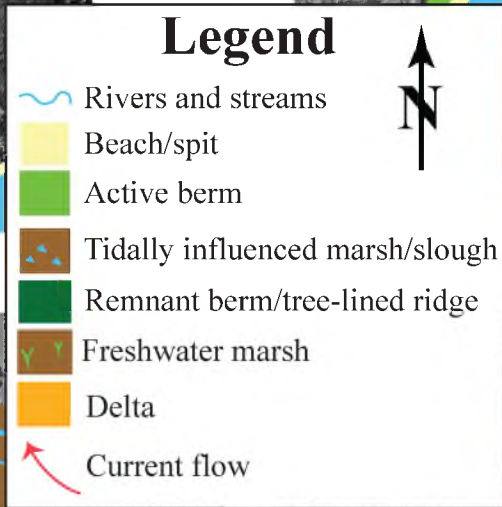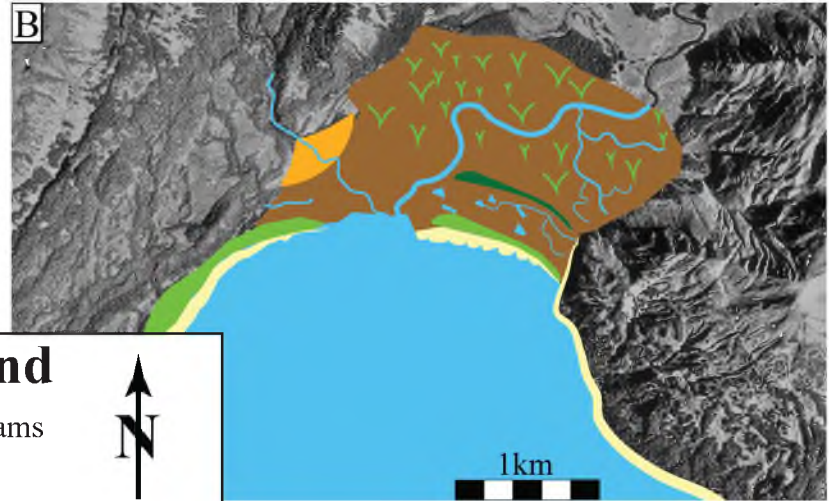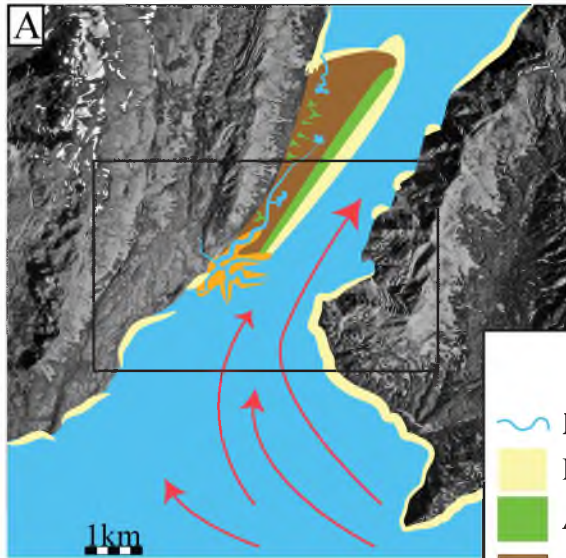
Figure 29. Paleogeaphic maps depicting Katalla before the 1500 BP uplift event through ~1100 BP. Locations are shown by the black rectangle on Figure 28a. A) No recorded intersiesmic subsidence between the 2100 BP event and the 1500 BP event. A possible spit may have formed off of the Don Miller Hills to the east. B) The 1500 BP event raised the previously intertidal marshes above sea level and the beach to an intertidal slough. C) Subsidence around 1100 BP resubmerged at least three freshwater marshes.
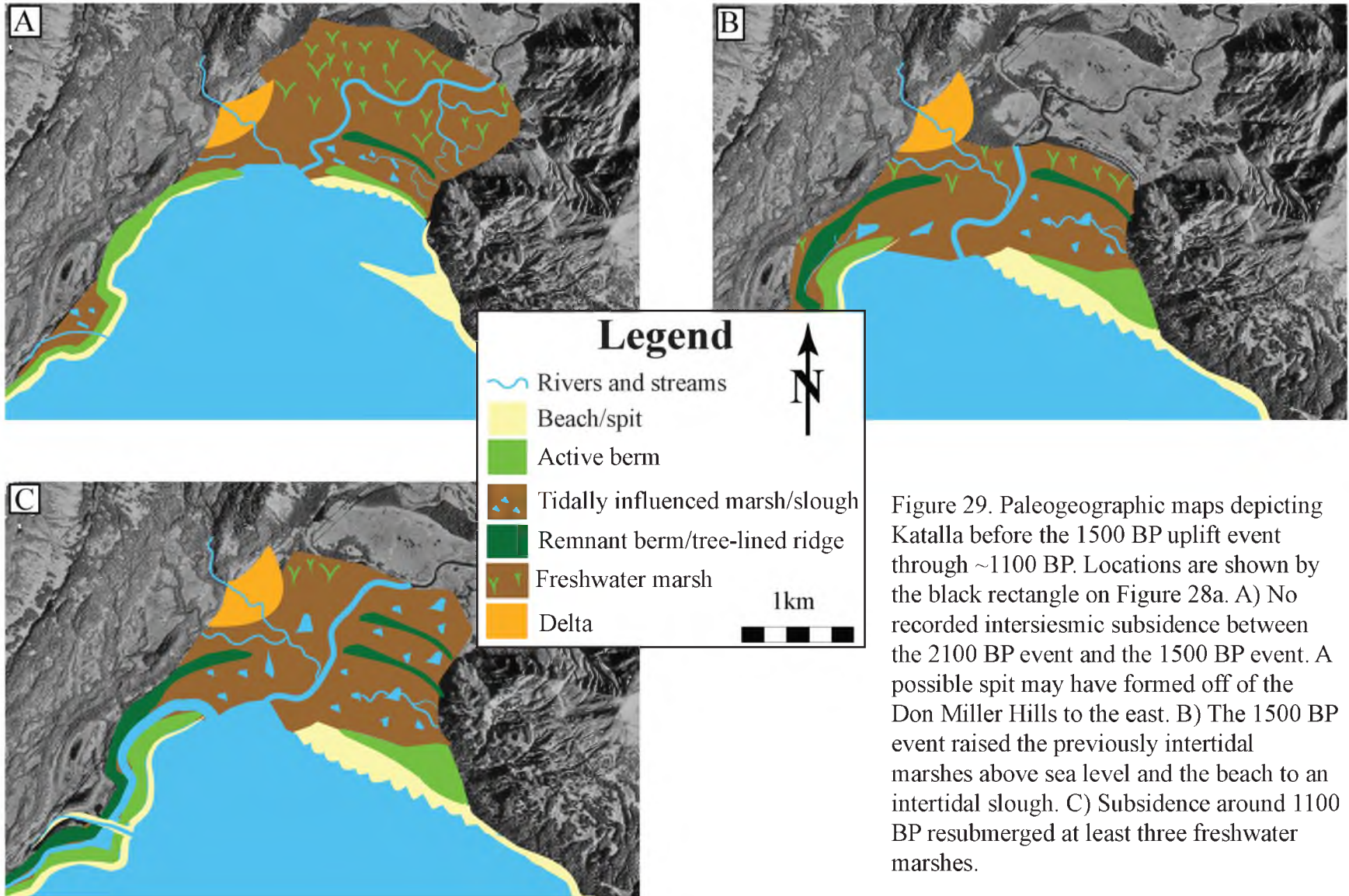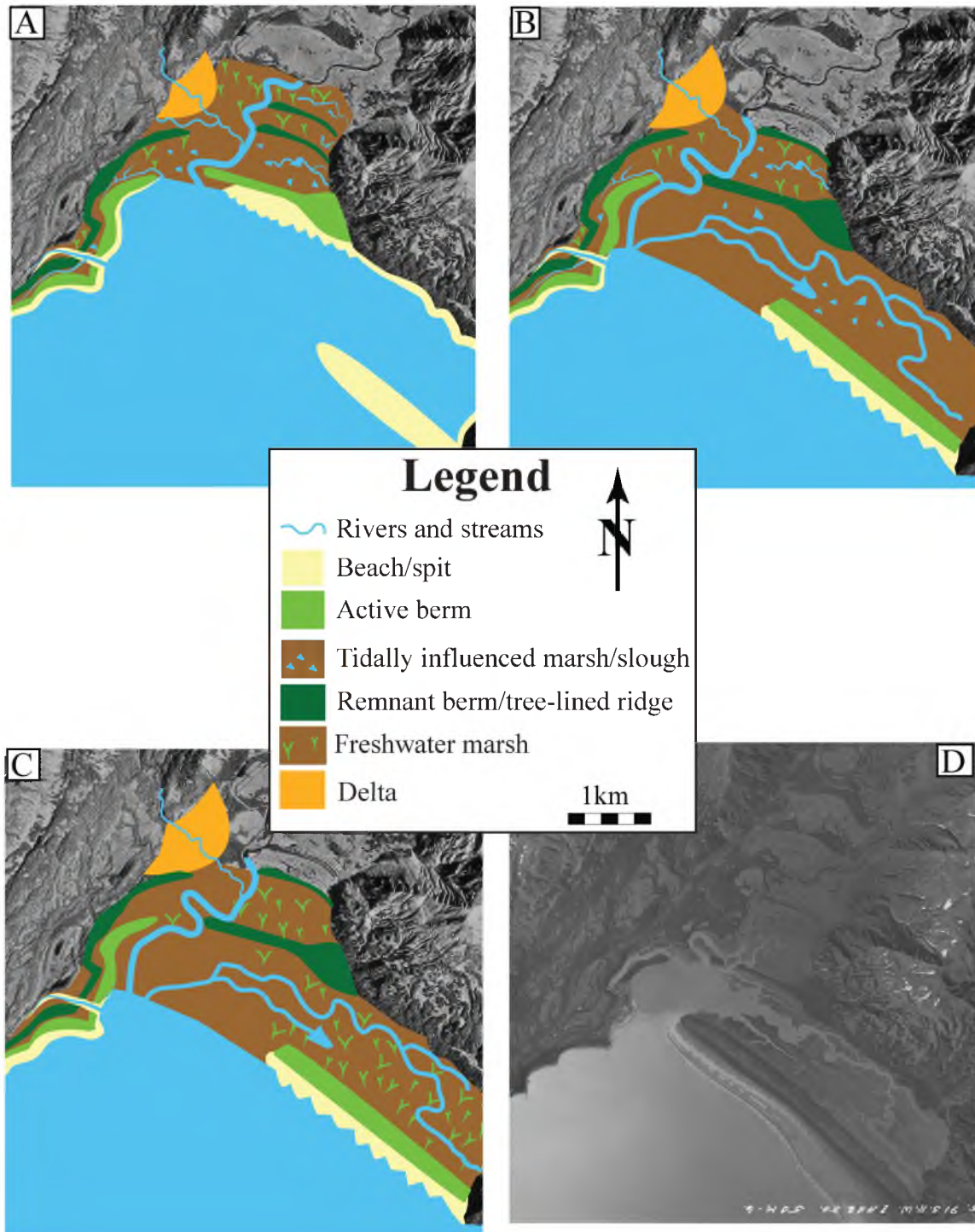
Figure 30. Paleogeographic maps depicting Katalla after the 900 BP uplit event to AD 1950. Locations are shown by the black rectangle on Figure 28a. A) The 900 BP uplift lifted all but one tidal slough to a freshwater marsh environment. B) Between 500 BP and 900 BP, a relative sea level caused an open marine environment to become a tidal slough, perhaps due to building of the spit at the southern end of the Don Miller Hills. C) The 500 BP uplift raised the tidal slough to a freshwater marsh. D) Intersiesmic subsidence drowned the marsh as seen in air photos.

CHAPTER 5

DISCUSSION

Today's landscape reflects at least 7000 years of southward progradation of the

shoreline as the Katalla River estuary filled with sediment and the sea level fell, stranding

former marine deposits on the piedmont and in the valley. The well-sorted, porous, and

better-drained gravel and sandy deposits beneath the berms support thick stands of

hemlock and Sitka spruce. The intervening freshwater marshes are vegetated by shrubs

and grasses that overlie a complicated stratigraphy that records a history of fluctuating

uplift and subsidence between marine, brackish water, and nonmarine environments. This

history of relative sea level change, infilling of the estuary, and southward migration of

the coast is obtained by interpreting and dating the Quaternary deposits that fill the

former sloughs and bury the eroded platforms. The history is complicated by

superposition of deposits and processes associated with the last vestiges of glaciation,

lateral migration of coastal and fluvial environments, and relative sea level change caused

by a combination of global sea level change, local isostatic rebound, and earthquakes.

Overall, there is compelling evidence for several meters of net uplift in the Katalla River

Valley.

The history of uplift and subsidence that occurred coseismically and interseismically in Katalla is complex. The only direct measurement of coseismic uplift occurred after the 1964 earthquake (Plafker, 1965). When interpreting the paleogeography of Katalla over the last 2600 years, vertical displacements fluctuated between periods of net uplift and subsidence. That is, there are two time periods of net subsidence—1500 BP to 900 BP and 500 BP to 1964 AD—one time period with net uplift roughly zero—2600 BP to 1500 BP—and two time periods with net uplift—900 BP to 500 BP and 1964 to present. However, it is too soon to tell whether or not interseismic subsidence will not come to dominate over coseismic uplift in 1964. If the amount of coseismic uplift and interseismic subsidence were equal to each other, and were the same for each earthquake, then net uplift would be zero. The cross section (Figure 21a) indicates some interseismic subsidence particularly in Marsh EF. The 2600 BP and 2100 BP contacts are at a lower elevation than the younger contacts. However, the 900 BP contact and 1500 BP contacts are both higher than the two youngest contacts which strongly suggests net uplift. The 7000-year-old shells near Ridge I also indicate net uplift since their deposition.

One possible cause of this relative sea level fall is a global sea level fall and subsequent progradation of the valley. We reject this hypothesis because there is no evidence of a eustatic sea level drop; in fact, global sea level has slowly risen over the last 6000 years (Church *et al.*, 2001). Additionally, a gradual drop in sea level would be evident in the stratigraphic cores, which is not the case.

Another alternative cause of relative sea level fall is due to increased sedimentation from the Katalla River. If sedimentary deposition is greater and faster than

removal by ocean currents, then the valley would prograde to the south. This too is unlikely as there are no sedimentalogical data showing a gradual progradation. In the lower half of the valley where the cores were taken, the stratigraphy indicates abrupt sea level falls, consistent with coseismic displacements. The only gradual sedimentary facies change appears to be interseismic when marine deposits buried former subaerial and shallow marine deposits.

Isostatic adjustment after glacial retreat could be another cause of a relative drop in sea level. While it is likely that the Katalla River Valley rebounded after the glacial retreat, the amount of uplift does not compare to the difference in height from the head of the valley to the mouth. Furthermore, the calculations show the isostatic adjustment period was relatively short and no longer influences the Katalla Valley (Richards, 2000).

There are two potential shortcomings to the isostatic analysis presented by Richards (2000) that need to be considered before one can eliminate isostatic rebound as a mechanism for net uplift in the Katalla Valley. First, the analysis was a one-dimensional or 'point load' isostatic rebound model that neglects the effects of ice loading distributed over a lithosphere with a finite equivalent elastic thickness, and also assumed that ice loading was removed instantaneously. The results of this type of calculation tend towards a maximum credible rebound at a point. Although the history of ice withdrawal from the valley is poorly determined, it is plausible that some uplift by rebound was still underway within a few thousand years after the assumed 10 ka date of ice withdrawal. Secondly, the valley is located only several tens of kilometers from large piedmont glaciers. These include the Bering, Stellar, and Martin River Glaciers, each of which has waxed and waned in surface area during the late Holocene (Hamilton, 1994).

Lateral growth and retreat of these glaciers may have caused vertical displacements within the valley that are not accounted for. Presumably, short-term shifts in the ice masses of the piedmont glaciers would be reflected in transitional rather than abrupt changes in the depositional environment of marine to nonmarine and the opposite, deposition. Observations of depositional changes in the cores from the Katalla Valley did not reveal gradational changes from marine to nonmarine deposition during uplift or relative sea-level fall, however. Rather, the evidence supports abrupt uplift, that, with one exception circa 500 BP, correlate in time with megathrust earthquakes during the last several thousand years.

Therefore, we conclude that the topography and shape of the valley are probably due to net tectonic uplift through time. Sedimentary cores that contain records of earthquakes are progressively older from south to north within the valley. If net uplift were equal to zero, then the megathrust events recorded in the cores at Katalla would be in all of the marshes. More likely, there would be few marshes to core, because the coast would be located farther inland near the head of the valley. While tectonic uplift is the driving factor in the long-term relative sea level fall, it is possible that increased sedimentation also has a role. There are smaller ridges between Ridges D and E in the Katalla River Valley, which may indicate progradation unrelated to tectonic uplift.

The general cycle of tectonic uplift followed by progradation in the Katalla River Valley is illustrated in Figures 31a and 31b. First a submerged portion south of the valley is uplifted and a berm or spit forms. This is followed by another uplift event and the former beach becomes either a freshwater or brackish marsh with a new berm in front of it. Beaches are able to form in the valley because they are partially protected from direct

wave action by the Don Miller Hills, which project outwards to the coast along the eastern side of the valley.

The terraces located on the Ragged Mountain piedmont reflect uplift and an emerging shoreline through time. Due to the direct wave action it receives from the east, large beaches do not form along the piedmont. Instead, the formally glacial scoured bedrock is cut by the wave action into a marine platform and a berm is deposited on top. A narrow beach may form in front of the berm. After an uplift event, the platform is raised and may become a tidal inlet or a freshwater marsh. Another platform-ridge sequence takes shape to the east. Eventually, the southern ridges may amalgamate into one. This process is shown in Figures 31c and 31d.

Although net uplift is apparent in the Katalla area, the overall trend of vertical displacement along the coast is subsidence. In sediment cores, subsidence manifests as marine sediment gradually overlying freshwater sediment or peat. With the exception of the 1964 event, every sharp contact of peat over marine sediment recorded in Quaternary stratigraphy from the Alaganik Slough to the west and Cape Suckling to the east is overlain by marine sediment (Carver and Plafker, 2008, Shennan *et al.*, 2009). Therefore, it is anomalous that Katalla—situated between those two endpoints—is experiencing net uplift.

We propose three hypotheses to explain net uplift in Katalla and partially explain extension along the Ragged Mountain fault and the anomalous 500 BP event. In all cases, the amount of net uplift is modest, and within the range of 2-5 m. Isostatic rebound caused by Late Holocene fluctuations in ice masses is not considered because 1) we found no evidence for gradational changes in stratigraphy related to rebound, and 2) the

history of piedmont glacier fluctuations is too poorly known to create accurate and

meaningful models of spatially distributed rebound in the Katalla Valley.

The first hypothesis proposes that imbricate thrusting drives net uplift. This

hypothesis fits into the overall nature of convergence along the boundary of the Yakutat

terrane and the North American plate. As the Yakutat terrane is subducted and accreted,

steeply dipping reverse faults propagate toward the surface to accommodate shortening of

the crust (Figure 32). Recent studies show the Kayak Island zone actively accommodates

convergence of the Yakutat terrane at 3.5±1.0 mm/yr. The zone extends onshore to

connect with the Bering Glacier Structure and the Suckling Hills fault, both of which are

east of the Katalla River Valley (Bruhn *et al.*, 2004; Chapman *et al.*, 2011). The imbricate

thrust beneath the Katalla River Valley may also be a result of this shortening. The

Bering Deformation zone, as described by Elliot (2011), is a zone of increased

counterclockwise motion relative to stable North America. The Bering Deformation zone

is the area between the Bering Glacier and the Copper River Delta, which includes

Katalla. The rotation exhibited by the new GPS data published by Elliot (2011) show that

the Bering Deformation zone is actively accommodating shortening described by

Chapman *et al.* (2011). As this block began rotation, the Kayak Island zone and its

onshore equivalents formed a new structural boundary that may be the current eastern

extension of the Aleutian megathrust (Chapman *et al.*, 2011). A local imbricate fault may

rupture during megathrust events, as happened at Kodiak Island during the Good Friday

Earthquake (Plafker, 1965), or it may rupture independently, causing anomalous events

like the 500 BP uplift event. This hypothesis, however, does not easily explain the

interseismic subsidence following the 500 BP event, but westward slip along the Ragged

Mountain fault may be similar to that which occurred during the Tohoko-Oki earthquake in Japan in 2011 (Ito *et al.*, 2011).

The second hypothesis speculates that net uplift is driven by aseismic anticlinal flexure or folding. This hypothesis is similar to the first in that an antiformal stack under the Katalla Valley accommodates shortening along the convergent boundary in a similar fashion to an imbricate fault. Uplift occurs due to repeated stacking of crustal rocks under the Katalla Valley as opposed to one high angle fault (Figure 32). This hypothesis not only explains net uplift, and possibly the 500 BP event, but also fits well with the bedrock geology of Katalla. The Poul Creek Formation, located on either side of the valley, is adjacent to the younger Redwood Formation east of the Don Miller Hills. At the head of the valley, the Tokun Formation crops out with the Sillwater north of it. The Tokun formation is older than the Stillwater Formation. As a plunging antiform erodes, the core of the anticline is exposed and is surrounded by younger strata on either side. This is evident in Katalla (Figure 4). The Tokun Formation at the head of the valley suggests that the axial plane is plunging toward the southeast. An antiformal stack beneath Katalla does not easily explain backsliding along the Ragged Mountain fault, however. The Ragged Mountain could be part of a syncline that is adjacent to the antiform beneath Katalla. The uphill facing scarps would not be a result of normal faulting, but of intralimb slip within the syncline. The geometry of the Ragged Mountain fault is not consistent with this hypothesis, and a steep syncline does not easily form in this tectonic regime.

The third hypothesis is that uplift is driven by exhumation of the footwall of the Ragged Mountain fault (Figure 32). As the hanging wall of the fault moves westward, the footwall, which underlies the Katalla Valley slowly rebounds. This hypothesis explains

apparent extension along the Ragged Mountain fault, as well as the few meters of net uplift over the last several thousand years. Unlike the first two hypotheses, however, this does not easily fit with the ongoing convergence of the Yakutat terrane and the North American plate. Additionally, trenching along the Ragged Mountain fault in the mid-2000s revealed reverse fault splays, which would not be present if the Ragged Mountain was backsliding (R. Bruhn, 2012 pers. comm.).

All three of these hypotheses reasonably explain net uplift in Katalla, but do not easily explain extension along the Ragged Mountain fault and/or fit into the larger tectonic regime. Of the three, an antiformal stack beneath Katalla is the preferred hypothesis. This is because it not only explains net uplift, but there is bedrock evidence of a remnant antiform. Antiforms and high-angle reverse faults are present throughout the region both onshore and off. In the Pamplona zone, east of the Kayak Island zone, seismic data show multiple anticlines growing offshore (Worthington *et al.*, 2010). The Kayak Island zone is a series of northwest dipping reverse faults, which are parallel to the proposed antiform beneath the Katalla Valley. The Ragged Mountain fault remains an enigma, however. Perhaps it is just backsliding along its original boundary as a result of the upward flexure in Katalla. Perhaps the trenching data are accurate and the extensional scarp is due to folding over the hanging wall after thrusting. The offset of the Quaternary landslide at the southern end of the Ragged Mountain fault indicates normal-sense offset in the last 10,000 years, leading to the preferred interpretation that it is indeed backsliding. These questions cannot be resolved, however, without further research and analysis of the Ragged Mountain fault.

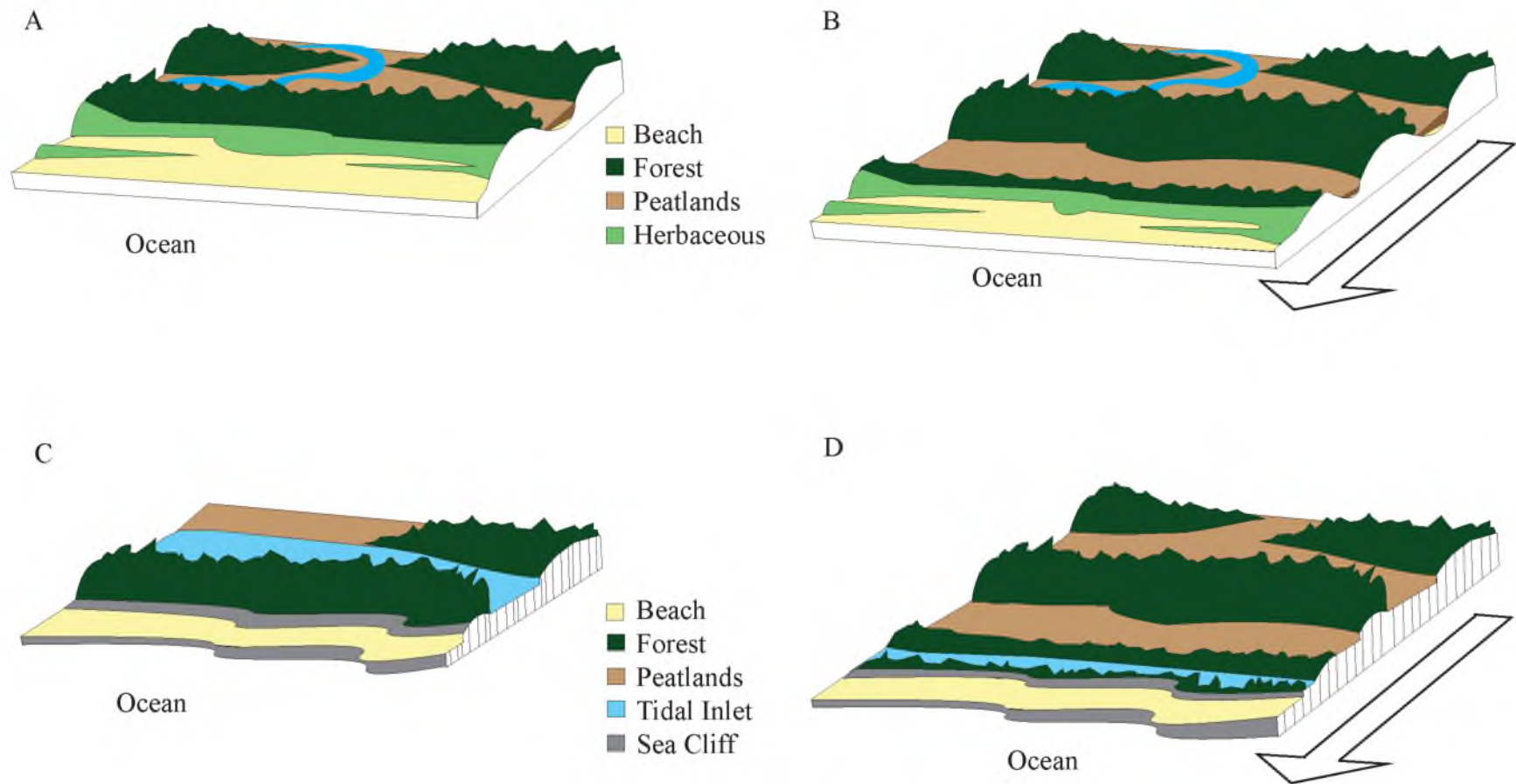Figure 31. Schematic diagram of response of a coast to coseismic uplift (after Boggs, 2000). A) Oblique view of an idealized beach ridge sequence prior to a megathrust event. B) After each uplift, relative sea-level drops and the shoreline progrades out. C) Oblique view of an idealized wave-cut platform sequence prior to a megathrust event. D) After uplift, relative sea level drops and a new cliff is formed.
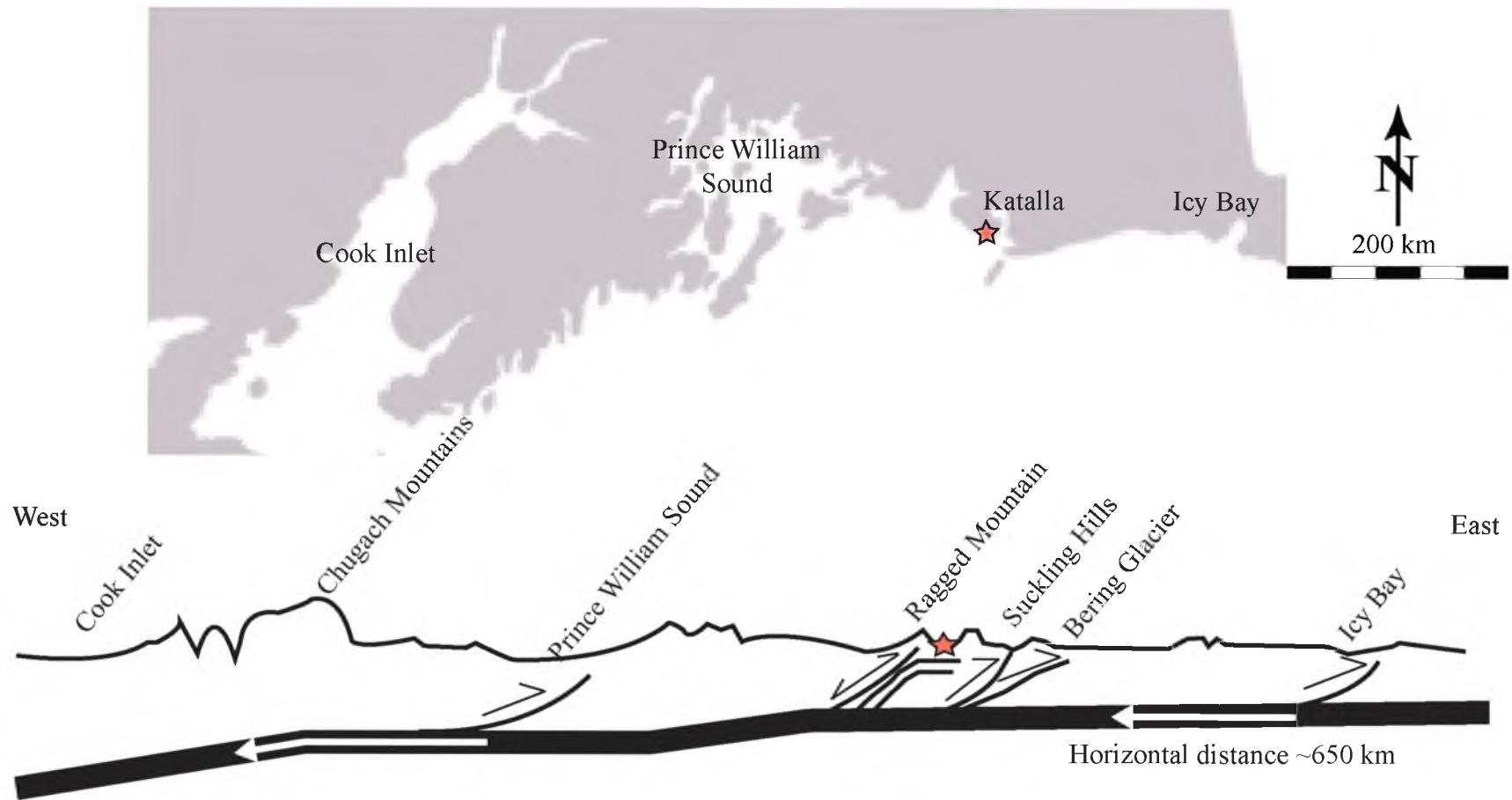
Figure 32. Schematic cross section of the plate boundary between Cook Inlet and Icy Bay adapted from Shennan *et al.* (2013 in press). See Figure 1 for location. Imbricate faults are either known from surface offsets or inferred. Three different mechanisms may be acting underneath Katalla to cause net uplift. The first is imbricate faulting, similar to faults beneath the Prince William Sound and the Suckling Hills. The second is an antiformal stack (shown). The third is that uplift is driven by exhumation in the footwall as the Ragged Mountain backslides along its original thrust boundary.

CHAPTER 6

CONCLUSIONS

This study of the seismic evolution of a tectonically active landscape utilized high-resolution LIDAR DEMs and air photographs to create new geomorphic maps of the Katalla River Valley and the Ragged Mountain piedmont. The geomorphic maps include features that were not previously mapped due to poor quality DEMs and the presence of thick vegetation. Radiocarbon dating was also utilized to determine the ages of peat deposits in six marshes on the piedmont of Ragged Mountain and in the Katalla River Valley.

The geomorphic maps and radiocarbon dates from this study and from others were used to correlate the ridges on the Ragged Mountain piedmont with those in the Katalla River Valley. These correlations led to the interpretation that the ridges were often deposited contemporaneously, even though the Katalla River now transects them.

Freshwater peat sharply overlying saltwater sediments is interpreted to record an abrupt drop in relative sea level. At Katalla, this pattern is interpreted as uplift of the land due to a large earthquake. The radiocarbon dates of the basal peat confirm that Katalla was uplifted during megathrust events documented elsewhere in coastal Alaska. These dates add to the already large database of Aleutian megathrust events.

One uplift event documented in a lower marsh in Katalla suggests that there is a local structure underneath the Katalla River Valley that uplifted it at least once. This structure is confined to the Katalla River Valley because there is no evidence of the 500 BP event in the nearby Alaganik Slough and the Puffy Slough.

This study also concluded that the Ragged Mountain fault is a thrust fault that was recently reactivated with normal slip. Normal-sense offset is indicated by offset of a Quaternary landslide as well as by the geometry of the fault scarp. There is no evidence that the Ragged Mountain fault ruptures coseismically with the Aleutian megathrust.

We propose three hypotheses to explain the net uplift in Katalla as well as the anomalous 500 BP event and backsliding along the Ragged Mountain fault: 1) uplift driven by buried imbricate thrusting, 2) uplift driven by slow asiesmic anticlinal folding that is accommodating shortening, and 3) uplift driven by exhumation as the upper plate of the Ragged Mountain fault moves west.

The results of this study emphasize the importance of LIDAR when studying highly vegetated regions, as well as stratigraphy when studying seismically active landscapes. The multidisciplinary approach allowed for a comprehensive analysis of Katalla that led to the conclusions stated above. It further underscored the complexity of subduction and accretionary margins and provided more evidence toward the Aleutian megathrust earthquake databases.

In order to fully understand this relatively small, but complex area, additional studies need to be undertaken. These could include coring more marshes in the northern part of the Katalla River Valley for evidence of uplift, examining the stratigraphy of the ridges along the piedmont of Ragged Mountain and in the Katalla River Valley to better

determine their depositional environments, and investigating the Ragged Mountain fault in the field for evidence of past rupture.

APPENDIX

Table 3. LIDAR acquisition details (from Pavlis and Bruhn, 2010)

LIDAR instrumentation	Optech 1233 Airborne Laser Terrain Mapper
Aircraft:	Piper Chieftain
Flight Altitude:	600 m
Aircraft Speed:	70 m/s
Scan Frequency and Angle:	28Hz±20°
Swath Width:	437 m
Overlap:	220 m
Beam Divergence:	0.3 millirads
Resolution:	1 m
Maximum Number Returns:	2
Relative Accuracy:	Vertical 0.05-.2m; horizontal 0.11
Ground Return Densities (test plot):	
Open Terrain	2.37 hits/m^2
Forest and/or Shrub	1.04 hits/m^2
Processing Software:	Surfer 8 and Terra Scan
Identification of Ground Returns:	See http://terrasolid.fi/en/products/terrascan
Digital Elevation Model (DEM) from ground returns:	Kriging algorithm, linear variogram
Data Availability:	http://calm.geo.berkeley.edu/nclam/ddc.html

Table 4. Comparison of site locations and names with previous studies by Richards (2000) and Sirkin and Tuthill (1971). Locations shown on Figure 5.

Location	Name in this Paper	2011 sites	2007 sites	Lat/Long	Richards (2000)	Sirkin and Tuthill (1972)
Marsh A						
Ridge A					A	
Marsh AB						
Ridge B					B1 and B2	
Marsh BC	[1]Core 1a [1]Core 1b		WP 464 WP 467	60 10.638N 144 26.938W 60 11.523N 144 28.956W		KBL1
Ridge C					C	KBR2
Marsh CD	[2]Core 2 [3]Core 3 Core 4	KR1101 KR1110 KR1111		60 12.389N 144 29.328W 60 12.387N 144 29.262W none		KBL2
Ridge D	Core5	KR1112		none for KR1112	D	KBR3
Marsh DE	[2]Core 6 [4]Core7 [2]Core 8 Core 9	KR1106 KR1107 KR1108 KR1109		60 12.591N 144 29.043W 60 12.584N 144 29.022W 60 12.469N 144 29.036W none for KR1109		KBL3
Ridge E	Pit1	pit 4		none for pit4	E	KBR4
Marsh EF	[3]Core 10 Core 11	KR1103 KR1105		none for KR1103 none for KR1105		KBL4

[1]Dated in 2007 and 2012
[2]Dated in 2012
[3]Dated in 2011 and 2012
[4]Dated in 2011

Table 4 (continued). Comparison of site locations and names with previous studies by Richards (2000) and Sirkin and Tuthill (1971). Locations shown on Figure 5.

Location	Name in this paper	2011 sites	2007 sites	Lat/Long	Richards (2000)	Sirkin and Tuthill (1972)
Marsh FG						KBL5
Ridge G					G	KBR6
Marsh GH						KBL6
Ridge H					H1	KBR7
Marsh HI						KBL7
Ridge I					H2 and I	KBR8
Marsh IJ						KBL8
Ridge J						KBR9
Marsh JK						KBL9
Ridge K					J	KBR10
Marsh KL						KBL10
Ridge L					K	KBR11
Marsh LM						KBL11
Ridge M					L	KBR12
Marsh MN						KBL12
Ridge N					M	KBR13
Marsh N					N	KBL13

Table 4 (continued). Comparison of site locations and names with previous studies by Richards (2000) and Sirkin and Tuthill (1971). Locations shown on Figure 5.

Location	Name in this Paper	2011 sites	2007 sites	Lat/Long	Richards (2000)	Sirkin and Tuthill (1972)
Terrace 4 Ridge 3	Pit2	Pit 1		60 11.607N 144 31.160W		
Terrace 3	Core 13a Core 13b	KR1113		60 11.554N 144 31.686W		
Ridge 2	Pit 3	Pit 2		60 11.822N 144 31.430W		
	Pit 4	Pit 3		60 11.819N 144 31.450W		
	Pit 5a Pit 5b	Pit 4		60 11.596N 144 31.845W		
Terrace 2	Core 14a			none		
	Core 14b			none		
	Core 14c			none		
	Core 14d			60 11.661N 144 31.781W		
	[2]Core 14e	KR1114		60 11.682N 144 31.877W		
Ridge 1	Pit6	Site3		60 11.730N 144 31.914W		
Terrace 1	[3]Core15	KR1115		60 12.075N 144 31.848W		

[2]Dated in 2011
[3]Dated in 2011 and 2012

Table 5. Elevation data from digital models and from Richards' GPS measurements (2000). All elevations expressed in meters.

Location	GDEM	SRTM	Richards	Lidar
Katalla Valley				
Marsh A			-	-
Ridge A	-1.02±1.65	-5.78±2.60	-	-
Marsh AB			-	-
Ridge B			6.9	-
Marsh BC	-.56±1.53	-3.2±2.9		-
Ridge C			7.7	-
Marsh CD			-	-
Ridge D	.026±1.08	-7.4±2.88	5.2	-
Marsh DE			5.4	-
Ridge E			5.9	-
Marsh EF	2.28±2.46	1.44±3.06	6.7	-
Ridge F			-	-
Marsh FG	3.02±2.50	2.55±2.39	6.7	-
Ragged Mountain Piedmont				
Terrace 1	-	-	1.8	2
Ridge 1	-	-	7.9	5
Terrace 2	-	-	-	6
Ridge 2	-	-	-	9.5
Terrace 3	-	-	-	11
Ridge 3	-	-	-	14
Terrace 4	-	-	17.3	19

Granitic Gneiss

Quartzite

Porphyritic Andesite

Quartzite

Figure 33. Photos of small boulders on the Katalla Coast with a 15cm pencil for scale. Note variety in petrology, all of which are exotic to Orca Group, Stillwater Formation and Poul Creek Formation.

Figure 34. Photo of medium boulder on Terrace 4 at approximately 60 11.607 N, 144 31.160 W. Shovel for scale is approximately 1 m long. Boulder is partially rounded, likely due to wave action.

Figure 35. Large boulder seen from the air located on Terrace 1 at about 60 11.377 N, 144 31.801 W. The boulder is about 4 m in diameter.

REFERENCES

Anonymous. 1907, August 10. No doubt about the Katalla break-water now under construction. Plans of projectors wisely made. *Katalla Herald* 1:1:1

Atwater, B.F., 1987, Evidence for great Holocene earthquakes along the outer coast of Washington state: Science, v. 236, p. 942-944

Boggs, K., 2000, Classification of community types, succession sequences, and landscapes of the Copper River Delta, Alaska. General Technical Report PNW-GTR-469. Portland, OR: U.S. Department of Agriculture, Forest Service, Pacific Northwest Research Station. 244 p.

Bowman, S., 1990, Radiocarbon Dating: Los Angeles, California, University of California Press, 64 p.

Bruhn, R.L., Pavlis, T.L., Plafker, G., Serpa, L., 2004, Deformation during terrane accretion in the Saint Elias orogen, Alaska: Geological Society of America Bulletin, v. 116, no. 7/8, p. 771-787

Bruns, T.R., 1983, Model for the origin of the Yakutat block, an accreting terrane in the northern Gulf of Alaska: Geology, v. 11, p. 718-721

Carver, G., Plafker, G., 2008 Paleoseismicity and neotectonics of the Aleutian subduction zone – an overview, *in* Freymueller, J.T., Haeussler, P.J., Wesson, R., Ekstrom, G., eds, Active Tectonics and Seismic Potential of Alaska: Washington, D.C., American Geophysical Union, v. 179, p. 43-64

Chapman , J.B., Pavlis, T.L., Gulick, S., Berger, A., Lowe, L., Spotila, J., Bruhn, R., Vorkink, M., Koons, P., Barker, A., Picornell, C., Ridgway, K., Hallet, B., Jaeger, J., McCalpin, J., 2008, Neotectonics of the Yakutat Collision: Changes in deformation driven by mass redistribution, *in* Freymueller, J.T., Haeussler, P.J., Wesson, R., Ekstrom, G., eds, Active Tectonics and Seismic Potential of Alaska: Washington, D.C., American Geophysical Union, v. 179, p. 65-81

Chapman, J.B., Worthington, L.L., Pavlis, T.L., Bruhn, R.L., Gulick, S.P., 2011, The Suckling Hills fault, Kayak Island zone and accretion of the Yakutat microplate, Alaska, Tectonics, v. 30

Christeson, G.L., Gulick, S.P.S., van Avendonk, H.J.A., Worthington, L.L., Reece, R.S., Pavlis, T.L., 2010 The Yakutat terrane: Dramatic change in crustal thickness across the Transition fault, Alaska: Geology, v. 38, no. 10, p. 895-898

Elliot, J.L., Larsen, C.F., Freymueller, J.T., Motyka, R.J., 2010, Tectonic block motion and glacial isostatic adjustment in southeast Alaska and adjacent Canada constrained by GPS measurements: Journal of Geophysical Research, vol. 115

Elliot, J.L, 2011, Active tectonics in southern Alaska and the Role of the Yakutat block constrained by GPS measurements [PhD Thesis]: Fairbanks, University of Alaska Fairbanks, 167 p.

Fleisher, P.J., Muller, E.H., Peteet, D.M., Lachniet, M.S., 1999, Arctic Enigma: Was Alaska's late Pleistocene Bering Glacier really out of step with its neighbors? New terrestrial evidence suggests otherwise: Geotimes, January, p. 16-21

Fletcher, H.J., Freymueller, J.T., 1999, New GPS constraints on the motion of the Yakutat Block, Geophysical Research Letters, v. 26, no 19, p. 3029-3032

Gawthrop, W.H., Page, R.A., Reichel, M., Jones, A., 1973, The southeast Alaska earthquake of July 1973. EOS Trans American Geophysical Union 64, 263

Hamilton, T.D., 1994, Late Cenozoic glaciation of Alaska, *in* Plafker, G., and Berg, H.C., eds., The Geology of Alaska: Boulder, Colorado, Geological Society of America, Geology of North America, v. G-1, p. 813-844

Hemphill-Haley, E., 1993, Taxonomy of recent and fossil (Holocene) diatoms (Bacillariophyta) from northern Willapa Bay, Washington. US Geological Survey Open File Report, 93-289, 154 p.

van Heteren, S., Oost, A.P., van der Spek, A.J.F., Elias, E.P.L, 2006, Island-terminus evolution related to changing ebb-tidal-delta configuration: Texel, the Netherlands: Marine Geology, v. 235, p. 19-33

Ito, Y., Tsuji, T., Osada, Y., Kido, M., Inazu, D., Hayashi, Y., Tsushima, H., Hino, R., Fujimoto, H., 2011, Frontal wedge deformation near the source region of the 2011 Tohoku-Oki earthquake, Geophysical Research Letters, v. 38, no 7

Janson, L.E., 1975, The copper spike: The story of the Copper River and Northwest Railway: Anchorage, Alaska, Todd Communications, 175 p.

Jenson, S.G., Aagaard, T., Badlock, T.E., Kroon, A., Hughs, M., 2009, Berm formations and dynamics on a gently sloping beach; the effect of water level and swash overtopping: Earth Surface Processes and Landforms, v. 34

Jessop, D.E., 2005, The rise and fall of Katalla: 'The coming metropolis of Alaska', Alaska History, v. 20, n. 1

Kachadoorian, R., 1960, Engineering Geology of the Katalla Area, Alaska: U.S. Geological Survey Miscellaneous Investigations Series Map I-308, scale 1:63,360, 1 sheet.

Kanamori, H., 1977, Seismic and aseismic slip along subduction zones and their tectonic implications, *in* Talwani, M., Pitman, W.C., eds., Island Arcs, Deep Sea Trenches and Back-Arc Basins 1: Washington DC, p. 163-174

Keller, E.A., Pinter, N., 1996, Active tectonics: Earthquakes, uplift and landscape: Upper Saddle River, New Jersey, Simon & Schuster, 338 p.

Koons, P.O., Hooks, B. P., Pavlis, T., Upton, P., Barker, A. D., Three-dimensional mechanics of Yakutat convergence in the southern Alaskan plate corner: Tectonics, v. 29

Libby, W., 1955, Radiocarbon Dating, 2nd ed: Chicago, Illinios, The University of Chicago Press, 164 p.

Lindhorst, S., Fürstenau, J., Christian Hass, H., Betzler, C., 2010, Anatomy and sedimentary model of a hooked spit (Sylt, southern North Sea), Sedimentology, v. 57, p. 935-955

Martin, G.C., 1908, Geology and mineral resources of the Controller Bay region, Alaska: U. S. Geological Survey Bulletin 335, 141 p.

McCalpin, J.P., Bruhn, R.L., Pavlis, T.L., Gutierrez, F., Guerrero, J., Lucha, P., 2011, Antislope scarps, gravitational spreading, and tectonic faulting in the western Yakutat microplate, south coastal Alaska: Geosphere, vol. 7, no. 5, p. 1-16

NASA Land Processes Distributed Active Archive Center (LP DAAC). ASTER L1B. USGS/Earth Resources Observation and Science (EROS) Center, Sioux Falls, South Dakota. 2001.

National Oceanic and Atmospheric Administration, 2011, NOAA tide predictions: Cordova: http://tidesandcurrents.noaa.gov/get_predictions.shtml?year=2011&stn=1200+Cordova (accessed November 2012).

Palmer, A.J.M., Abbot, W.H., 1986, Diatoms as indicators of sea-level change, *in* Van de Plassche, O. eds., Sea-level research: a Manual for the Collection of and Evaluation of Data. Geo Books, Norwich, p. 457-488.

Plafker, G., Moore, J.C., Winkler, G.R., 1994, Geology of the southern Alaska margin, *in* Plafker, G., and Berg, H.C., eds., The Geology of Alaska: Boulder, Colorado, Geological Society of America, Geology of North America, v. G-1, p. 389-449

Plafker, G., 1965, Tectonic deformation associated with the 1964 Alaska earthquake: Science, v. 148, no. 3678, p. 1675-1687

Plafker, G., 1972, Alaskan earthquake of 1964 and Chilean earthquake of 1960: Implications for arc tectonics: Journal of Geophysical Research, v. 77, no. 5, p. 901-925

Plafker, G., 1987, Regional geology and petroleum potential of the northern Gulf of Alaska continental margin, *in* Scholl, D.W., Grantz, A., and Vedder, J.G., eds,. Geology and resource potential of the western North America and adjacent ocean basins—Beaufort Sea to Baja California: Houston, Texas, Cicum-Pacific Council for Energy and Mineral Resources, Earth Science Series, v. 6, p. 229-268

Richards, S., 2000, Holocene history of the Katalla River Valley, Alaska [M.S. thesis]: Salt Lake City, University of Utah, 132 p.

Ruppert, N., 2008, Stress map for Alaska from earthquake focal mechanisms, *in* Freymueller, J.T., Haeussler, P.J., Wesson, R., Ekstrom, G., eds, Active Tectonics and Seismic Potential of Alaska: Washington, D.C., American Geophysical Union, v. 179, p. 351-367

Shennan, I., Bruhn, R. L., Plafker, G., 2009, Multi-segment earthquakes and tsunami potential of the Aleutian megathrust: Quaternary Science Reviews, vol. 28, p. 7-13

Shennan, I., Barlow, N., Bruhn, R.L., Good, K., Watchman, E., 2013, Late Holocene great earthquakes and plate segmentation of the eastern part of the Aleutian megathrust, Geology (in press)

Shennan, I., 2009, Late Quaternary sea-level changes and paleoseismology of the Bering Glacier region, Alaska: Quaternary Science Reveiws, vol. 28 p. 1762-1773

Sirkin, L.A., Tuthill, S., 1971, Late Pleistocene palynology and stratigraphy of Controller Bay Region, Gulf of Alaska: Etudes sur le Quaternaire le Monde, vol. 1 p. 197-208

Tysdal, R. G., Hudson, T., Plafker, G., 1976, Surface features and recent movement along the Ragged Mountain fault, south-central Alaska, US Geological Survey Miscellaneous Field Studies Map MF-782, scale 1:24,000, 1 sheet.

USGS, 1950, www.earthexplorer.usgs.gov, (accessed February 20, 2013)

USGS 2004, Shuttle Radar Topography Mission, 1 Arc Second scene
SRTM_u03_n008e004, Unfilled Unfinished 2.0, Global Land Cover Facility,
University of Maryland, College Park, Maryland, February 2000.

Worthington, L.L., Gulick, S.P.S., Pavlis, T.L., 2008, Identifying active structures in the
Kayak Island and Pamplona zones: Implications for offshore tectonics of the
Yakutat Microplate, Gulf of Alaska, *in* Freymueller, J.T., Haeussler, P.J., Wesson,
R., Ekstrom, G., eds, Active Tectonics and Seismic Potential of Alaska:
Washington, D.C., American Geophysical Union, v. 179, p. 257-268

Worthington, L.L., Gulick, S.P.S., Pavlis, T.L., 2010, Coupled stratigraphic and structural
evolution of a glaciated orogenic wedge, offshore St. Elias orogen, Alaska:
Tectonics, vol. 29

Winkler, G.R., Plafker, G., Goldfarb, R. J., Case, J. E., 1992, The Alaska Mineral
Resource Assessment Program: Background information to accompany geologic
and mineral-resource maps of the Cordova and Middleton Island Quadrangles,
Southern Alaska: US Geological Survey Circular

Winkler, G.R., Plafker, G., 1993, Geologic map and cross sections of the Cordova and
Middleton Island Quadrangles, southern Alaska: U.S. Geological Survey
Miscellaneous Investigations Series Map I-1984, scale 1:250,000, 1 sheet.